THEORETICAL AND EXPERIMENTAL STUDIES OF NOTCHED COLUMNS SUBJECTED TO AXIAL COMPRESSIVE LOADS[1]

by

H. Liebowitz[2]

Technical Report #1

THE GEORGE WASHINGTON UNIVERSITY

(NASA-CR-126175) THEORETICAL AND EXPERIMENTAL STUDIES OF NOTCHED COLUMNS SUBJECTED TO AXIAL COMPRESSIVE LOADS H. Liebowitz (George Washington Univ.) Mar. 1969 111 p

N72-71876

Unclas

00/99 26254

STUDENTS FACULTY STUDY R
ESEARCH DEVELOPMENT FUT
URE CAREER CREATIVITY CO
MMUNITY LEADERSHIP TECH
NOLOGY FRONTIE SIGN
ENGINEERING APPI NG
GEORGE WASHIN IV

SCHOOL OF ENGINEERING

THEORETICAL AND EXPERIMENTAL STUDIES OF NOTCHED COLUMNS SUBJECTED TO AXIAL COMPRESSIVE LOADS[1]

by

H. Liebowitz[2]

Technical Report #1

March 1969

Acknowledgement for support is given to Office of Naval Research, Reynolds Metals Company, and National Aeronautics and Space Administration (NASA Grant NGR-09-010-030).

[1]Keynote address given at the 21st Annual General Meeting of The Aeronautical Society of India in Madras, India, April 4, 1969.

[2]Dean of the School of Engineering and Applied Science, The George Washington University; Washington, D. C. 20006.

ABSTRACT

This paper is chiefly concerned with the recent work developed on the fracture and carrying capacity of long, slender notched columns subjected to concentric and eccentric axial compressive loading. A study was made of the effects of cracks of various depths and root radii on the load carrying capacity of long and short columns with notches on one side and on two opposite sides of these columns. It was shown by Liebowitz[1-5,9] and his students that the load carrying capacity of eccentrically loaded columns, particularly those having fatigue cracks or notches with a root radius smaller than 0.003 inch, may be reduced significantly. This effect also varies significantly with the type of boundary conditions studied. The failure criterion developed is based upon the principles of fracture mechanics which are briefly described. This paper includes a summary of the work of Liebowitz[1] in the Treatise on Fracture in addition to his latest research investigations[2-5,9] concerned with notched columns.

INTRODUCTION

The effect of notches on the behavior of columns under axial compression has not received any attention until the recent work of Liebowitz and his students was published. Liebowitz et al[2-4] studied experimentally the stability and fracture of cracked columns under compression. Liebowitz and Claus[5] have subsequently analyzed the fracture of notched columns utilizing the stress intensity factor obtained from Neuber's[6] stress concentration expressions. Details of this and other work was presented by Liebowitz[1]. Okamura et al[7] calculated the deflection, load carrying capacity, stress intensity factor and fracture load of a slender and single-edge-cracked column with hinged ends under an eccentric compression. Vanderveldt and Liebowitz[8] studied the carrying capacity and fracture of glass fiber composite notched columns having pinned-ends and loaded in compression. Theoretical studies of the failure of notched columns with fixed-ends were made by Liebowitz and Claus[9]. They gave a theoretical basis for some of the experimental results obtained by Vanderveldt and Liebowitz[10] for columns with fixed-fixed ends. Liebowitz and Claus[9] work utilized a failure criterion based on the stress-intensity concept which some recent work by Liu et al[11] obtained solutions to the fixed-fixed ends for notched columns loaded eccentrically by utilizing the stress intensity solutions given by Gross and Srawley[12] and Brown and Srawley[13]. In addition

to these studies, Vanderveldt and Liebowitz[14] obtained theoretical and experimental results for fixed-pinned columns, and Cotterell[15] also determined the theoretical buckling load for a column with a single-edge-notch.

FRACTURE MECHANICS

Linear Crack Stress Field Analysis

Fracture Mechanics consists of the characterization of the crack tip stress field in terms of either the stress intensity factor, K, or the energy rate, G, and observation of crack extension behavior associated with various values of K or G. These fundamental modes of crack surface displacements are usually considered for a stationary crack and are shown in Fig. 1. For a homogeneous isotropic material containing a crack in the xz plane, their stress fields are associated with the three modes of crack surface displacements. For crack surface displacements (mode I), the stress field is symmetric with respect to the xz plane; for mode II, the stress field is "skew-symmetric" with respect to the xz plane; for mode III, crack surface displacements are due to the "anti-symmetric" stress field. Irwin[16,17] presented the analysis for the three displacement modes of crack tip stress analysis.

The following Eqs. (1) and (2) are those of Cauchy-Riemann and represent the condition that the function, $\overline{Z} = \mathrm{Re}\overline{Z} + i\,\mathrm{Im}\overline{Z}$ is analytic:

$$\frac{\partial \mathrm{Re}\overline{Z}}{\partial x} = \frac{\partial \mathrm{Im}\overline{Z}}{\partial y} = \mathrm{Re}Z \tag{1}$$

and

$$\frac{\partial \mathrm{Im}\overline{Z}}{\partial x} = -\frac{\partial \mathrm{Re}\overline{Z}}{\partial y} = \mathrm{Im}Z \tag{2}$$

Eliminating $\mathrm{Im}\bar{Z}$ and $\mathrm{Re}\bar{Z}$, by differentiating with respect to x and y, from Eqs. (1) and (2) gives

$$\left(\frac{\partial^2}{\partial x^2} + \frac{\partial^2}{\partial y^2} \right) \mathrm{Re}\bar{Z} = 0 \, . \tag{3}$$

$$\left(\frac{\partial^2}{\partial x^2} + \frac{\partial^2}{\partial y^2} \right) \mathrm{Im}\bar{Z} = 0 \, . \tag{4}$$

The above are harmonic functions as both the real and imaginary parts of the function $\bar{Z}$ satisfy Laplace's equation. Westergaard[18] introduced a stress function

$$\Phi_I = \mathrm{Re}\bar{\bar{Z}}_I + y\mathrm{Im}\bar{Z}_I \tag{5}$$

where $\bar{Z} = \frac{d\bar{\bar{Z}}}{dz}$, $Z = \frac{d\bar{Z}}{dz}$, $Z' = \frac{dZ}{dz}$ (6)

and subscript I refers to the opening mode.
Using the Airy stress function Φ where

$$\sigma_x = \frac{\partial^2 \Phi}{\partial y^2} \, , \quad \sigma_y = \frac{\partial^2 \Phi}{\partial x^2} \, , \quad \tau_{xy} = - \frac{\partial^2 \Phi}{\partial x dy} \tag{7}$$

The stress components are determined from Eqs. (1) and (2) as

$$\sigma_x = \mathrm{Re}Z_I - y\mathrm{Im}Z'_I \, , \tag{8a}$$

$$\sigma_y = \mathrm{Re}Z_I + y\mathrm{Im}Z'_I \, , \tag{8b}$$

$$\tau_{xy} = - y\mathrm{Re}Z'_I \, . \tag{8c}$$

For the problem of a crack in an infinite plate, the function Z_I is taken as

$$Z_I = \frac{g(z)}{[(z + c)(z - c)]^{1/2}} . \tag{9}$$

Substituting variables where

$$\xi = z - c \tag{10}$$

results in

$$Z_I = \frac{g(\xi + c)/(\xi + 2c)^{1/2}}{(\xi)^{1/2}} = \frac{f(\xi)}{(\xi)^{1/2}} \tag{11}$$

Therefore, near the crack tip

$$Z_I|_{\xi \to 0} = \frac{K_I}{(2\pi\xi)^{1/2}} \tag{12}$$

Using appropriate relations of polar coordinates and substituting Eq. (12) into Eq. (8) leads to the following relationships for the two dimensional stress distribution, near the leading edge of a tensile crack, as

$$\sigma_x = \frac{K_I}{(2\pi r)^{1/2}} \cos\frac{\theta}{2}\left(1 - \sin\frac{\theta}{2}\sin\frac{3\theta}{2}\right) . \tag{13a}$$

$$\sigma_y = \frac{K_I}{(2\pi r)^{1/2}} \cos\frac{\theta}{2}\left(1 + \sin\frac{\theta}{2}\sin\frac{3\theta}{2}\right) \tag{13b}$$

$$\tau_{xy} = \frac{K_I}{(2\pi r)^{1/2}} \sin\frac{\theta}{2}\cos\frac{\theta}{2}\cos\frac{3\theta}{2} \tag{13c}$$

where

$$K_I = \lim_{\xi \to 0} (2\pi\xi)^{1/2} Z_I \tag{14}$$

The stress intensity K_I could be determined for the case of an infinite plate having a crack along the x axis from x = - c to x = c by assuming the stress function

$$Z_I = \frac{\sigma z}{[(z + c)(z - c)]^{1/2}} \tag{15}$$

Substituting Eq. (15) into Eq. (14) gives

$$K_I = \lim_{\xi \to 0} (2\pi\xi)^{1/2} \left\{ \frac{\sigma(\xi + c)}{[(\xi)(\xi + 2c)]^{1/2}} \right\} \tag{16}$$

$$K_I = \sigma(\pi c)^{1/2} \tag{17}$$

Other values of stress intensity for various plates with cracks may be seen in articles by Irwin[17] and Paris and Sih[19]. Some of these values are given as

Semi-infinite plate with a through crack of length c and with σ parallel to the edge

$$K = 1.13\ \sigma(\pi c)^{1/2} \tag{18}$$

For a strip of width W with a central crack of length 2a perpendicular to a longitudinally applied stress σ

$$K = \sigma[\pi c \sec(\pi c/W)]^{1/2} \tag{19}$$

where $c \leq 0.3\ W$

For a circular (penny-shaped) crack of radius, c, in an infinite three dimensional body with uniform stress σ applied perpendicular to the crack

$$K_I = 2\sigma\ (c)^{1/2}\ (\pi)^{-1/2} \tag{20}$$

For an infinite plate with an array of colinear cracks of length 2c spaced on centers, 2a, apart with applied uniform biaxial tension σ at infinity

$$K_I = \sigma(\pi c)^{1/2} \frac{2a}{\pi c} \tan \frac{\pi c}{2a}^{1/2} \tag{21}$$

The stresses close to the leading edge of a tensile crack for modes II and III are similarly obtained as for the case of mode I.

For mode II, the stresses are

$$\sigma_x = \frac{-K_{II}}{(2\pi r)^{1/2}} \sin\frac{\theta}{2}\left(2 + \cos\frac{\theta}{2}\cos\frac{3\theta}{2}\right), \tag{22a}$$

$$\sigma_y = \frac{K_{II}}{(2\pi r)^{1/2}} \cos\frac{\theta}{2}\sin\frac{\theta}{2}\cos\frac{3\theta}{2}, \tag{22b}$$

$$\tau_{xy} = \frac{K_{II}}{(2\pi r)^{1/2}} \cos\frac{\theta}{2}\left(1 - \sin\frac{\theta}{2}\sin\frac{3\theta}{2}\right). \tag{22c}$$

For mode III, the stresses are

$$\tau_{xz} = -\frac{K_{III}}{(2\pi r)^{1/2}} \sin\frac{\theta}{2}, \tag{23a}$$

$$\tau_{yz} = \frac{K_{III}}{(2\pi r)^{1/2}} \cos\frac{\theta}{2}. \tag{23b}$$

The displacements in the x and y directions could be found for mode I by utilizing Hooke's Law, strain and displacement relationships and the stress components given in Eqs. (8) as

$$u = \frac{K_I}{\frac{E}{2(1+\nu)}} \left(\frac{r}{2\pi}\right)^{1/2} \cos\frac{\theta}{2}\left(1 - 2\nu + \sin^2\frac{\theta}{2}\right) . \tag{24}$$

$$v = \frac{K_I}{\frac{E}{2(1+\nu)}} \left(\frac{r}{2\pi}\right)^{1/2} \sin\frac{\theta}{2}\left(2 - 2\nu - \cos^2\frac{\theta}{2}\right) . \tag{25}$$

It is interesting to note that the crack tip stresses and displacements are directly proportional to a parameter K. This parameter may be related to the elastic strain energy rate with respect to crack area where

$$K^2 = GE \qquad \text{(plane stress)} \tag{26}$$

$$K^2 = GE/(1-\nu^2) \qquad \text{(plane strain)} \tag{27}$$

Irwin observed that by definition G corresponds to a generalized force in mechanics and introduced the terminology "crack extension force". Previously Griffith's theory, which permitted the development of fracture mechanics, was based upon fracture occuring when the release of elastic strain energy per increment of crack area was equal to the surface energy over the same increment of area. The condition critical for onset of rapid fracture was a point of stable balance between stress-field energy release rate and rate of plastic work near the crack to be followed by a

region of unstable rapid crack propagation. However, due to Wells' thermal measurements, there were opposite type of implications that the point of onset of rapid fracture was an abrupt instability point followed by a stable region in which the work rate and loss of stress-field energy were balanced through a considerable range of crack speeds. The instability point could be preceded by a slow region of crack extension in which the crack extension process was also stable.

Equation (27) may be determined from the following derivation:

The work done in closing up the crack in Fig. 2 is

$$\delta W = 2 \int_0^{\alpha} 1/2 \; \sigma y \; v dr \qquad (28)$$

where

$$\sigma_y = \frac{K_I}{[2\pi(\alpha-r)]^{1/2}} \quad , \qquad \theta = 0 \qquad (29)$$

$$v = K_I r^{1/2} \; 2(2/\pi)^{1/2} \; (1-\nu^2)/E \quad , \quad \theta = 0 \qquad (30)$$

Since $G\delta A = \delta W - \delta V$

$$G_I = \frac{K_I^2(1-\nu^2)}{E} \qquad \text{plane strain}$$

Similarly

$$G_I = K_I^2/E \qquad \text{plane stress}$$

the above relationships for stress intensity values are useful

in practical problems. Critical flow sizes may be determined for various structures and materials. For the plane-strain case, which results in the lowest value for stress intensity, Brown and Srawley[13] present some very useful experimental procedures to be used by the practicing engineer. Extension of the stress-intensity concept for determining the response of structural elements was developed by Liebowitz et al[1-5,9]. This paper does not treat the plasticity analysis concept for cracks since the aluminum specimens tested failed in plane strain and therefore experienced little plastic flow.

Failure and Carrying Capacity of Notched Columns

Beginning with work by Inglis[20] and [21] to the present time, a large number of studies, both theoretical and experimental, have been conducted in this area of determining the sensitivity of cracks in materials. Recently Sih and Liebowitz[22] confirmed Griffith's claim in 1924 that his original energy expression, published in 1921, is indeed erroneous. Most of these, however, have dealt with failure of precracked members in tension or in pure bending. Apparently, the effect of flaws on the buckling or critical load was not treated until recently (Liebowitz et.al[1-5]). For research on buckling of unnotched columns, see Hoff[23], Timoshenko and Gere[24], Langhaar[25], and Donnell[26].

Studies have been made by Dr. Liebowitz and his students on columns subjected simultaneously to axial compression and

bending. Experiments conducted exploit the combined effects of notch depth, root radius, column length, single and double notches, and eccentricity of loading.

The data from these experiments are compared to results obtained from similar columns without notches to determine the effects of notches on the load-carrying ability and/or the failure loads. Fatigue cracks and notches of root radii equal to 0.003 inch or smaller have a significant effect on reducing the load-carrying capacity of eccentrically loaded aluminum columns.

The analysis developed is based upon using the slender unnotched column analysis and stress intensity values obtained from appropriate stress concentration relationships developed by Neuber but where the radius of the notch approaching zero. The results presented in sharply notched components treated in this chapter may be of significance in many areas of engineering, particularly where slender columns are employed to achieve high-strength-to-weight performance. For example, the results are applicable to the aeronautical and aerospace industries, since aircraft and missiles have slender column construction in wing and fuselage sections. Flaws may develop in these structures from mechanical vibrations, aerodynamic loads, rocket fuel exhaust, leakage of rocket fuel, or acoustical fatigue.

Euler Buckling Load

The Euler buckling load P_E, for elastic unnotched columns is well known (Euler[27,28]) as

$$P_E = \nu^2 \pi^2 EI/L^2 \tag{31}$$

FIG. 3. is valid for elastic, unnotched columns with pinned ends.

Euler Critical Stress

The Euler stress corresponding to the above load is

$$\sigma_E = \nu^2 \pi^2 E/(L/R)^2 \tag{32}$$

where, in the above Eqs. (31) and (32), E is Young's modulus, I is the moment of inertia, of the section of the column about its neutral axis, L is the effective length of the column, ν is dependent upon the boundary conditions at the ends of the column and R is the radius of gyration of the section as is defined as equal to $(I/A)^{1/2}$, where A is the cross sectional area of the column. From Fig. 4, it is seen that the results of the theoretical and experimental findings for the straight columns agree quite well. Buckling tests (Figs. 5 and 6) on various lengths of columns, with and without initial eccentricities, were performed; in particular, extensive tests were conducted on 12-inch columns. It should be noted that the Euler buckling load, which is for an idealized column, may be obtained from experiments on straight columns. In order to maintain a straight column during the test with increasing load, it is necessary to adjust the column horizontally at the ends of the column so that there is no bowing effect of the column. This straightening may be achieved by adjusting the

screw in the rig, as shown in Fig. 7. Finally, a load will be reached at which it is no longer possible to straighten the column; at this time the critical load may be determined (Fig. 4).

Slender Column Analysis, Knife-Edged Column, (Based upon Neuber's Expressions)

The maximum combined stress σ_{max}, for an unnotched column loaded eccentrically (Fig. 10a), can be written as

$$\sigma_{max}\Big|_{L/2} = \mp e \frac{P}{Z} \sec\left(\frac{\pi}{2}\sqrt{P/P_E}\right) - \frac{P}{A} \qquad (33)$$

where e is the eccentricity of loading, P is the failure load, Z is the section modulus, and A is the area of the cross section. In order to determine the maximum stress at the outer fiber at b in Fig. 10a, on the compression side of the column, both minus signs should be used in Eq. (33), while the maximum stress at a will require the use of the plus sign of the first term and the minus sign of the second term of Eq. (33).

The approximate maximum stress could be determined by employing stress-concentration formulas developed by Neuber[6].

For example, he considered the effect of deep and shallow hyperbolic external notches (Fig. 10b) for cases of pure tension and bending. The maximum stress at the root of the notch may be determined for tension as

$$\sigma_{max} = \frac{P}{2ab} \frac{[(a/\rho) + 1](\sqrt{a/\rho})}{[(a/\rho) + 1] \arctan(\sqrt{a/\rho}) + (\sqrt{a/\rho})} \qquad (34)$$

where $\frac{P}{2ab}$ is the nominal stress,

and for pure bending, as

$$\sigma_{max} = \frac{2P(e + \delta)\ (a/\rho)\ (\sqrt{a/\rho})}{a^2b\ [(\sqrt{a/\rho}) + [(a/\rho) - 1]\ \text{arc tan}\ (\sqrt{a/\rho})]} \qquad (35)$$

where $\frac{2P(e+\delta)}{a^2b}$ is the nominal stress, ρ is the radius of curvature of the root of the notch and a is half the width of the net cross section at the root of the notch. Equations (34) and (35) may be combined with appropriate signs to give the resulting stress at a notch in a column subjected to an axial compressive load and a bending load. The superposition of Eqs. (34) and (35) is valied within the limits of the linear theory of elasticity.

One difficulty in using Eqs. (34) and (35) is that the dimensions of the net section area are required to obtain the maximum stress for each incremental load. Obviously, errors are introduced in using Eqs. (34) and (35) for determining the maximum stress in notched columns. Furthermore, Neuber's expression for stress concentration is not valid for fatigued crack specimens where ρ approaches zero.

It is also possible to determine the approximate stress in columns subjected to eccentric compression loads, by using the nominal stress calculated from the beam column formula in Eq. (34) and substituting this value for stress into the approximate Neuber's stress-concentration expressions, as for example

those given in Eqs. (34) and (35). Therefore, the maximum stress of the notched column is

$$\sigma_{max} = e\frac{P}{Z}\sec\left(\frac{\pi}{2}\sqrt{\frac{P}{P_E}}\right)\frac{4\frac{a}{\rho}\sqrt{\frac{a}{\rho}}}{3\left[\sqrt{\frac{a}{\rho}} + \left(\frac{a}{\rho} - 1\right)\arctan\sqrt{\frac{a}{\rho}}\right]} - \frac{P}{A}\frac{2\left(\frac{a}{\rho} + 1\right)\sqrt{\frac{a}{\rho}}}{\left(\frac{a}{\rho} + 1\right)\arctan\sqrt{\frac{a}{\rho}} + \sqrt{\frac{a}{\rho}}} \tag{36}$$

It should be noted that Eq. (36) is similar to the algebraic difference of Eqs. (34) and (35), except for the values of the nominal stresses.

For a double notched member under tension, the stress concentration is given in Eq. (34). The stress-intensity factor is defined by

$$K = \lim_{\rho \to 0} \frac{\sigma_{max}(\pi\rho)^{1/2}}{2} \tag{37}$$

After substituting Eq. (34) into Eq. (37) and allowing the notch radius to go to zero, the stress-intensity expression becomes

$$K_T = \frac{P}{b}(a\pi)^{-1/2} \tag{38}$$

For a double notched member under pure bending, the stress concentration is given in Eq. (35). Again, the stress-intensity factor is defined by Eq. (38). After combining Eqs. (35) and

(37) and allowing the notch radius to go to zero, the stress-intensity expression of bending becomes

$$K_B = \frac{2M}{(a)^{3/2} b\pi^{1/2}} \tag{39}$$

For columns subjected to axial compressive loading and bending moments, it may be assumed that the stress-intensity expression then can be obtained from superposition and written as

$$K = -K_T \pm K_B \tag{40}$$

The point of interest in this case is the root of the opening crack; therefore, the positive value of K_B is taken, and the final expression becomes

$$K = \frac{P}{b(a\pi)^{1/2}} \left[\frac{2(e + \delta)}{a} - 1 \right] \tag{41}$$

Neuber's stress-concentration equations for members with double (shallow) notches under tensile loads and in pure bending are, respectively,

$$\frac{\sigma_{max}}{P/2ab} = 3 (c/2\rho)^{1/2} - 1 + \frac{4}{2 + (c/2\rho)^{1/2}} \tag{42}$$

and

$$\frac{\sigma_{max}}{3M/(2a)^2 b} = 3 (c/2\rho)^{1/2} - 1 + \frac{4}{2 + (c/2\rho)^{1/2}} \tag{43}$$

By a development similar to that used for deep notches, the final expression for the stress intensity, where shallow notches are present, becomes

$$K = \frac{3P}{4ab} (\pi c)^{1/2} \left[\frac{6 (e + \delta)}{a} - 1 \right] \tag{44}$$

The slender column analysis utilizes the analytical expression for the stress at the midpoint of the column subjected to a concentrated force loaded eccentrically. Of course, the horizontal deflection δ could also have been derived theoretically and then used in Eq. (41), but there was some interest in determining the stress-intensity factor by using long slender column specimens; there is some novelty in using these specimens since deflection measurements are utilized, while conventional tests usually require compliance and other type measurements.

As in the above methods, the approximate stress in a column subjected to axial compression and bending, within the linear range, is equal to the sum of the stresses due to compression and the stresses due to bending. Consequently, using Eqs. (34) and (35) and the stress-intensity relationships for the sharp crack (Eqs. (38) and (39) results in the following:

$$K = K_{TOT} = K_B + K_C = \frac{4}{3} (a/\pi)^{1/2} \sigma_{NB} - 2(a/\pi)^{1/2} \sigma_{NT} \tag{45}$$

where K_{TOT} is the total stress-intensity factor, K_B is the stress intensity for bending, K_C is the stress intensity for compression

which is equal to $-K_T$ (stress intensity for tension), σ_{NB} is the nominal bending stress at one-half the length of the column, and σ_{NT} is the nominal tensile stress at one-half the length of the column. Therefore, by using Eq. (33) and $\sigma_{NT} = P/A$, the total stress intensity becomes

$$K = \left(\frac{4}{3}\sqrt{\frac{a}{\pi}}\right) \frac{Pe}{(I/d)\cos\left(\frac{kL}{2}\right)} - 2\sqrt{\frac{a}{\pi}}\,\frac{P}{A} \qquad (46)$$

Since $d = a$, $A = 2ab$ and $I = \frac{1}{12}(b)(2a)^3$, the total stress-intensity factor becomes

$$K = K_{TOT} = \frac{4}{3}\sqrt{\frac{a}{\pi}}\,\frac{Pea}{(2ba^3/3)} \cdot \frac{1}{\cos\left(\frac{kL}{2}\right)} - 2\sqrt{\frac{a}{\pi}} \cdot \frac{P}{2ab} \qquad (47)$$

Rearranging terms gives the following for the stress intensity:

$$K = \frac{2Pe}{b\sqrt{\pi}} \cdot \frac{1}{a^{3/2}} \cdot \frac{1}{\cos\left(\frac{kL}{2}\right)} - \frac{P}{\sqrt{\pi}\,a^{1/2}\,b} \qquad (48)$$

$$K = \frac{P}{(\pi a)^{1/2}\,b}\left[\frac{2e}{a}\sec\left(\frac{kL}{2}\right) - 1\right] \qquad (49)$$

where

$$k^2 = P/EI \qquad (49a)$$

The stress-intensity value in Eq. (47) may also be expressed as a function of the Euler load, P_E.

Since

$$\frac{kL}{2} = \frac{L}{2}\,(P/EI)^{1/2} \tag{50}$$

and

$$EI = P_E L^2/\pi^2 \tag{51}$$

the following is obtained for

$$\frac{kL}{2} = \frac{\pi}{2}\,(P/P_E)^{1/2} \tag{52}$$

Using Eqs. (49), (50), and (52), the stress intensity becomes

$$K = \frac{P}{(\pi a)^{1/2} b}\left[\frac{2e}{a\cos\left(\frac{\pi}{2}\sqrt{P/P_E}\right)} - 1\right] \tag{53}$$

or

$$K = \frac{P}{(\pi a)^{1/2} b}\left[\frac{2e}{a}\sec\left(\frac{\pi}{a}\sqrt{P/P_E}\right) - 1\right] \tag{54}$$

For some of the calculations and tests performed by Liebowitz et al[1-5,9], the following values were used:

$K = 38{,}000$ lb-inch$^{-3/2}$, b=h=0.5 inch and $P_E = 2930$ lb.

Therefore, the stress intensity, for these particular tests, is

$$K = 38{,}000 = (1.13)\,\frac{P}{\sqrt{a}}\left[\frac{2e}{a\cos\,(0.029\sqrt{P})} - 1\right] \tag{55}$$

Equation (55) appears to be sensitive in determining, by trial-and-error process, the maximum load P.

Equations (53) and (54) are very useful in obtaining the maximum load-carrying capacity that a notched column can withstand when subjected to a load applied eccentrically. Table I indicates the experimental values obtained by Liebowitz et al for the maximum load on a knife-edged column and also the values obtained by using Eq. (55). It is interesting to note that, for crack lengths from 0.02 inch to about 0.15 inch, the prediction of the maximum load from Eq. (55) is quite good while, for larger values of crack length, the results are not as favorable.

In determining the load from Eq. (55), a value of $K = 38{,}000$ lb-inch$^{-3/2}$ was used. Undoubtedly, there is some error in using this value. In a recent report by Davis et al, the stress-intensity value varied from $K = 22{,}000$ to $K = 35{,}000$ and was a function of the type of test and direction of the sample material studied. Some investigators have been using a value of $K = 32{,}000$. The new test procedures recommended by Brown and Srawley[13] should lead to more consistent results for determining the stress intensity. These test procedures could also be applied to the specimens investigated by Liebowitz et al[1-5] and Liebowitz and Claus[5,9]. The slender column engineering analysis may also be used in determining the stress-intensity values.

Discussion of Experimental and Theoretical Results for Critical Load of Knife-Edged Columns

Tests were conducted on columns having lengths of 6, 9, 12, 15, 18, 24, and 30 inches. The majority of the tests were performed on columns 12 inches long, but an adequate number of other lengths were also studied.

The results for unnotched columns subjected to a concentric axial load are shown in Fig. 3. In these tests, with the eccentricity equal to zero, the columns were continually adjusted, during the loading, to insure straightness. The required adjustments were always very small. Some tests were also conducted using double notched columns. For the case of zero eccentricity, no appreciable difference for the Euler buckling load was observed for notched and unnotched columns. This result is apparently correct, since the column is subjected solely to an axial load and not permitted to bend. Consequently, the cracks close under compressive load and have virtually no effect on straight columns which are made to remain straight until buckling. A series of tests was also run on 12-inch-long unnotched columns at various eccentricities of loading. In these tests, the columns were loaded well beyond the inflection point on the load deflection curve.

The same eccentricities were used for the unnotched and notched columns. The depth of notch (or crack) was varied. The deflection in the horizontal direction was measured at approximately the center of the column. Load deflection curves

obtained for various crack depths are shown in Figs. 11 and 12. Although experiments were conducted on columns with one and two notches, Figs. 11 and 12 show only the results of columns with a single notch; the results for the double notch are discussed later. The notch was on the side of the column farthest from the axis of the applied load.

The failure load was measured using seven crack depths at five eccentricities. A comparison between the response of the notched bars at various eccentricities with those of the unnotched bars is tabulated in Figs. 11 and 12. The comparison shows that a fatigue crack in a column under axial load reduces its load-carrying ability. The load-carrying capacity of the column is further reduced as the depth of the crack is increased. Furthermore, increasing the eccentricity of the applied load decreases the load-carrying ability. Finally, it appears that the horizontal deflection is approximately constant for a given crack depth. This can be seen from Fig. 13, where failure load has been plotted versus the corresponding maximum horizontal deflection. The largest decrease in load-carrying ability from the notched to the unnotched column was 55%, which occurred for a notch depth of 0.195 inch and an eccentricity of 1.250 inches. The failure loads were plotted versus the notch depths at various eccentricities (Fig. 14). The values presented at zero notch depth are the maximum loads obtained for the tests on the unnotched columns for the eccentricities indicated.

The effect of the root radius of the crack was also studied (Fig. 15). The majority of the results were obtained using a

notch with a fatigue crack extension. In Fig. 15, results have also been given for 0.003-inch and 0.0625-inch root radii; the large root radius resulted in higher failure loads than those for small root radius for the tests conducted in this research. No appreciable difference was found between the fatigue crack and the 0.003-inch-radius crack. However, the 0.0625-inch root radius appears to have no effect on preventing the load from reaching a maximum value before failure, because the corresponding load deflection curves have approximately zero slope at failure.

The results of the effect of putting a notch on both sides of the column are shown in Fig. 16. Note that the total notch depth for the double V-notch indicated in the table on this figure is equal to the sum of the length of the crack on each side of the column. These tests indicate that a double notch is less disastrous than a single notch with a crack depth equal to the total crack depth of the double notch. Symmetry appears to be maintained for a double notch but is not maintained for a single notch.

The results of a series of tests on the effects of slenderness ratio, depth of notch, and eccentricity on the maximum load-carrying capacity of the column are shown in Figs. 17 and 18. Two eccentricities were considered, namely, 1.000 inch in Fig. 17 and 0.090 inch in Fig. 18. A variety of notches were considered, namely, a single 0.110-inch-deep notch and double notches 0.020 and 0.110 inch deep. From Figs. 18 and 19, it

appears that the load-carrying ability of 7075-T6511 aluminum columns having slenderness ratios larger than 250, and for eccentricities of 0.090 and 1.000 inch, is not noticeably affected by notches. However, as the slenderness ratio decreases from a value of 250, the effect of notches on the load-carrying capacity of the column increases. For small slenderness ratios, the weakening effect of the notches is most pronounced, especially for the 1.000-inch eccentricity.

To determine whether a preferred orientation caused by manufacturing processes existed in the rolled bar, four columns taken from the same bar were tested. A single identical notch was put into each of these columns but placed on their four different sides for the four tests. Differences in the load-carrying capacity and transverse deflection were less than the experimental accuracy.

Slender Column Analysis, Knife-Edges (Based Upon Stress Intensity Factors)

As shown in Fig. 19 from Okamura et al, the lateral deflection at the mid-section, δ, increases slowly with the load at first, then rapidly after the applied compression passes a certain value. As both the deflection and the compression increase, the applied bending moment at the cracked-section increases rapidly. This bending induces tensile mode, i.e. mode I, crack tip stress field. If the material is brittle, the column may fracture before the load carrying capacity is reached.

It has been substantiated that when the stress intensity factor at a crack tip reaches the fracture toughness of a brittle material, the cracked member fractures.

The stress intensity factor of a beam under bending is given by Gross and Srawley as

$$\frac{K_B bh^2}{6Mc^{1/2}} = Y_B = 1.99 - 2.47\left(\frac{c}{h}\right) + 12.97\left(\frac{c}{h}\right)^2 - 23.17\left(\frac{c}{h}\right)^3 + 24.80\left(\frac{c}{h}\right)^4 \tag{56}$$

The moment, M, at the cracked section of the column is

$$M = Pe\left(\frac{\delta}{e} + 1\right) \tag{57}$$

Since

$$\frac{\delta}{e} = \frac{1 - \frac{h}{6e}\beta\lambda L \sin \lambda L}{\cos \lambda L - \beta\lambda L \sin \lambda L} - 1 \quad , \tag{58}$$

the moment at the mid-section is

$$M = \frac{Pe\left(1 - \frac{h}{6e}\beta\lambda L \sin \lambda L\right)}{\cos \lambda L - \beta\lambda L \sin \lambda L} \tag{59}$$

Substituting into and rearranging

$$\frac{(1-\nu^2)\ K_B^{\ 2}}{E} = \frac{M}{2B}\frac{dC}{dc} \quad , \tag{60}$$

results in

$$\frac{K_B}{Eh^{1/2}} = \frac{1}{2}\left(\frac{h}{L}\right)^2 \frac{e}{h}\lambda^2 L^2 \left[\frac{1 - \frac{he}{6e}\beta\lambda L \sin \lambda L}{\cos \lambda L - \beta\lambda L \sin \lambda L}\right]\left(\frac{c}{h}\right)^{1/2} Y_B \tag{61}$$

When the quantity $(h/6e)\ \beta\lambda L \sin \lambda L$ is negligible, Eq. (61) can be rearranged as

$$\frac{K_B h^{1/2}}{6e} = \frac{1}{2}\left(\frac{h}{L}\right)^2 \frac{\lambda^2 L^2}{\cos \lambda L - \beta\lambda L \sin \lambda L} \left(\frac{c}{h}\right)^{1/2} Y_B \qquad (62)$$

According to Eq. (60), the stress intensity factor of a single-edge cracked column under an eccentric compression is related to five dimensionless parameters. The parameter, $\lambda L = (P/EI)^{1/2} L$ is the usual column parameter which compares the rigidity of the column to the load. The parameter $\beta = EI/2kL$ contains the effect of a crack. It compares the flexural rigidity of a cracked column with that of an uncracked one.

The function $\{(c/h)^{1/2} Y_B(c/h)\}$ is plotted against c/h in Fig. 20. With Eqs. (61) or (62), the critical bending stress intensity factor at fracture, K_B, of a cracked column, can be calculated. However, the net stress intensity factor at the crack tip is reduced by the compression. Therefore the fracture toughness, K_{TOT}, of the column is

$$K_{TOT} = K_B - K_T \qquad (63)$$

where K_T is the stress intensity factor at fracture due to the axial compression. K_T can be calculated from

$$\frac{K_T bh}{P_c^{1/2}} = Y_T = 1.99 - 0.41\left(\frac{c}{h}\right) + 18.70\left(\frac{c}{h}\right)^2 - 38.48\left(\frac{c}{h}\right)^3 + 53.85\left(\frac{c}{h}\right)^4 \qquad (64)$$

If eccentricity is large, bending is dominant, then K_T can be neglected.

It is appropriate to point out that the fracture mechanics is applicable only if fracture is rather "brittle". The important requirement for brittle fracture is that the specimen size is sufficiently large relative to the plastic zone size at fracture.

Figures 21 and 22 show the comparison of the calculated deflection with the deflection measured by Liebowitz et al[2]. The solid curves are calculated and the dashed ones are measured. A value of 10.5×10^6 psi is used for E, and 13.25" for 2L. Consider the simple-minded model used for the calculation, the agreement between the calculated and the measured values are very good. The maximum deviation is approximately 5% in load.

In Fig. 23, the ratio of the load carrying capacity of a cracked column and the buckling load of an uncracked column (P_{cr}/P_o) is plotted against ($\frac{c}{h}$) for six values of $(1-\nu^2)\frac{h}{L}$ such as: 0.01, 0.02, 0.04, 0.1, 0.2, and 0.4. The figure shows that a crack does reduce the load carrying capacity of a column. However the effect of a crack decreases with both $\frac{c}{h}$ and $\frac{h}{L}$. For a very slender column or a column with a small crack, the critical load of the column is not affected much by the crack. For a column with a crack 0.6h long and the column having a value of 0.01 for $(1-\nu^2)\frac{h}{L}$ the load carrying capacity is reduced only 11% from that of an uncracked column. The value of 0.01 for $(1-\nu^2)\frac{h}{L}$ corresponds to a slenderness ratio of 620. For a crack length c = 0.2h, the load carrying capacity is reduced only 8% for $(1-\nu^2)\frac{h}{L} = 0.20$,

which corresponds to a slenderness ratio of 31. For longer crack and shorter column, the load carrying capacity decreases rapidly. Liebowitz et al[2] measured the load carrying capacities of concentrically loaded single edge cracked columns of 12" long with various notch depths. For notch depth ratios (c/h) of 0.18, 0.34, and 0.39, the calculated ratios of P_{cr}/P_o are 0.98, 0.91 and 0.88 respectively. The reduction in load carrying capacity is not appreciable.

Eccentricity has an effect on the load carrying capacity of a cracked column, which has been discussed earlier in the paper. The above discussion is valid only for an elastic cracked column which can sustain a large deflection. Often the tensile crack tip stress field causes fracture before reaching the load carrying capacity given by

$$\beta\lambda L \tan \lambda L = 1 \tag{65}$$

and

$$\frac{1}{3(1-\nu^2)\frac{h}{L} F(\frac{c}{h})} = \lambda L \tan \lambda L \ . \tag{66}$$

A similar approach to this problem using the stress intensity expressions was also made by Cotterell[15].

Slender Column Analysis, Fixed-Fixed Edges (Based upon Neuber's Expressions)

The procedure followed is an extension of the criterion developed for the knife-edged column which was based on the

stress-intensity (K) factor concept. The K factor concept. The K factor was defined in Eq. (37).

Using Neuber's results for stress distributions in hyperbolic notches, a combined K factor accounting for both bending and compressive stresses was derived by Liebowitz and Claus[5] in Eq. (47). The K factor is valid for double, symmetric hyperbolic notches with a throat width of 2a.

Since the nominal stresses are functions of the applied load P and K is a material property, Eq. (37) is interpreted as a failure criterion giving the maximum carrying load. Furthermore, the boundary conditions of the column are taken into account through the selection of the nominal stresses.

It is known that if a perfectly concentric load were applied to a perfectly straight column, buckling, not bending, would occur. To take into account the observed bending, an equivalent initial crookedness of the column

$$y_o(x) = \delta \sin \frac{\pi x}{L} \tag{67}$$

is assumed. Using standard, classical techniques the bending stress at the middle and at the outer fiber of a fixed-end column of width 2a under an axial load P is

$$\sigma_b = \frac{P\,a}{I(1-\alpha)} \left[1 - \frac{\pi\alpha}{2u \sin u} \right] \tag{68}$$

where

$$\alpha = PL^2/(\pi^2 EI) \quad \Big| \quad u = (L/2)(P/EI)^{1/2} \quad \Big| \quad P_{cr} = 4\pi^2 EIL^{-2}$$

$$\alpha = 4P/P_{cr} \quad \Big| \quad u = (P/P_{cr})^{1/2} \quad \Big|$$

This stress is taken as the nominal bending stress in Eq. (37). The nominal compressive stress is taken to be $-P(2ah)^{-1}$. Here b is the thickness of the bar.

Substituting the nominal bending stress Eq. (68) and the nominal compressive stress into Eq. (45) allows rewriting the K factor as

$$K = A\left[1 - \frac{2(P/P_{cr})^{1/2}}{\sin\left[\pi(P/P_{cr})^{1/2}\right]}\right] - P(\pi a)^{-1/2}b^{-1}$$

$$A = 2P\,\delta\pi^{-1/2}b^{-1}a^{-3/2}\left[1 - 4(P/P_{cr})\right]^{-1} \qquad (69)$$

This relation is regarded as a failure criterion for the notched columns with fixed-ends. K is an experimentally determined material property so that Eq. (69) can be solved numerically for the failure load P. Of course Eq. (69) is valid only for $P<P_{cr}$.

Several comments are in order regarding Eq. (69). First, the moment of inertia in the bending stress Eq. (68) was taken to be the reduced cross-sectional moment since the nominal stress at the notch root was the nominal stress desired. Second, it was found experimentally that the notch did not affect the buckling (P_{cr}) load of the straightened column. Hence P_{cr} was calculated using the full cross-section.

Comparison of Theoretical Results with Those From Experiments on Fixed-Fixed Edged Columns

The failure criterion Eq. (69) was solved numerically for the failure load P for columns of various lengths with notches of various depths. The calculated failure loads were then compared with the experimental results reported[10]. A summary of these results is presented in Figs. 24-36. In Figs. 24-27 the maximum load is plotted against total notch depth for columns 10.25, 16.25, 22.25, and 28.25 inches long. Experimental points are shown for both single and double notches for comparison. Although the single notch data seem to agree well with the calculated values of the maximum load, remember that the assumptions used in deriving the failure criterion restrict the validity of that criterion to the symmetric, double notch case. It is simply noted that the same criterion appears to be successful in the asymmetric, single notch case also. Further research needs to be done to clarify this point.

In Figs. 28-36 the maximum load is plotted against column length for various notch depths. Calculations were done using notch depths from 0.020 inches to 0.230 inches. It is seen from these figures that agreement between calculated and measured maximum loads is acceptably good. An initial eccentricity of 0.1 inches gives good agreement with experimental results.

Slender Column Analysis, Fixed-Fixed Edges (Based upon Stress intensity approach)

From Liu et al[11], the total deflection, δ, at the mid-section is given as

$$\frac{\delta}{\delta_o} = \left\{ \frac{\pi}{\pi^2-(2\lambda L)^2} \left[\pi \sin \lambda L + 2\lambda L (\cos \lambda L - 1) + \right.\right.$$

$$\left. + \beta\lambda L(\pi - 2\lambda L \sin \lambda L) \right] +$$

$$\left. + \beta\lambda L \frac{h}{6\delta_o} (\cos \lambda L - 1) \right\} / (\sin \lambda L + \beta\lambda L \cos \lambda L). \quad (70)$$

The bending moment at the cracked section causes a positive tensile mode crack tip stress field, and the positive mode I stress field is reduced by the compression. The stress intensity factors, K_B and K_T, of a cracked beam under pure bending and of a single edge notched plate under tension were calculated by Gross and Srawley[12] and are given in Eqs. (61) and (64).

The bending moment at the cracked section is

$$M = P\delta + M_o$$

$$= \frac{P\delta_o \left[\frac{\pi}{\pi^2-(2\lambda L)^2} (\pi \sin \lambda L - 2\lambda L) + \beta\lambda L \frac{h}{6\delta_o} \cos \lambda L \right]}{(\sin \lambda L + \beta\lambda L \cos \lambda L)} \quad (71)$$

Substituting into Eq. (61) and rearranging the equation, one

obtains

$$\frac{K_B}{Eh^{1/2}} = \frac{1}{12}\left(\frac{h}{L}\right)^2\left(\frac{c}{h}\right)^{1/2} Y_B \left[\frac{(\lambda L)^2}{(\sin \lambda L + \beta\lambda L \cos \lambda L)}\right]$$

$$x\left[\frac{\pi}{\pi^2-(2\lambda L)^2}(\pi \sin \lambda L - 2\lambda L)\frac{6\delta_o}{h} + \beta\lambda L \cos \lambda L\right] \quad (72)$$

The net stress intensity factor of the column is the difference between those of bending and compression

$$K_{TOT} = K_B - K_T$$

$$= K_B \left[1 - \frac{1}{\delta + \frac{M_o}{P}} \frac{h}{6}\frac{Y_T}{Y_B}\right] \quad (73)$$

The functions $(c/h)^{1/2} Y_B$ and Y_T/Y_B are plotted vs. (c/h) in Figs. (40) and (41).

In Fig. (41) a sample calculation for both K_{TOT} and K_B is plotted vs. $(\lambda L)^2$ with δ_o/h as parameter. The dashed lines are for K_B and the solid lines are for K_{TOT}. At low load levels, and at low values of δ_o/h, the difference between K_B and K_{TOT} is considerable. This indicates that the compressive stress intensity factor is significant. As the load or δ_o increases, the bending stress intensity factor becomes dominant, and the compressive stress intensity factor becomes neglible.

When the bending moment at the mid-section is below Ph/6, the crack is closed. Therefore the crack does not have any effect on the compliance of the column. As the moment increases

beyond Ph/6, the crack begins to open. In this study the compliance is assumed to increase to the full value of a cracked column, when the moment is larger than Ph/6. But the crack is not fully open until $K_B > K_T$. When this condition is written in terms of the moment at the mid-section, it becomes

$$M = P\delta + M_o > \frac{Ph}{6} \frac{Y_T}{Y_B} \tag{74}$$

The actual variation of the compliance with moment in the region $Ph/6 < M < (Ph/6)(Y_T/Y_B)$ is not known, and it is shown schematically by the dashed line in Fig. (40).

The effect of the crack on the load carrying capacity decreases with h/L. This is also shown in Fig. (41).

Comparison of Theoretical and Experimental Results for Fixed-Fixed Edged Columns

In Fig. (41), the ratio P_{cr}/P_o is plotted vs. the ratio (c/h), with the quantity $(1-\nu^2)$ h/L as parameter.

In Fig. (42), the ratio P_{cr}/P_o is plotted vs. "c" for a set of columns of a square cross section 1/2" x 1/2" and various column lengths, 2L = 10.25", 16.25", 22.25", and 28.25". The columns were made of 7075-T6511 aluminum with single edge notches at the mid-section. In this figure, Euler loads are indicated. The open points are the measured points to be compared with the calculated dashed lines, and solid points correspond to solid lines. The calculated load carrying capacities

are higher than the measured ones. The maximum loads of these columns could have been limited by fracture.

Slender Column Analysis, One End Fixed and One End Pinned (Based on a Stress Intensity and Limit Analysis Approval)

In order to find a theoretical solution which would predict the load carrying capacity of the notched column with fixed-pinned ends and loaded eccentrically in compression, several theoretical analyses have been considered. None of the solutions were found to be completely acceptable, although the stress intensity and the limit analysis approach provided adequate solutions for small notch depths. These approaches are indicated below with a comment on their applicability.

Stress-Intensity Analysis

In this analysis the same procedure is used as that given by Liebowitz and Claus[5] excepting that the transverse columns deflection y(x) is for the column shown in Fig. 10. This transverse deflection of the fixed-pinned column with an eccentrically applied load, P, is given by

$$y(x) = e\left(\frac{\cos kL + kL \sin kL - 1}{\sin kL - kL \cos kL}\right) \sin kx - \cos kx + 1$$

$$-\left[k \sin kL + k \cos kL \left(\frac{\cos kL + kL \sin kL - 1}{\sin kL - kL \cos kL}\right)\right]x \qquad (75)$$

where e is the eccentricity of the load application, L is the length of the column, x is the distance from the pinned end to the notch

$$k = \left(\frac{P}{EI}\right)^{1/2} \qquad (76)$$

where E is Young's modulus and I the moment of inertia of the cross-section. The combined stress intensity factor, K, is given by Eq. (43).

Limit Analysis

Using limit analysis, the unnotched column with one end fixed and one end pinned with an eccentrally applied compressive load has been studied by Vanderveldt et al[30], and satisfactory results were obtained. Consequently, it was felt that the same analysis should be applied to the notched column.

The bending moment, M, at the notch is given by

$$M = P\ [y(x) + e] \tag{77}$$

where y(x) is found from Eq. (75).

The moment of inertia, I, used in the determination of y(x) is based on the unnotched cross-section of the column. The use of this moment of inertia is based on experimental observation, since it was noted that on plotting the curve of the load, P, versus the transverse deflection of the column y(x), the slope of the experimental curve, (P/y(x)) did not vary appreciably with large notch depths from that of the unnotched column. If, however, the net cross-section was considered for the computation of y(x), the theoretical slope (P/y(x)), did vary appreciably with increasing notch depths.

The axial force in the column is given by

$$N = -P \tag{78}$$

In the present analysis the column is rectangular with dimensions of 2a for the net width of the column at the notch and b for the depth of the column. Denoting the yield stress of the material by σ_o, two extreme cases of plastic behavior are worth mentioning. The first of these is the case of pure bending and is given by

$$M_o = \sigma_o \, ba^2 \tag{79}$$

the second case is that of axial yield and is given by

$$N_o = 2\sigma_o \, ba \tag{80}$$

where the net cross-section at the notch has been used to determine the yielding of the cross-section. Combining Eqs. (77) - (80) the following dimensionless variables may be defined

$$\begin{aligned} m &= \frac{M}{M_o} \\ n &= \frac{N}{N_o} \end{aligned} \tag{81}$$

For this problem the relationship between m and n is defined by

$$m = n^2 - 1 \tag{82}$$

and is shown in section CD in Fig. (43). The sign convention is the same as that used by Vanderveldt et al. From Eqs. (77)-(81) m may be determined in terms of n, i.e.

$$m = \frac{-2n}{a} \left[y(x) + e \right] \tag{83}$$

where x is taken as the distance from the pinned end of the column to the notch. Finally, substituting Eq. (83) into Eq. (82) to eliminate m, then solving for n and equating the resulting equation to Eq. (81) results in

$$\frac{-P}{\sigma_o b 2a} = \frac{-1}{a}\,[y(x) + e] - \sqrt{\frac{1}{a^2}\,[y(x) + e]^2 + 1} \qquad (84)$$

Equation (84) may be solved for the maximum load carrying capacity, P, of the notched fixed-pinned column having a compressive loading applied eccentrically.

Comparison of Theoretical and Experimental Results for the Fixed-Pinned Edged Columns

The agreement between experimental results and the theoretical results found from Eq. (84) above was useful for very small notch depths ($a/h \leq 0.1$). It must be pointed out, however, that the notches were not put into the columns at the point of maximum transverse displacement of the column. Rather, the notches were located approximately halfway between the pinned and fixed end of the column. Consequently the maximum carrying capacity of the column was not decreased appreciably by the notches, but was closely related to the maximum carrying capacity of the unnotched column. For very deep notches, the effect of the notches becomes more dominant and, therefore, will affect the maximum carrying capacity of the column. It should be recognized that the discrepancy between the theoretical and

experimental results for large notch depths may be due in part to the approach of using the deflections from the elastic solution and then using these deflections in the limit analysis solution in which a fully plastic condition was assumed.

The dimensionless load carrying capacity of the columns is P_M/P_B. P_M is the maximum experimental load carrying capacity of the column with a certain notch depth and loaded at a certain eccentricity. P_B is the experimentally determined maximum load carrying capacity of the concentrically loaded column buckling load with one end fixed and the other end pinned for the lengths of 11.75 in. and 29.75 in.

Figure 44 shows P_M/P_B versus c/h for the double notched column for an effective length of L = 11.75 in. From Fig. 44 it is evident that the maximum load carrying capacity of the fixed-pinned column is decreased due to the presence of the notches. Considering the effect of the dimensionless eccentricity, e/h, the effect of the notches becomes less dominant as e/h increases. This would appear to suggest that an eccentrically applied load to a fixed-pinned column decreases the effect of the notches. However in observing the unnotched columns, c/h = 0, the eccentricity, e, causes a 51% loss of maximum load carrying capacity for e/h = 1.0 and a 67% loss when e/h = 2.0, whereas for concentric loading, e/h = 0, the notch depth, c, may equal approximately 27% of the gross-cross section before causing a noticable loss in load carrying capacity of a double notched column. Similarly for e/h = 1.0, the total notch depth may be equal to about 40% and for e/h = 2.0, the

total notch depth may also be about 40% of the gross cross-section before causing an appreciable loss in maximum load carrying capacity of the columns.

The results shown in Fig. 45 are for the fixed-pinned column with a single notch of depth, c, and put in on the opening side of the column. The column has an effective length of L = 11.75 in. The notch is at the same distance from the pinned end as the notches were in the case of the double notched column. Except for e/h = 0, it appears that the maximum load carrying capacity of the column is not affected by the presence of the notch, until the notch depth exceeds 40% for e/h = 1.0 and e/h = 2.0. Since the magnitude of the maximum load carrying capacity does not appear to differ for the single notched column from that of the double notched column, it seems that the percentage of the gross cross-section that has been notched determines the loss of maximum load carrying capacity, if any, for the eccentricities e/h = 1.0 and 2.0.

In comparing the maximum load carrying capacity of the double notched column with that of the single notched column, shown in Figs. 44 and 45, respectively, it appears that a single notch in a column causes a larger loss of maximum load carrying capacity than a double notch in a column, as long as the same net cross-section at the notch exists. It must be pointed out that this increased loss of maximum load carrying capacity is particularly evident for e/h = 0 and does not become evident for e/h = 1.0 and 3/h = 2.0 until the total notch depth

has exceeded the "critical notch depth" of 40%. "Critical notch depth" is defined as that percentage of the cross-section which may be notched without causing a significant decrease in the maximum load carrying capacity of the column and with the notch located at L'/2.

Figures 46 and 47 show the maximum load carrying capacity of double and single notched columns respectively for fixed-pinned columns loaded in compression for the columns having an effective length of L = 29.75 in. It is evident that the effect of the eccentricity is considerably less than it was for the columns with length L = 11.75 in. For unnotched columns of L = 29.75 in. the effect of the eccentricity is as follows; for e/h = 1.0 the load carrying capacity decreases approximately 15% from that of the concentrically loaded unnotched column and for e/h = 2.0 the decrease is about 25% from the concentrically loaded unnotched column.

From Fig. 46, for the double notched column with L = 29.75 in. the "critical notch depth" appears to be less than 40% for the eccentrically loaded column where e/h = 1.0 or e/h = 2.0. However, for the column length of L = 29.75 in. the "critical notch depth" for e/h = 0 is larger than it was for the corresponding case with L = 11.75 in. The single notched column shown in Fig. 47 shows a "critical notch depth" less than for the single notched column shown in Fig. 45, for the case of eccentrically applied loading to the column. The concentrically loaded column e/h = 0 in Fig. 47 does not appear to show any "critical notch depth". The load carrying capacity decreases as the notch depth

increases, which is also the case for the concentrically loaded column with a length L = 11.75 in. as shown in Fig. 45.

From Figs. 48 and 49, it is clear that the effect of the notches on the maximum load carrying capacity decreases as the slenderness ratio of the columns increases. Furthermore the maximum load carrying capacity of the concentrically loaded notched columns does not show a large variation (maximum of 8%) in the load carrying capacity of the column as the slenderness ratios increases for the columns considered here. The eccentrically loaded notched columns however, shown in Figs. 48 and 49, do show a considera e change of the maximum load carrying capacity of the columns for the slenderness ratios considered here. For the double notch column results shown in Fig. 48, the maximum load carrying capacity of the notched (c' = 0.110 in.) column increases 34% for e/h = 1.0 and 37% for e/h = 2.0 as the slenderness ratio increases from L/ρ = 81 to L/ρ = 206. Similarly for the single notched (c = 0.110 in.) column, the maximum load carrying capacity of the column increases 37% for e/h = 1.0 and 42% for e/h = 2.0 as the slenderness ratio increases from 81 to 206 and as indicated in Fig. 49.

Finally, it is significant to point out that the results shown in Figs. 48 and 49 for the maximum load carrying capacity of the double and single notched column respectively show only a maximum difference of about 6% at L/ρ = 164 for e/h = 1.0 and a maximum difference of about 5% at L/ρ = 206 for e/h = 2.0, although the total notch depth, a, of the double notched column is twice the total notch depth of the single notched column.

This relatively small difference appears to indicate only a minor effect due to the notch on the closing (compression) side of the double notched column. In combination with the results found in Figs. 44-47, i.e. no decrease in maximum load carrying capacity as the notch depth increases, it appears that the total effect of the notches is insignificant for the columns considered in the present study. It appears that the maximum load carrying capacity is determined by the unnotched section of the column at the point where the maximum transverse displacement (at the highest stress level) of the column occurs.

The comparison of the maximum load carrying capacity of the columns with differing ends has been shown in Figs. 50 and 51 for the case with an effective length of the fixed-pinned columns equal to 29.75 in. Both the columns with the double notch (Fig. 50) and the single notch (Fig. 51) indicate that the notch in the fixed-pinned column causes the least loss of relative load carrying capacity of columns.

CONCLUDING REMARKS

For the aluminum 7075-T6511 columns considered, the following conclusions may be drawn:

1. Presence of a fatigue crack in a column reduces its load-carrying capacity when the load is applied eccentrically in compression.

2. The experimentally determined buckling load is not affected by the presence of two symmetrical and identical cracks for concentrically loaded straight columns. Experiments on concentric loaded columns were run only on knife-edged columns.

3. For slenderness ratios less than about 250, the sharp notches appear to have a significant effect on the load-carrying ability of the columns except for the fixed-pinned case. This effect is especially pronounced for large eccentricity of load application. For slenderness ratios greater than about 250, these notches do not appear to have quite as significant an effect on the load-carrying ability.

4. The load-carrying capacity decreases with increasing depth of notch for slenderness ratios less than about 250.

5. For a column length of 12 inches, the weakening effect of a fatigue crack becomes more pronounced when loads are applied at greater eccentricities.

6. The reduction in load-carrying ability of a 12-inch-long fatigue-cracked columns tested is the same as for a sharp notch with a root radius of 0.003 inch or less, as long as all the other dimensions remain the same.

7. A root radius of 0.0625 inch does not appear to result in catastrophic failures of the type exhibited by a fatigue crack in a knife-edged column having a slenderness ratio of 92.

8. In loading columns to failure, a fatigue crack on one side of the column is more disastrous than a fatigue crack of half the depth on both sides of the column.

9. For a slenderness ratio of 92 and a given depth of fatigue crack, failure appears to occur at a near-constant horizontal deflection, when the knife-edged column is loaded eccentrically in compression.

10. Columns made from rolled bar stock did not show any preferred orientation resulting from manufacturing processes in these studies.

11. It is possible to establish a reasonable failure criterion for double notched columns, from Neuber's (1937) stress-concentration equations for deep notches.

12. Small closing cracks have little effect on the failure load or the values of failure criteria. Large closing cracks have a distinct effect on the values of failure criteria.

13. The maximum carrying capacity of a knife-edged column having a single notch appears to be affected relatively less by the presence of the notch than is that of a fixed-end column having a single notch.

14. For low slenderness ratios (<200), the ratio of the load carrying capacity to the buckling load for the knife-edge column is higher than that for the fixed-end column.

15. When designing columns against the effect of notches, it is desirable to use as large a slenderness ratio as is feasible to avoid the detrimental effects of the notches.

16. Column failures for the eccentrically loaded notched columns considered here, appear to be due more to the failure of the unnotched column at the point of maximum transverse column displacement than due to the effect of the notches.

17. In general, for notched columns with differing end conditions and the notches approximately centrally located in the specimens, the effect of the notches is to decrease the maximum load carrying capacity of the columns most for the column with the fixed-fixed ends, somewhat less for the column with the pinned-pinned ends and least for the column with the fixed-pinned end.

18. Solutions using the stress-intensity approach at the notch or the limit analysis at the notch, are satisfactory only for small notch depths. These solutions may be much more accurate for notches at the point of maximum transverse displacement of the columns. The larger discrepancies obtained for larger notch depths may be due to the inaccuracy of using the deflections obtained from the elastic case and applying these in the limit analysis.

19. The notches in columns having fixed-pinned ends had been observed from tests to have the best effect on the loss of carrying capacity than notched columns having fixed-fixed ends and those having pinned-pinned ends.

In addition to the tests made on the 1/2" x 1/2" cross-section columns made of 7075-T6 aluminum, tests were performed on glass composite columns of similar cross section and length.

The material was a square MTS Glastic rod. This is a composite made up of glass fibers with an epoxy filler. This material, which contains 30% of glass fibers, is generally used for electrical applications. Tests were also conducted on composite specimens supplied by Universal Moulded Fiber Glass Corp. which has a glass fiber content about 70%. This material is usually used for structural applications. A summary of some of the test results is:

19. The presence of a single notch in an eccentrically loaded composite column has a much more detrimental effect on the maximum load carrying capacity of the column than the presence of a single notch of the same size in an aluminum column with approximately the same dimensions and which is also loaded eccentrically.

20. In the composite columns with notches, no sudden failures occurred in which the crack continued to propagate in the transverse direction throughout the width of the column as opposed to similar sized aluminum columns having notches where plane strain failure did occur.

21. Composite columns exhibit crack arresting properties (in that a transverse crack does not propagate in the transverse direction but changes its direction and propagates parallel to the fibers) as opposed to the aluminum columns where plane strain failure occurs in which case the transverse crack propagates in the transverse direction of the column.

22. In the composite columns, irrespective of the amount of glass fibers (i.e. for 30% and 70% glass), initially machined transverse cracks change direction and propagate in the longitudinal direction of the column while in the aluminum columns the cracks propagate in the transverse direction.

REFERENCES

1. Liebowitz, H., "Fracture and Carrying Capacity of Notched Columns", Treatise on Fracture - 7 Vols. (Edited by H. Liebowitz), Academic Press, Nov. 1967 - March (1968).

2. Liebowitz, H., Vanderveldt, H., and Harris, D. W., "Carrying Capacity of Notched Columns", Int. J. Solids Structures, Vol. 3 (1967), p. 489.

3. Liebowitz, H., Harris, D. W., and Vanderveldt, H., "Fracture of Long and Short Notched Columns", presented at the SESA Meeting, Ottawa, Canada, 1967 and published in the J. Exp. Mechs., Feb. 1968.

4. Liebowitz, H., Vanderveldt, H., and Sanford, R. J., "Stress Concentrations due to Sharp Notches" presented at the SESA Meeting, Ottawa, Canada, 1967 and published in the J. Exp. Mechs., Dec. 1967.

5. Liebowitz, H., and Claus, W. D., Jr., "Failure of Notched Columns", J. Engr. Fract. Mechs., April 1968.

6. Neuber, H., "Kerbspannungslehre", Springer, Berlin, 1937, (also available as 1958 English translation. Edwards Bros., Ann Arbor, Mich. Also, as 1958 A.E.C. report. "Theory of Notch Stresses", 2nd Edition, AEC-T2-4547. U.S. Atomic Energy Commission, Washington, D.C.)

7. Okamura, H., Liu, H. W., Chu, J., and Liebowitz, H., "A Cracked Column under Compression", J. Engr. Fract. Mechs. Dec. 1968.

8. Vanderveldt, H., and Liebowitz, H., Carrying Capacity and Fracture of Notched Glass Fiber Composite Columns, J. Composite Mats. April 1968.

9. Liebowitz, H., and Claus, W. D., Jr., "Failure of Notched Columns with Fixed Ends", J. Engr. Fract. Mechs. 1968.

10. Vanderveldt, H., and Liebowitz, H., "Fracture of Notched Columns", submitted to Int. J. Solids Structures.

11. Liu, H. W., Chu, C. S., and Liebowitz, H., "Cracked Columns under Compression-Fixed Ends", to be submitted to J. Engr. Fract. Mechs.

12. Gross, B., and Srawley, J. E., "Stress-Intensity Factors for Single-Edge-Notch Specimens on Bending or Combined Bending and Tension by Boundary Collocation of a Stress Function", NASA TN-D-2603, 1965.

13. Brown, W. F., Jr. and Srawley, J. E., "Plane Strain Toughness Testing of High Strength Metallic Materials", STP 410, Am. Soc. for Testing and Materials, 1967.

14. Vanderveldt, H., and Liebowitz, H., "Theoretical and Experimental Studies of Notched Columns having One end Fixed and One End Pinned", submitted to Int. J. of Solids Structures.

15. Cotterell, B., "On the Behavior of Notched Struts", presented at the ASME Mtg. in NYC, Dec. 1968, also appeared in ASME J. of Basic Engineering, Dec. 1968.

16. Irwin, G. R., "Fracture" Handbook der Physik, Vol. VI, Springer, Berlin, pp. 551-590, 1958.

17. Irwin, G. R., "Fracture Mechanics", Structural Mechanics, Proceedings of the First Symposium on Naval Structural Mechanics, Ed. by J. N. Goodier and N. J. Hoff, Pergamon Press, N.Y., 1960.

18. Westergaard, H. M., "Bearing Pressures and Cracks," Trans. ASME, J. of App. Mech., pp. A49-A53, June 1939.

19. Paris, P. C., and Sih, G. S., "Stress Analysis of Cracks", in Fracture Toughness Testing and Its Applications, ASTM S.T.P. No. 381, 1965.

20. Inglis, C. E., "Stresses in a Plate Due to the Presence of Cracks and Sharp Corners", Trans. Instn. Nav. Archit. 60, 219, 1913.

21. Griffith, A. A., "The Theory of Rupture", Proc. 1st Inst. Int. Congr. Appl. Mech., Delft, pp. 55-63, 1924.

22. Sih, G. C., and Liebowitz, H., "On the Griffith Energy Criterion for Brittle Fracture", Int. J. Solids. Structures, Vol. 3, pp 1-22, 1967.

23. Hoff, N. J., The Analysis of Structures Wiley, N.Y., 1956.

24. Timoshenko,S. P., and Gere, J. M., Theory of Elastic Stability, 2nd Edition, McGraw-Hill, N.Y., 1961.

25. Langhaar, H. L., Energy Methods in Applied Mechanics, Wiley, N.Y., 1962.

26. Donnell, L. H., "Applied Mechanics Surveys" (H. N. Abramson, H. Liebowitz, J. M. Crowley and S. Jukasz eds.), pp 315-316 Macmillian, N.Y., 1966.

27. Euler, L., "De curvis elastics (Additamentum). In Methodus inveniendi lineas curves maximi proprietate gaudentes". Lousanne, 1744.

28. Euler, L., In Histoire de l'Academic, Vol. 13, pp 252-282, Berlin, 1757.

29. Davis, S. O., Tupper, M. G., and Miemi, R. M., "Effect of Specimen Type and Crack Orientation on Fracture Toughness", Technical Report AFML-TR-38, Air Force Materials Laboratory, Wright-Patterson Air Force Base, Ohio, (1967).

30. Vanderveldt, H., Liebowitz, H., and Perrone, N., "Limit Analysis of the Response of a Fixed-Pinned End Column Loaded Eccentrically", submitted to Int. J. Solids Structures, 1968.

TABLE I.

Comparison of Theoretical and Experimental

Maximum Load, Pinned-Pinned Edge

LIST OF FIGURES

FIG. 1. Three modes of fracture.

FIG. 2. Edge of crack.

FIG. 3. Elastic unnotched column subjected to concentric load.

FIG. 4. Comparison of theoretically predicted Euler load with experimental results.

FIG. 5. Test specimen.

FIG. 6. Test equipment and specimen.

FIG. 7. Knife-edge assembly.

FIG. 8. Typical fracture surface of a fatigue cracked specimen.

FIG. 9. Specimen configuration.

FIG. 10a. Unnotched specimen loaded eccentrically.

FIG. 10b. Notched specimen loaded eccentrically.

FIG. 11. Load-deflection curve for a column with a 0.020-inch-deep notch with a fatigue crack extension.

FIG. 12. Load-deflection curve for a column with a 0.195-inch-deep notch with a fatigue crack extension.

FIG. 13. Effect of notch depth on failure load and maximum horizontal deflection of the column (all notches have a fatigue crack extension).

FIG. 14. Effect of depth of notch with a fatigue crack extension on failure load.

FIG. 15. Effect of notch depth and root radii on load-carrying ability of columns (eccentricity = 1.0 inch).

FIG. 16. Load deflection for a column with two V-notches on opposite sides and of varying depth (eccentricity = 1.0 inch).

FIG. 17. Effect of notches and slenderness ratio on the maximum carrying capacity of columns (eccentricity = 1.0 inch).

FIG. 18. Effect of notches and slenderness ratio on the maximum load-carrying capacity of columns (eccentricity = 0.090 inch).

FIG. 19. The deflection of a cracked column subjected to an eccentric compression load.

FIG. 20. $(c/h)^{1/2} Y_B$ (c/h) as a function of c/h .

FIG. 21. Load-deflection curve for a column with a 0.09" deep notch with a fatigue crack extension.

FIG. 22. Load-deflection curve for a column with a 0.195" deep notch with a fatigue crack extension.

FIG. 23. Load carrying capacity of a cracked column.

FIG. 24. Maximum load vs. total notch depth in fixed-fixed column, $\delta = \varepsilon = 0.01, 0.1$, L = 10.25.

FIG. 25. Maximum load vs. total notch depth in fixed-fixed column, $\delta = \varepsilon = 0.01, 0.1$, L = 16.25.

FIG. 26. Maximum load vs. total notch depth in fixed-fixed column, $\delta = \varepsilon = 0.01, 0.1$, L = 22.25.

FIG. 27. Maximum load vs. total notch depth in fixed-fixed column, $\delta = \varepsilon = 0.01, 0.1$, L = 28.25.

FIG. 28. Maximum load vs. length of fixed-fixed column, $\delta = \varepsilon = 0.1$, c = 0.11.

FIG. 29. Maximum load vs. length of fixed-fixed column, $\delta = \varepsilon = 0.1$, c = 0.14.

FIG. 30. Maximum load vs. length of fixed-fixed column, $\delta = \varepsilon = 0.1$, c = 0.18.

FIG. 31. Maximum load vs. length of fixed-fixed column, $\delta = \varepsilon = 0.1, 0.01$, $c = 0.22$.

FIG. 32. Maximum load vs. length of fixed-fixed column, $\delta = \varepsilon = 0.1$, $c = 0.25$.

FIG. 33. Maximum load vs. length of fixed-fixed column, $\delta = \varepsilon = 0.1, 0.01$, $c = 0.26$.

FIG. 34. Maximum load vs. length of fixed-fixed column, $\delta = \varepsilon = 0.1, 0.01$, $c = 0.30$

FIG. 35. Maximum load vs. length of fixed-fixed column, $\delta = \varepsilon = 0.1, 0.01$, $c = 0.32$.

FIG. 36. Maximum load vs. length of fixed-fixed column, $\delta = \varepsilon = 0.1, 0.01$, $c = 0.36$.

FIG. 37. $(c/h)^{1/2}$ $F(c/h)$ as a function of (c/h).

FIG. 38. (Y_T/Y_B) as a function of (c/h).

FIG. 39. Stress intensity factor of a cracked column.

FIG. 40. Compliance of a cracked column as influenced by bending moment at a cracked section.

FIG. 41. Load carrying capacity, P_{cr}, of a cracked column.

FIG. 42. Load carrying capacity of single edge notched columns, (7075-T6 AL.).

FIG. 43. Interaction curve for combined axial force and bending.

FIG. 44. (P_M/P_B) vs. (c/h), when column is double-notched and $L = 11.75$.

FIG. 45. (P_M/P_B) vs. (c/h), when column is single-notched and $L = 11.75$.

FIG. 46. (P_M/P_B) vs. (c/h), when column is double-notched and $L = 29.75$.

FIG. 47. (P_M/P_B) vs. (c/h), when column is single-notched and $L = 29.75$.

FIG. 48. (P_M/P_B) vs. (L/ρ), when column is double-notched.

FIG. 49. (P_M/P_B) vs. (L/ρ), when column is single-notched.

FIG. 50. (P_M/P_B) vs. (c/h), various end conditions and double notch.

FIG. 51. (P_M/P_B) vs. (c/h), various end conditions and single notch.

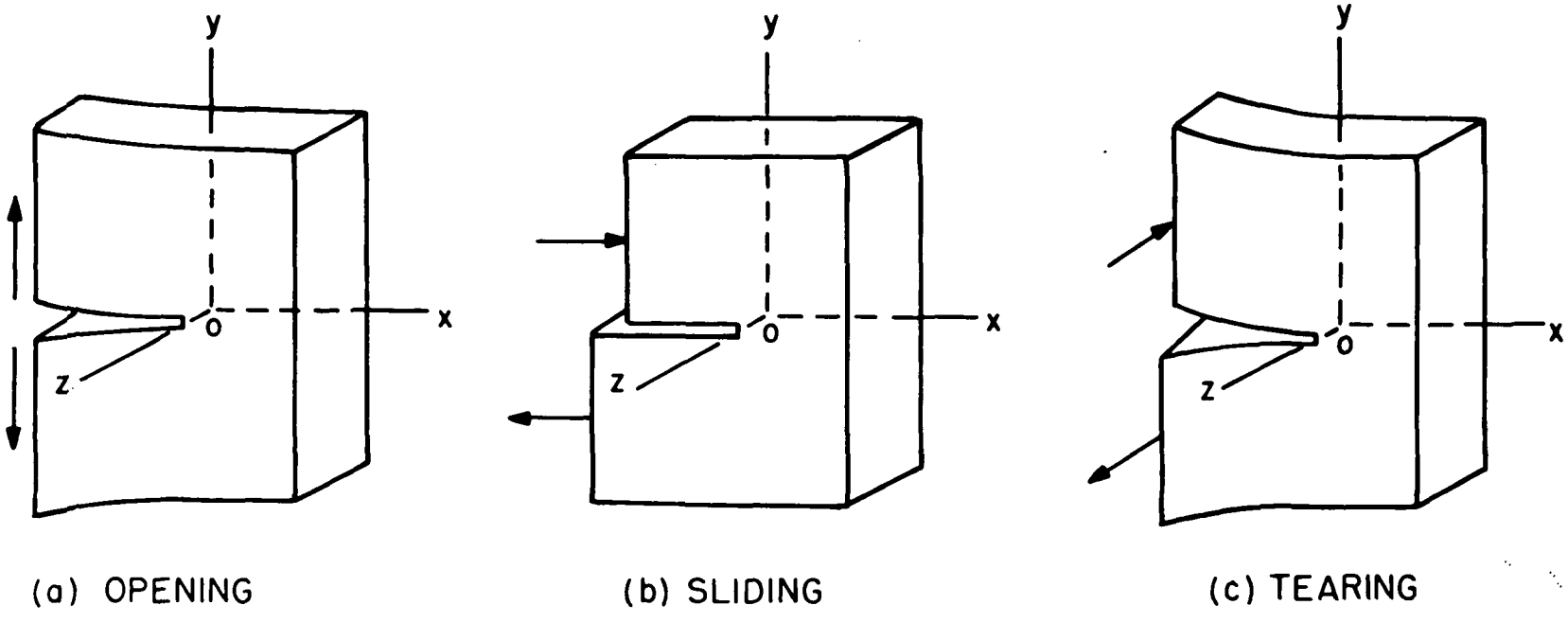

Figure 1. Three modes of fracture

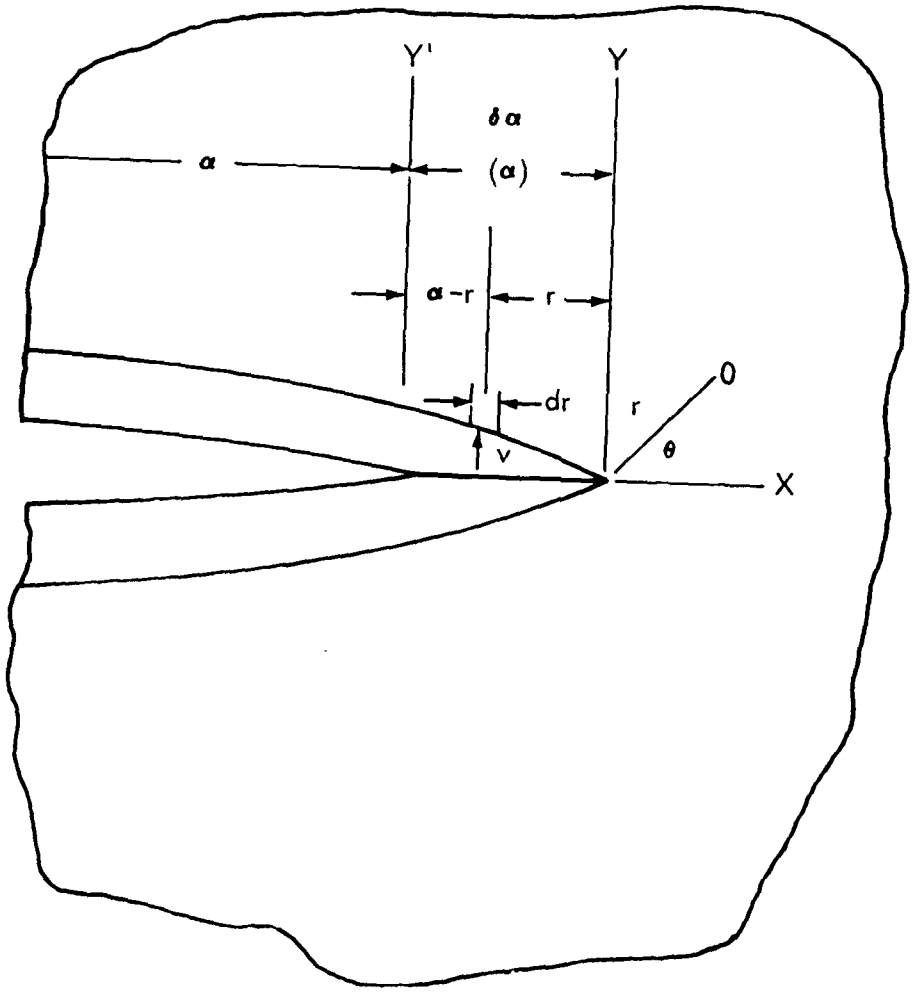

Figure 2. Edge of crack

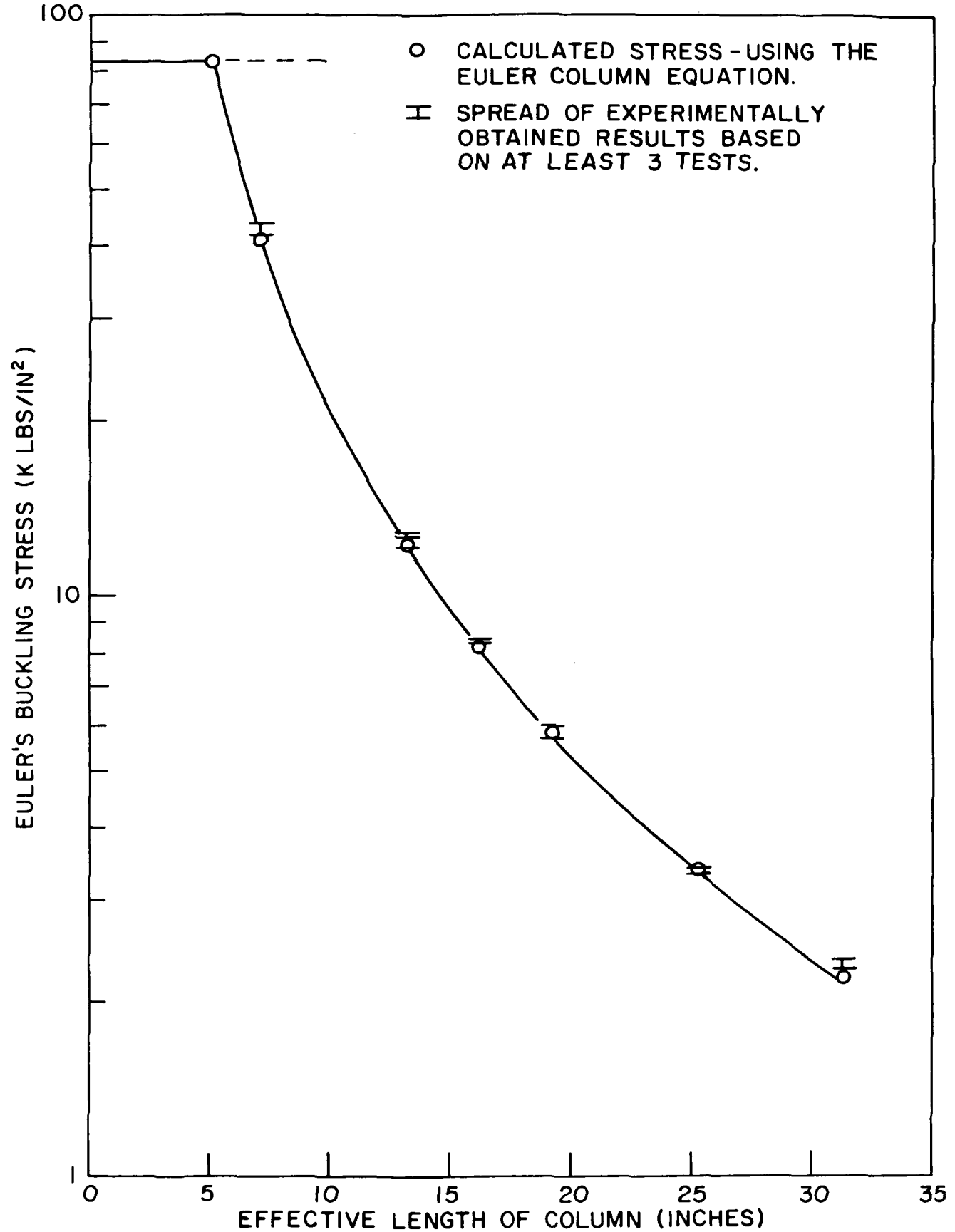

Figure 3. Elastic unnotched column subjected to concentric load

Eccentricity (in.)	Experimentally Determined Maximum Load (lb.)
0	3045*
0	3150
0.090	2440
0.250	2050
0.500	1590
1.000	1200
1.250	1020

*Euler buckling load which was calculated using a length of column plus the added length due to the knife edges.

Figure 4. Comparison of theoretically predicted Euler load with experimental results

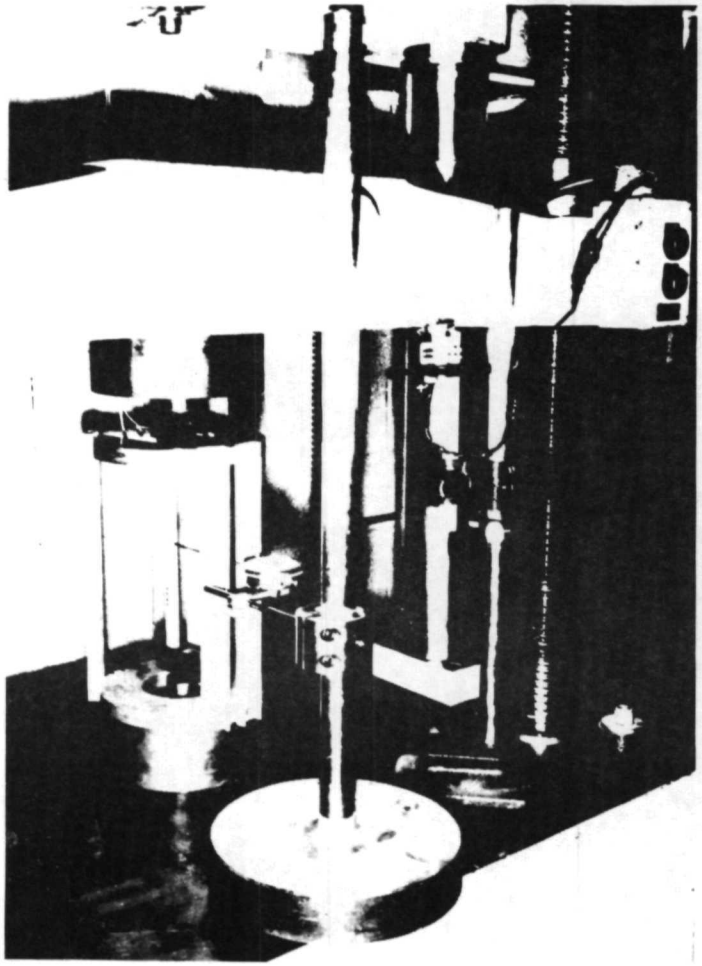

Figure 5. Test specimen

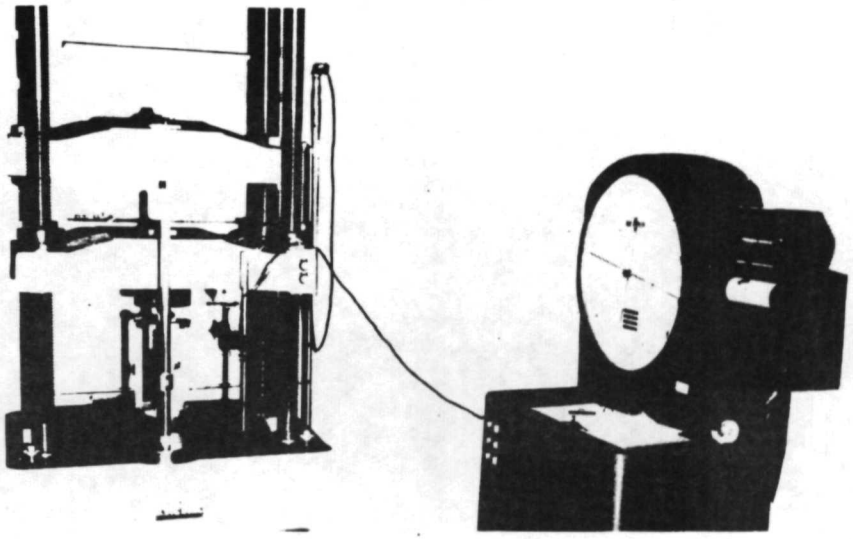

Figure 6. Test equipment and specimen

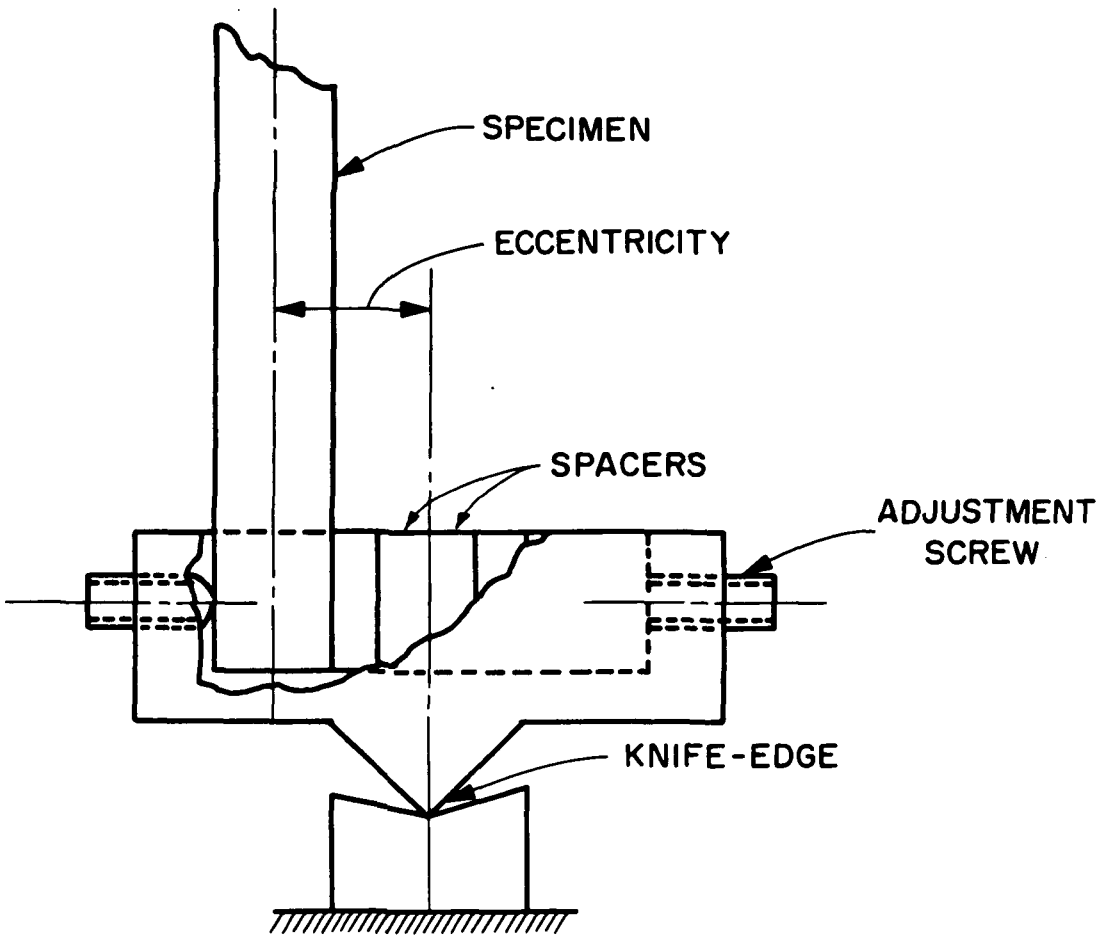

Figure 7. Knife-edge assembly

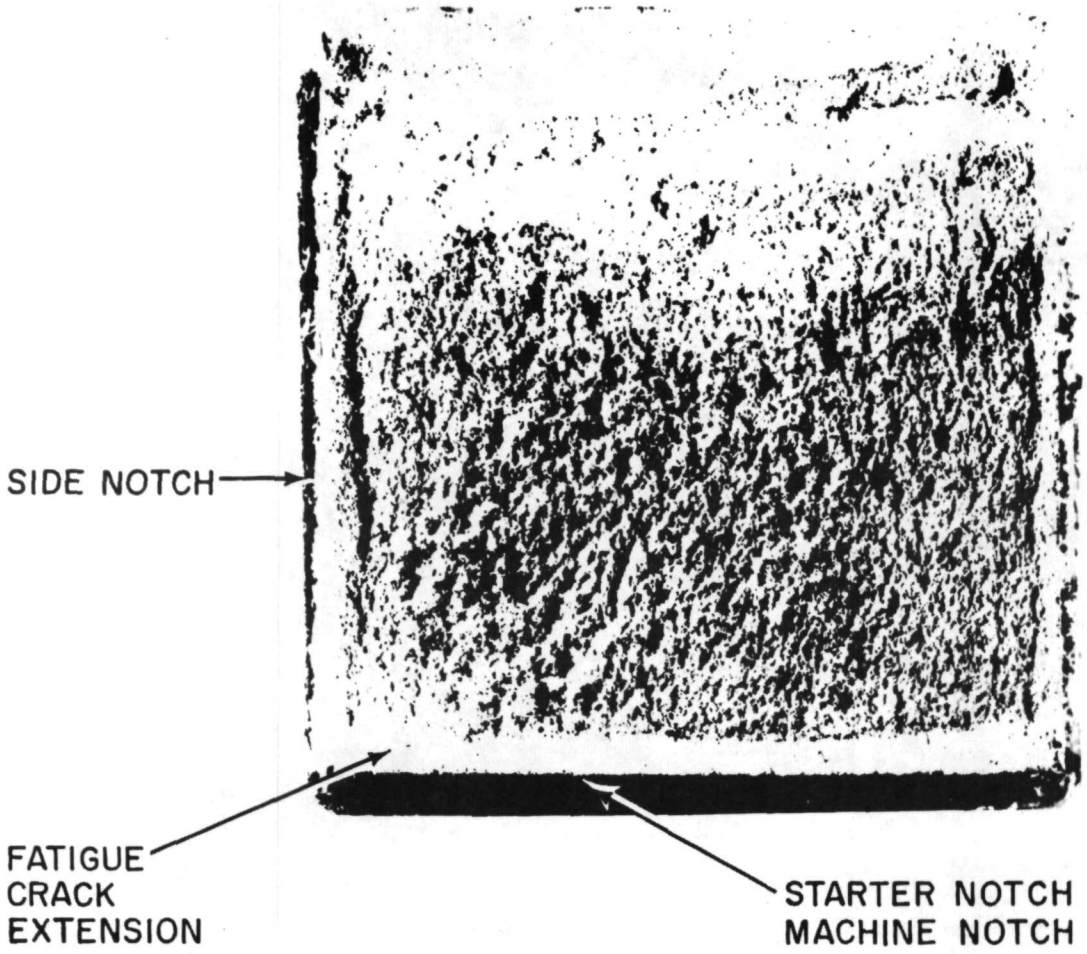

Figure 8. Typical fracture surface of a fatigue cracked specimen

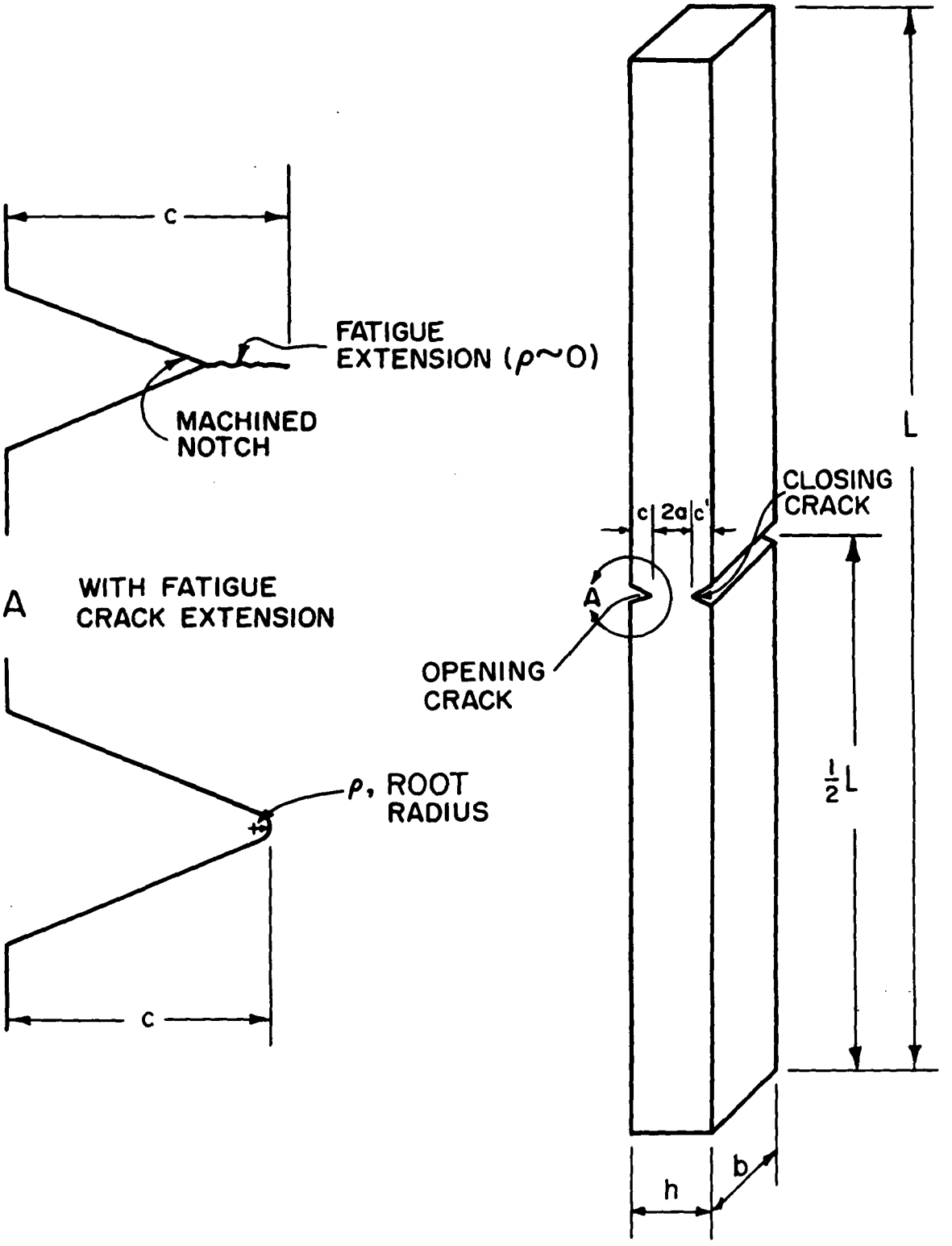

Figure 9. Specimen configuration

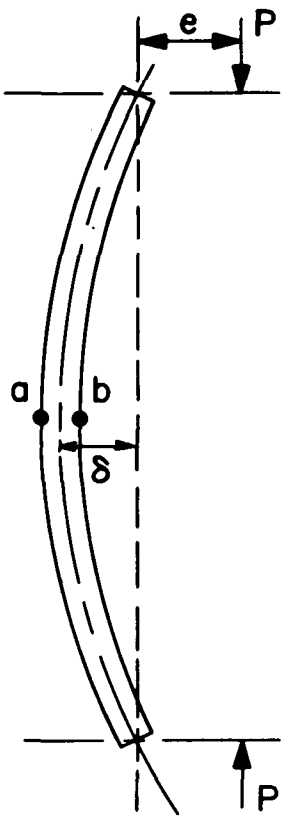

Figure 10a. Unnotched specimen loaded eccentrically

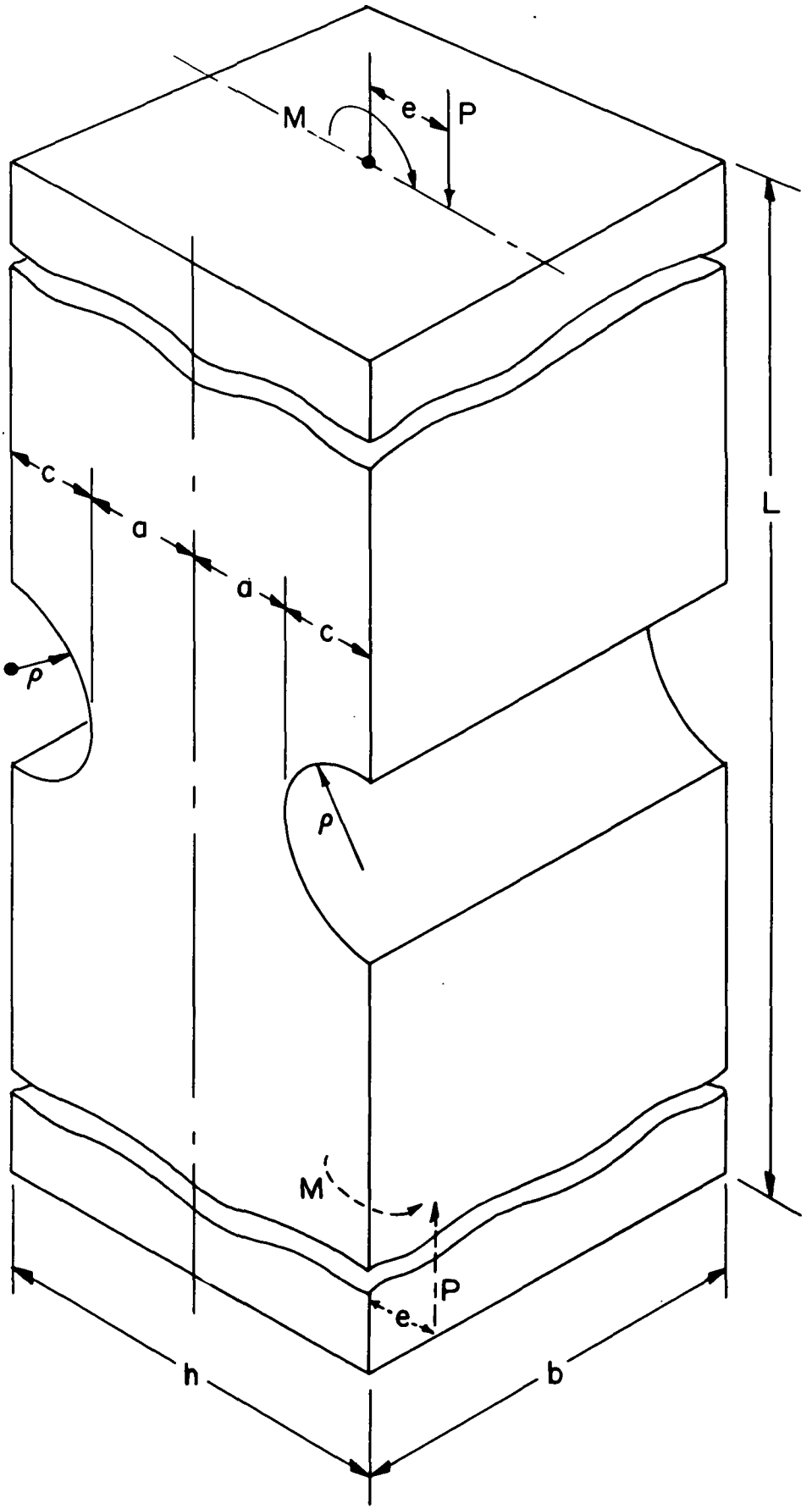

Figure 10b. Notched specimen loaded eccentrically

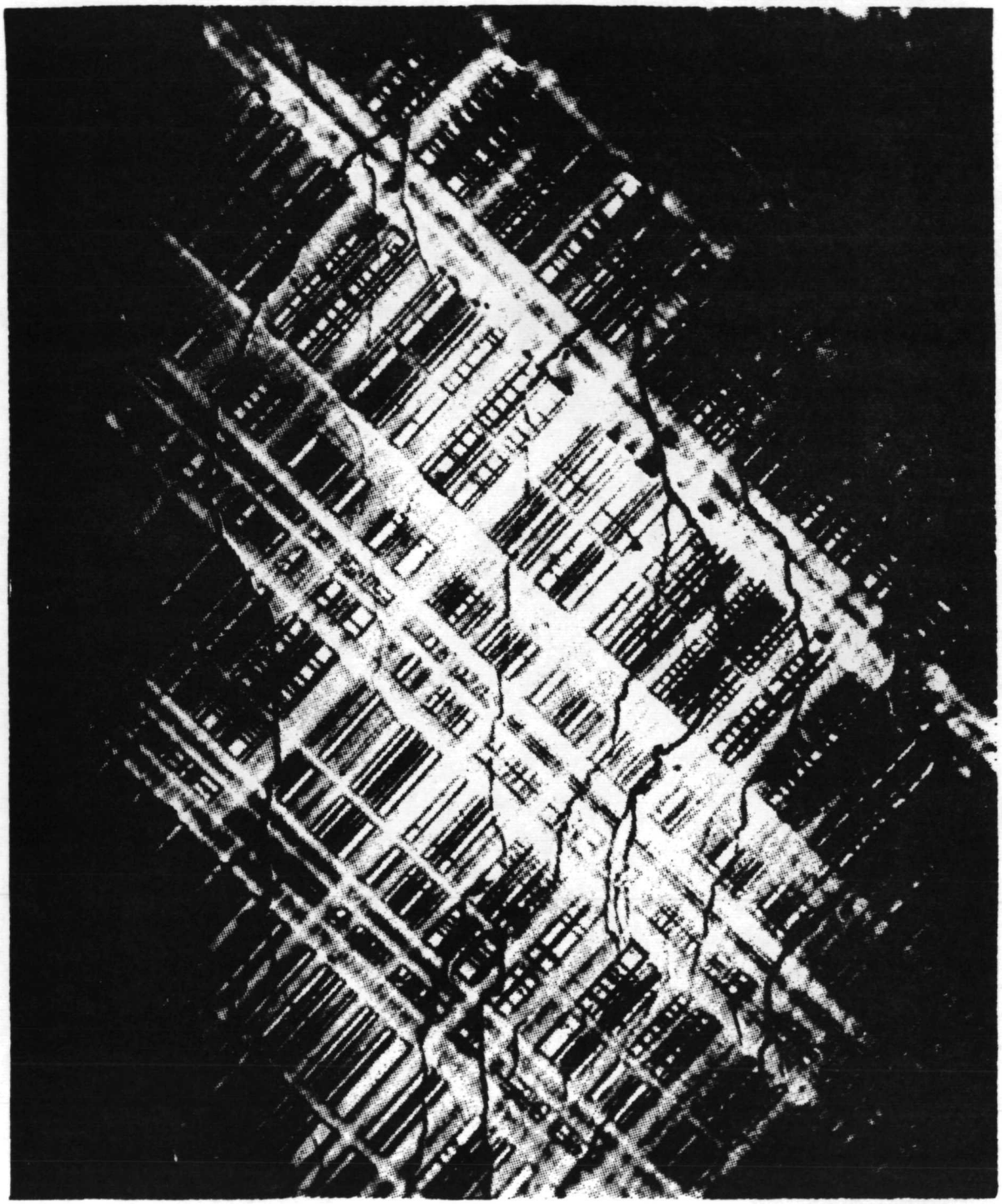

Microcracks in MgO stabilized by slip bands. × 150 (Johnston *et al.*)

Figure 11. Cracks propagating across slip bands

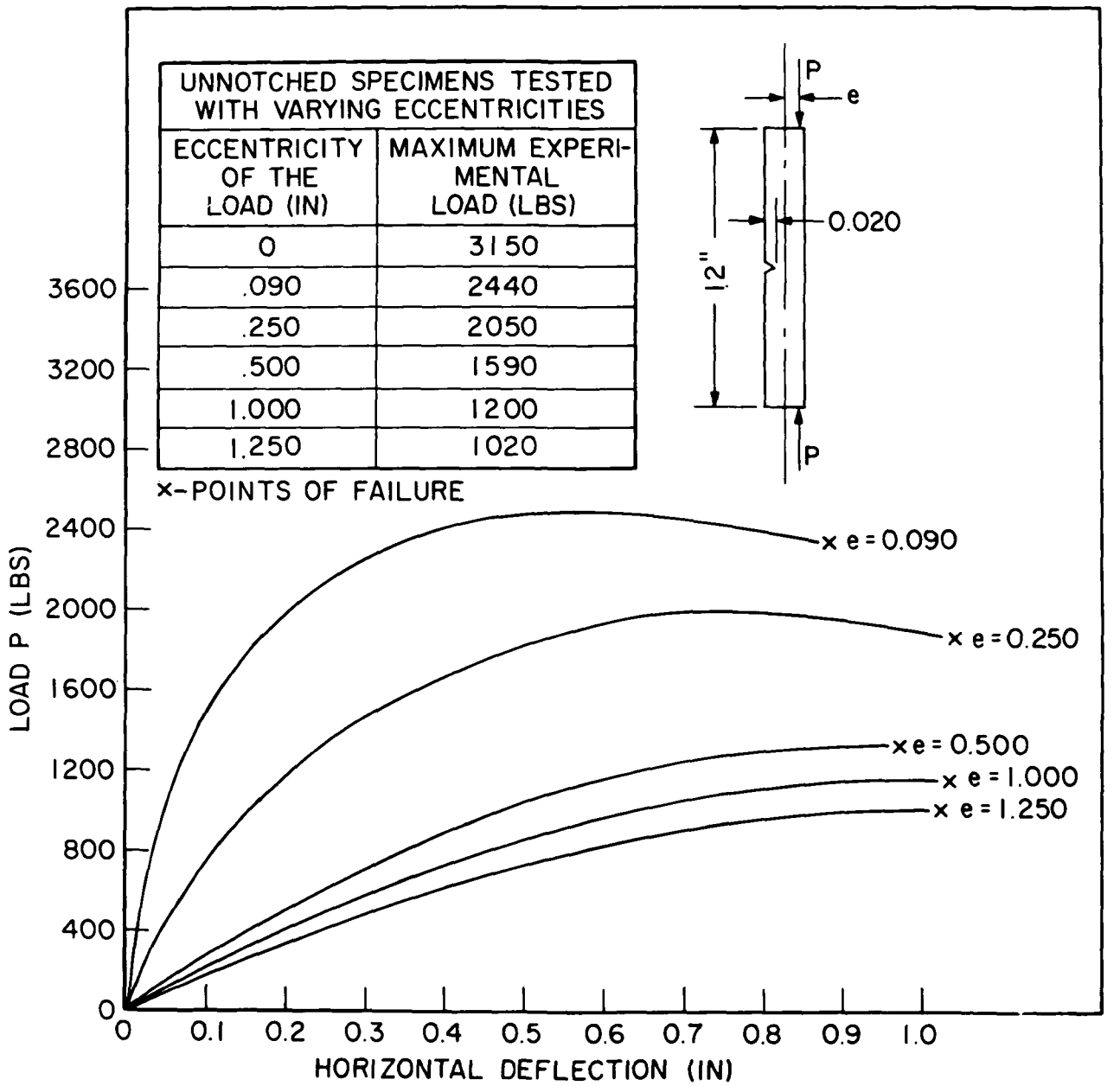

Figure 11. Load-deflection curve for a column with a 0.020-inch-deep notch with a fatigue crack extension

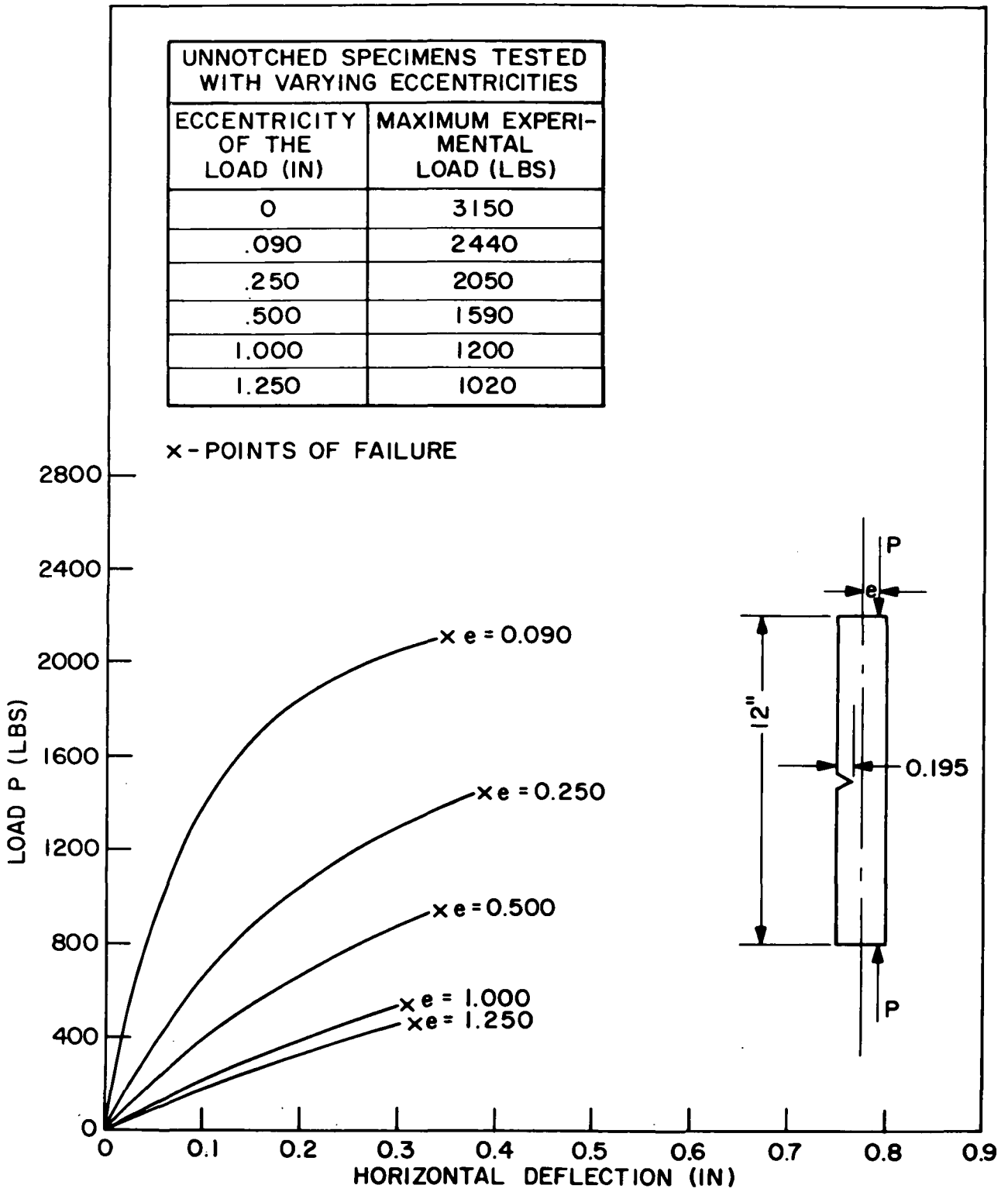

Figure 12. Load-deflection curve for a column with a 0.195-inch-deep notch with a fatigue crack extension

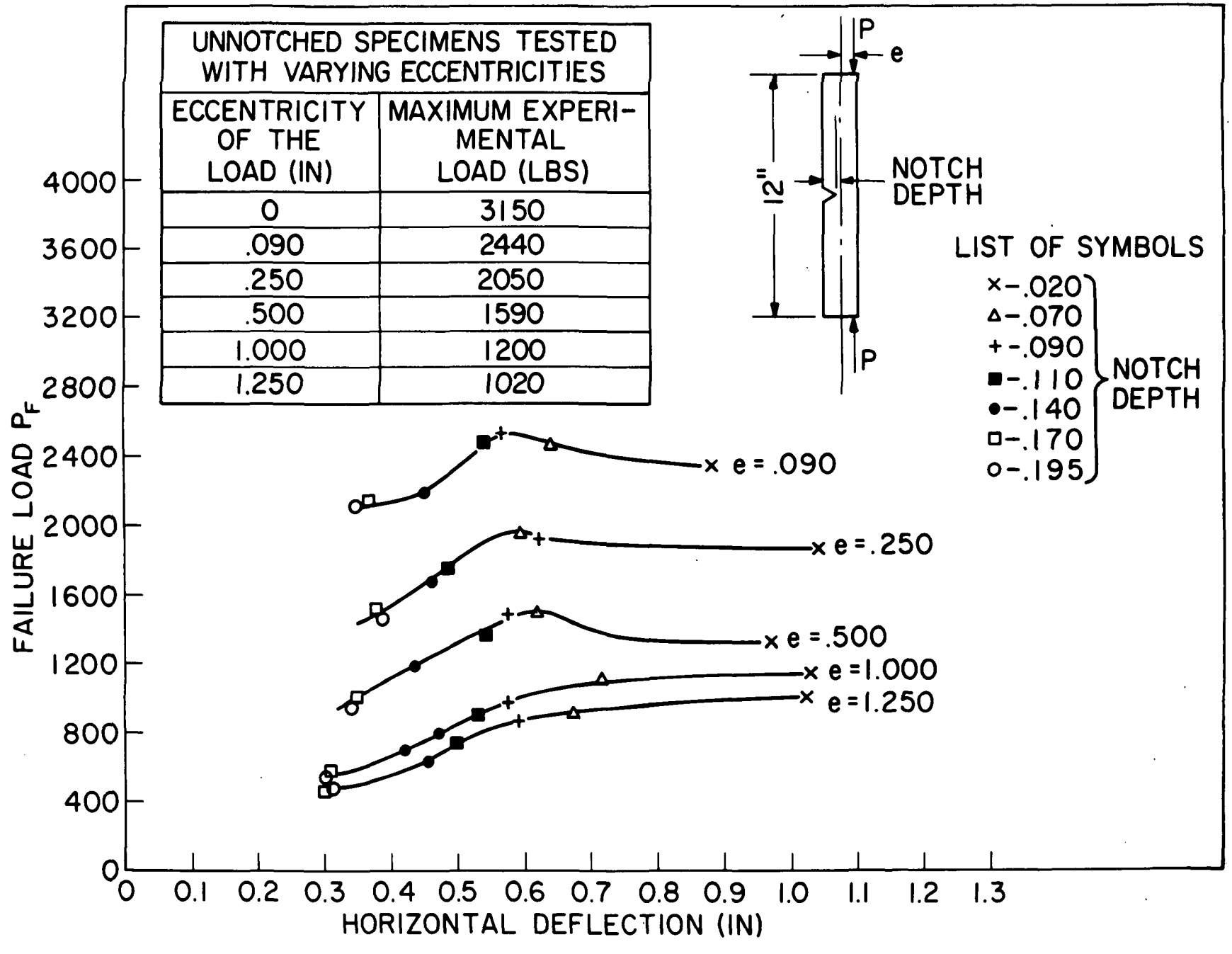

Figure 13. Effect of notch depth on failure load and maximum horizontal deflection of the column (all notches have a fatigue crack extension)

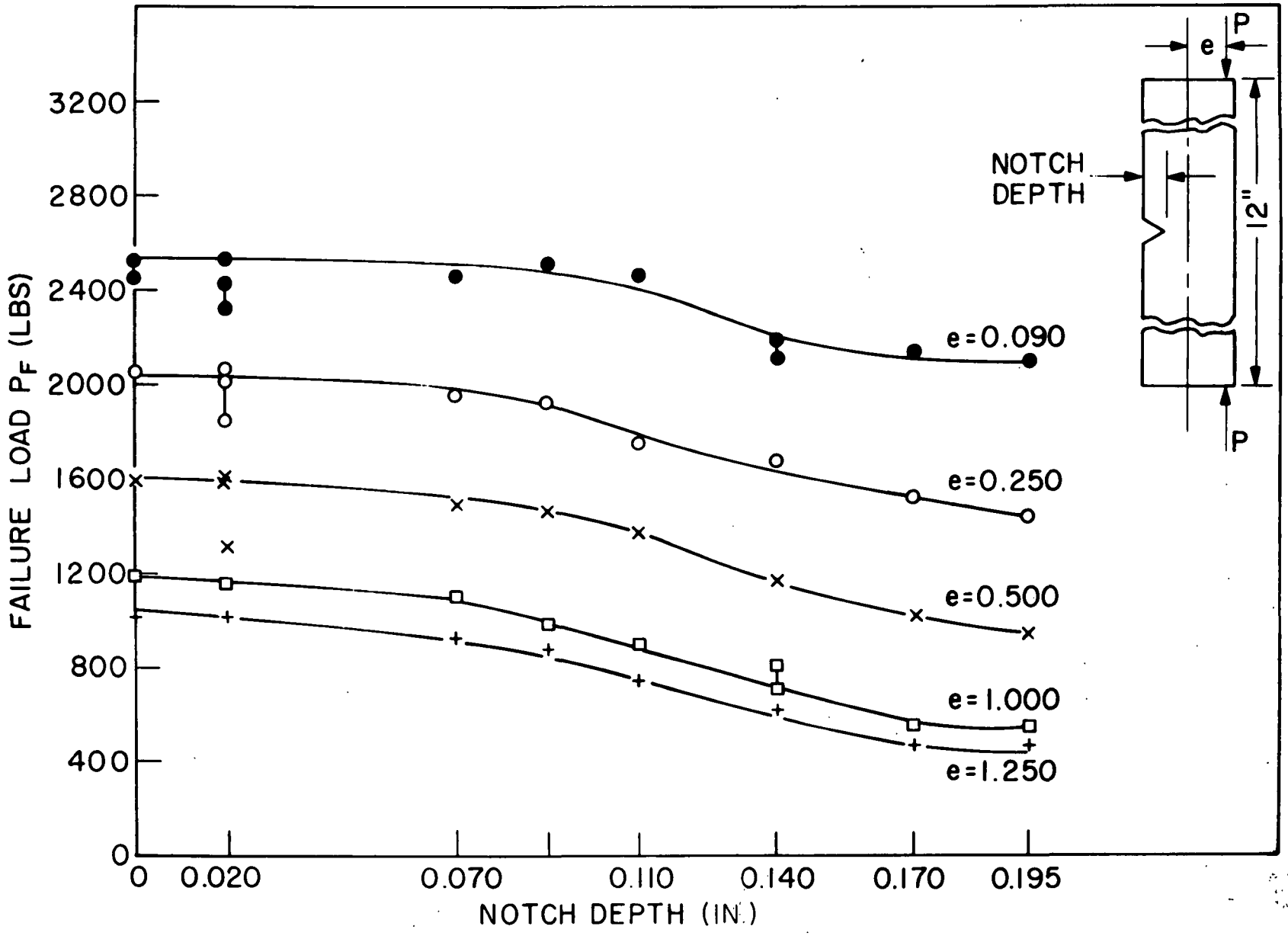

Figure 14. Effect of depth of notch with a fatigue crack extension on failure load

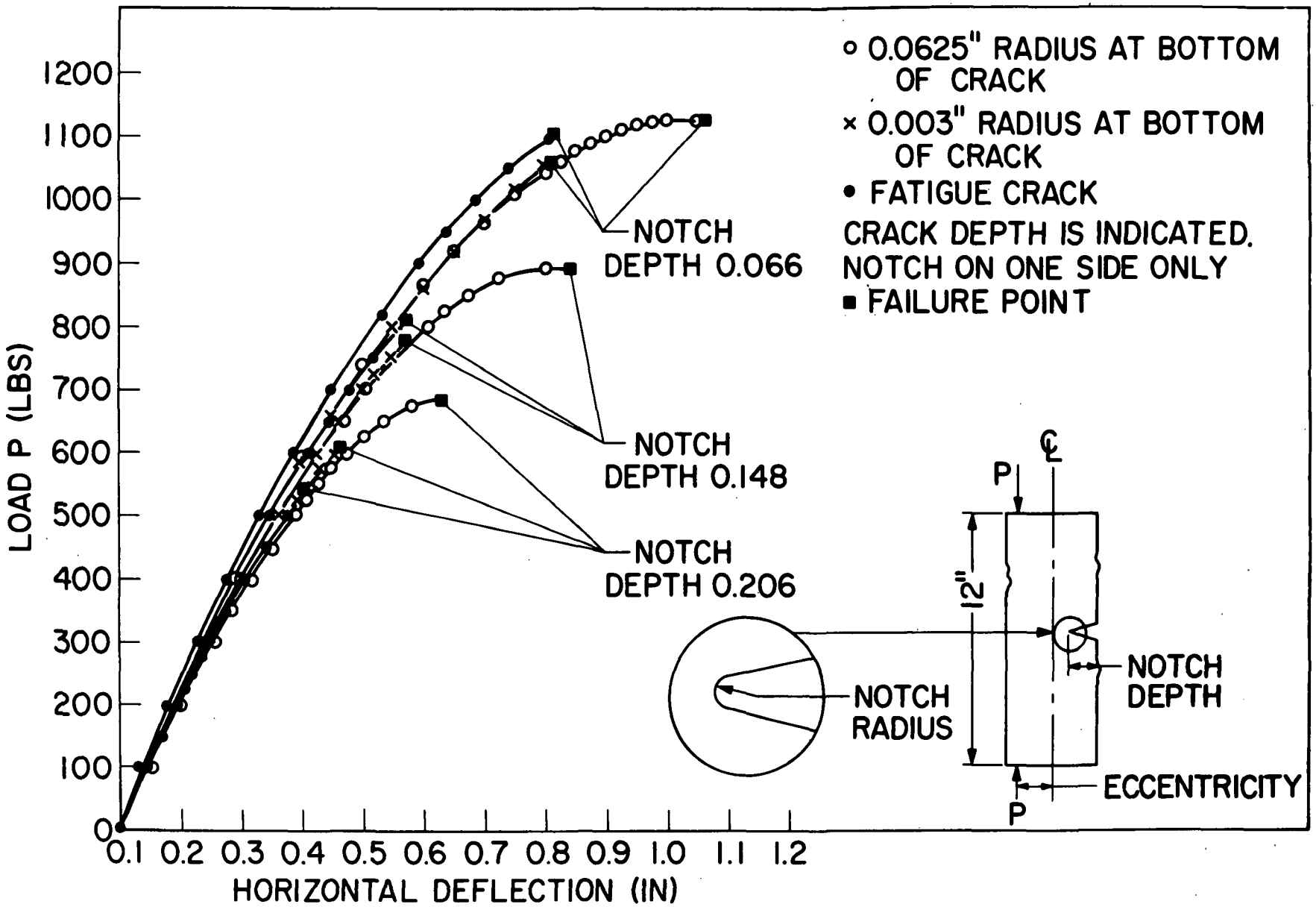

Figure 15. Effect of notch depth and root radii on load-carrying ability of columns (eccentricity = 1.0 inch)

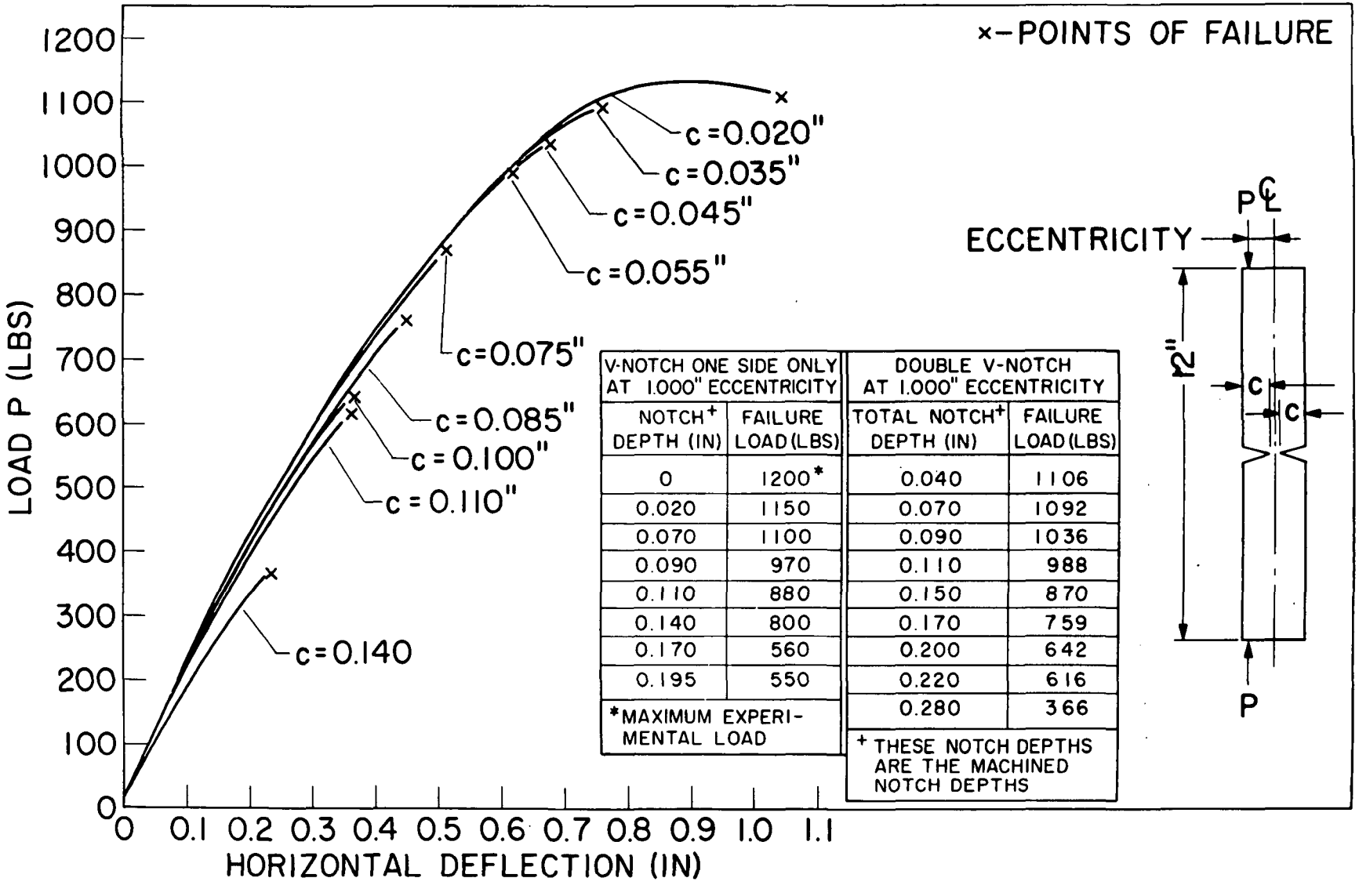

V-NOTCH ONE SIDE ONLY AT 1.000" ECCENTRICITY	
NOTCH+ DEPTH (IN)	FAILURE LOAD (LBS)
0	1200*
0.020	1150
0.070	1100
0.090	970
0.110	880
0.140	800
0.170	560
0.195	550

*MAXIMUM EXPERIMENTAL LOAD

DOUBLE V-NOTCH AT 1.000" ECCENTRICITY	
TOTAL NOTCH+ DEPTH (IN)	FAILURE LOAD (LBS)
0.040	1106
0.070	1092
0.090	1036
0.110	988
0.150	870
0.170	759
0.200	642
0.220	616
0.280	366

+ THESE NOTCH DEPTHS ARE THE MACHINED NOTCH DEPTHS

Figure 16. Load deflection for a column with two V-notches on opposite sides and of varying depth (eccentricity = 1.0 inch)

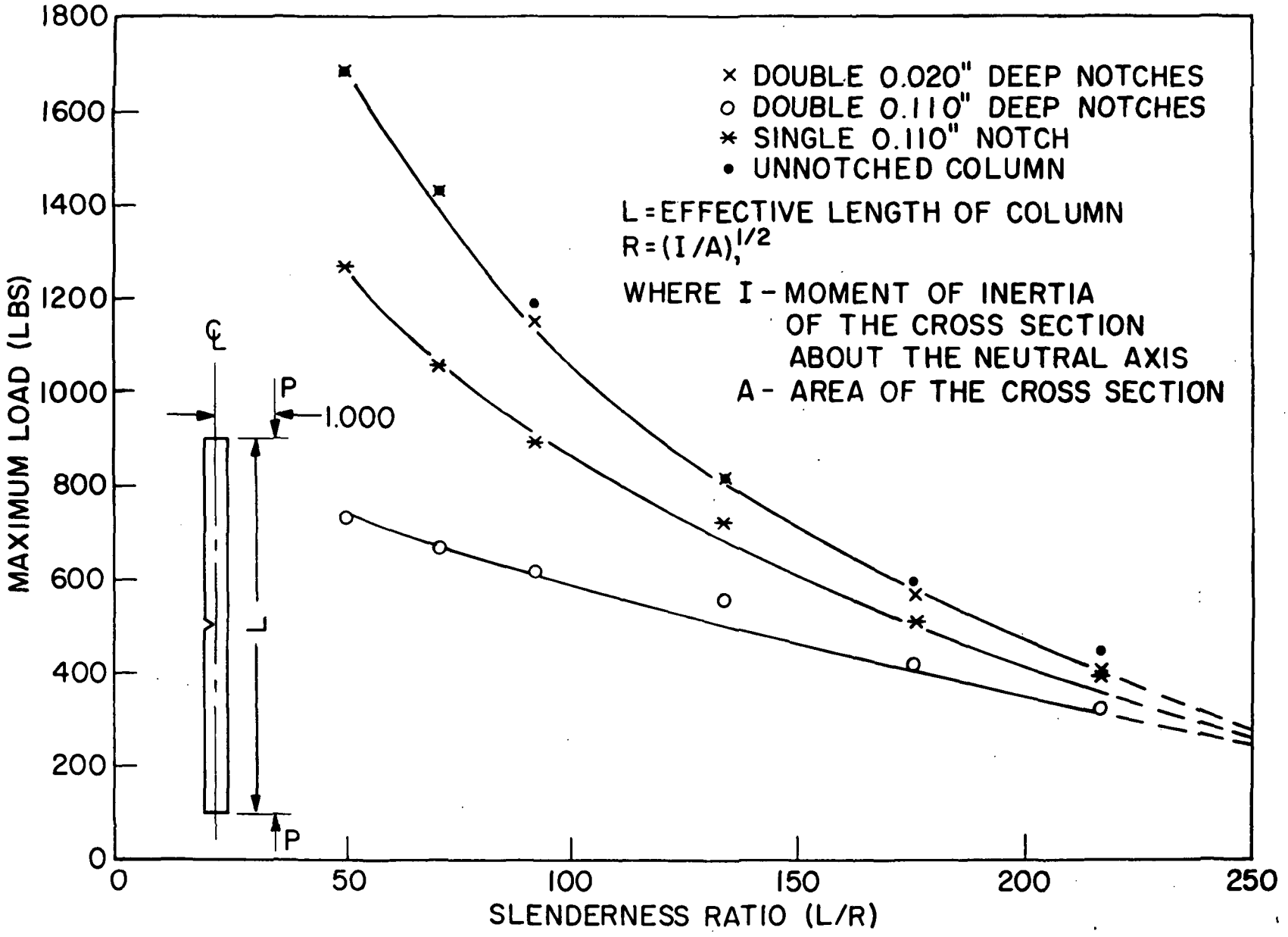

Figure 17. Effect of notches and slenderness ratio on the maximum carrying capacity of columns (eccentricity = 1.0 inch)

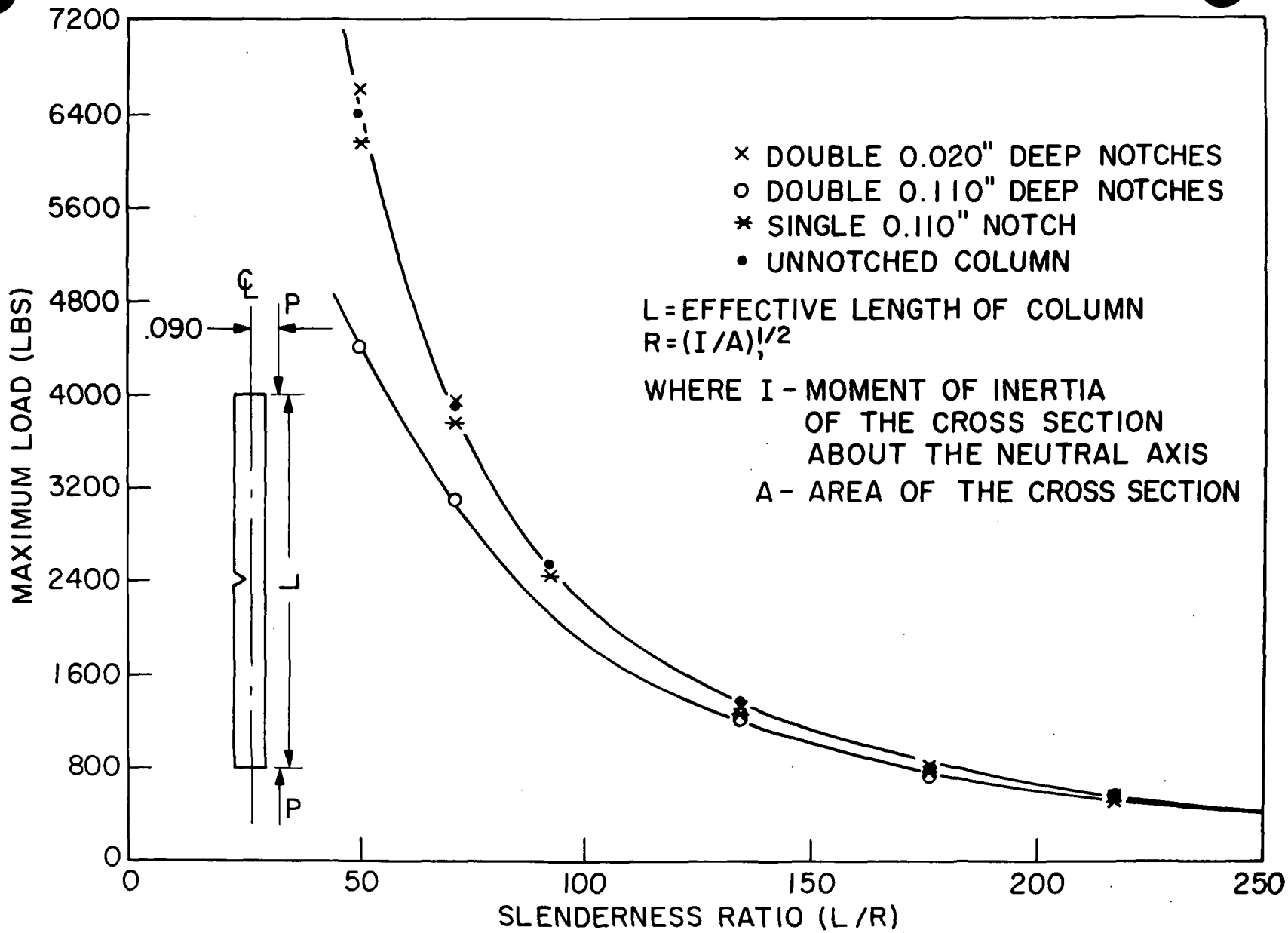

Figure 18. Effect of notches and slenderness ratio on the maximum load-carrying capacity of columns (eccentricity = 0.090 inch)

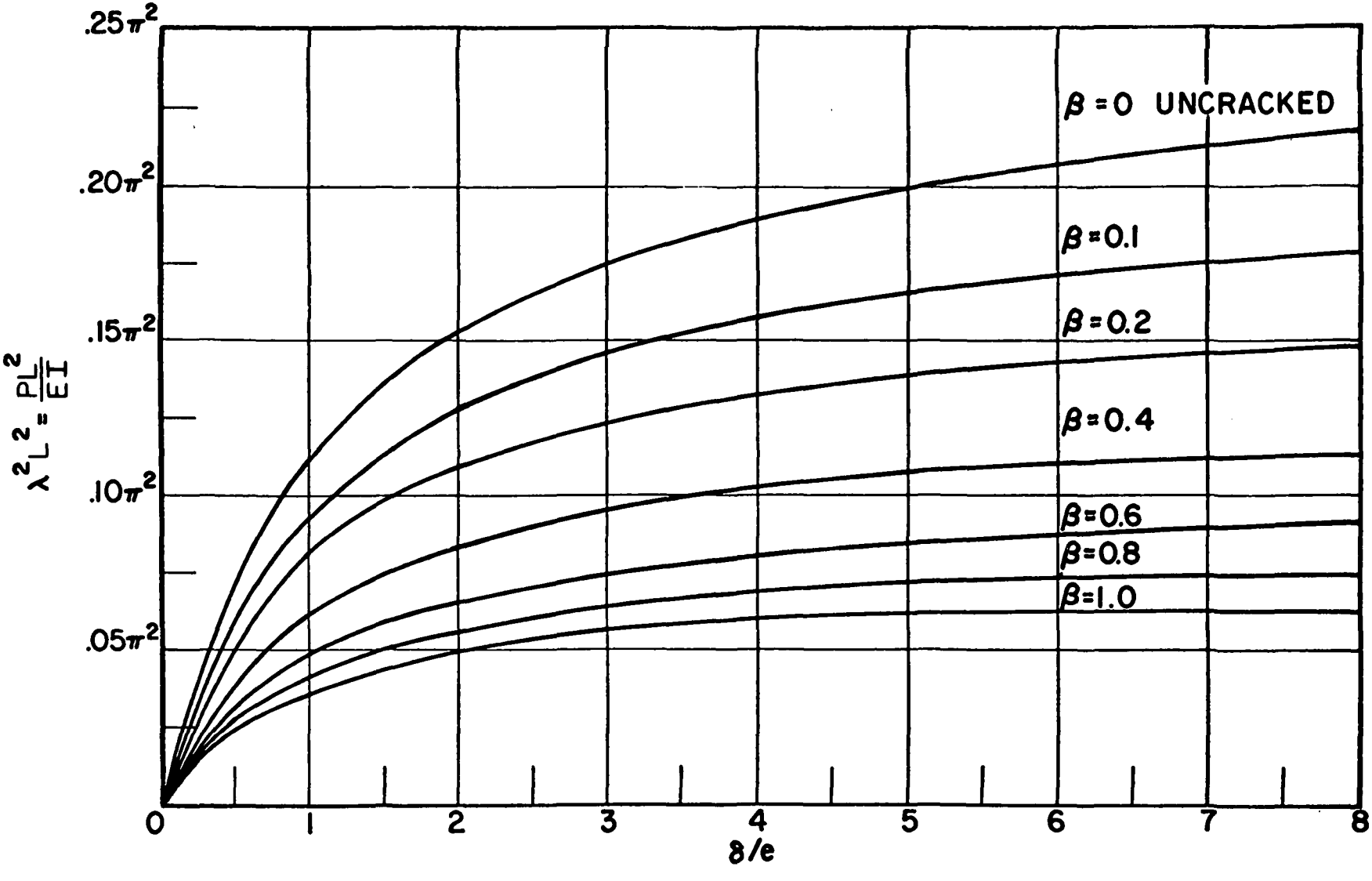

Figure 19. The deflection of a cracked column subjected to an eccentric compression load

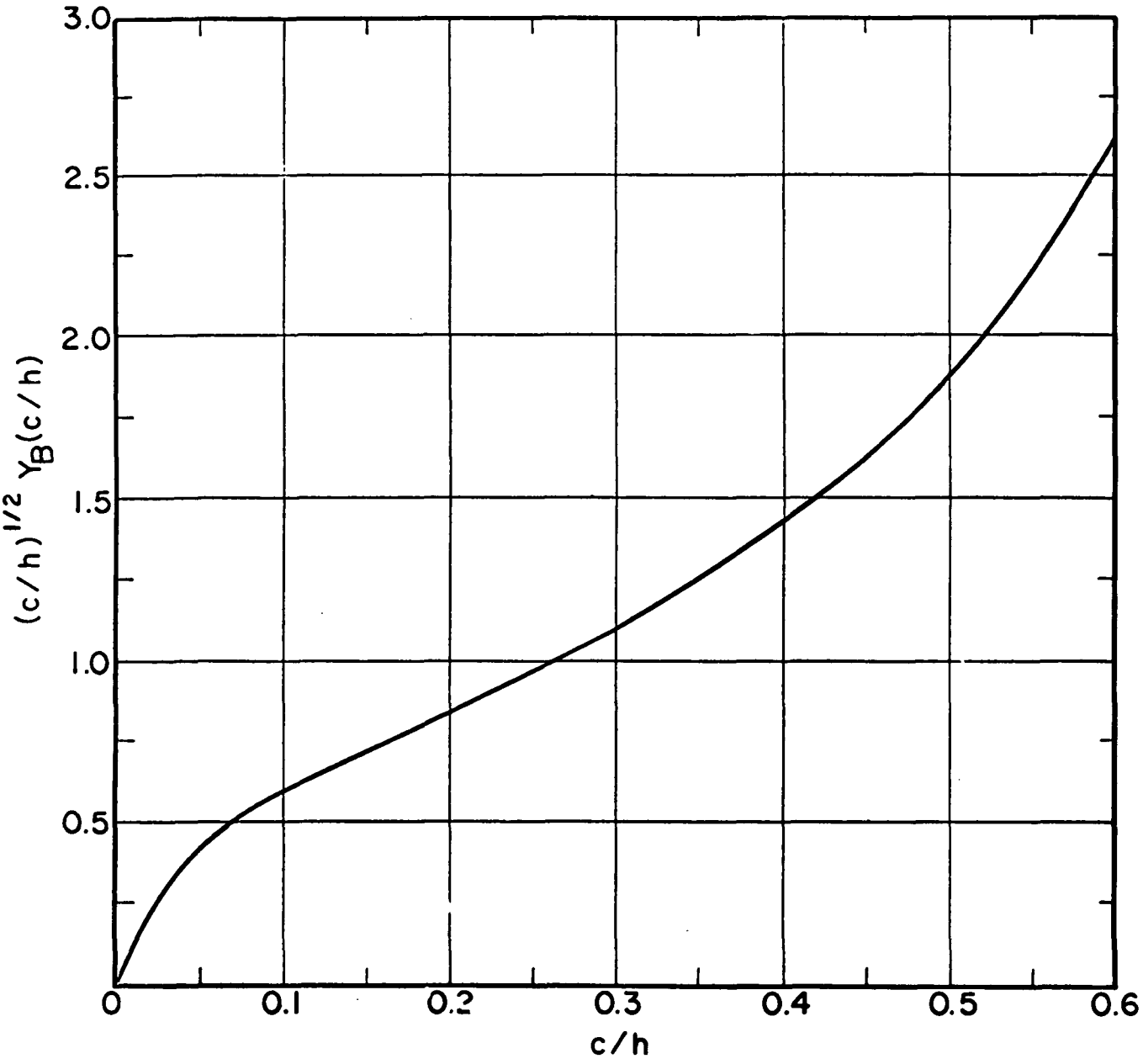

Figure 20. $(\frac{c}{h})^{1/2} Y_B (\frac{c}{h})$ as a function of c/h

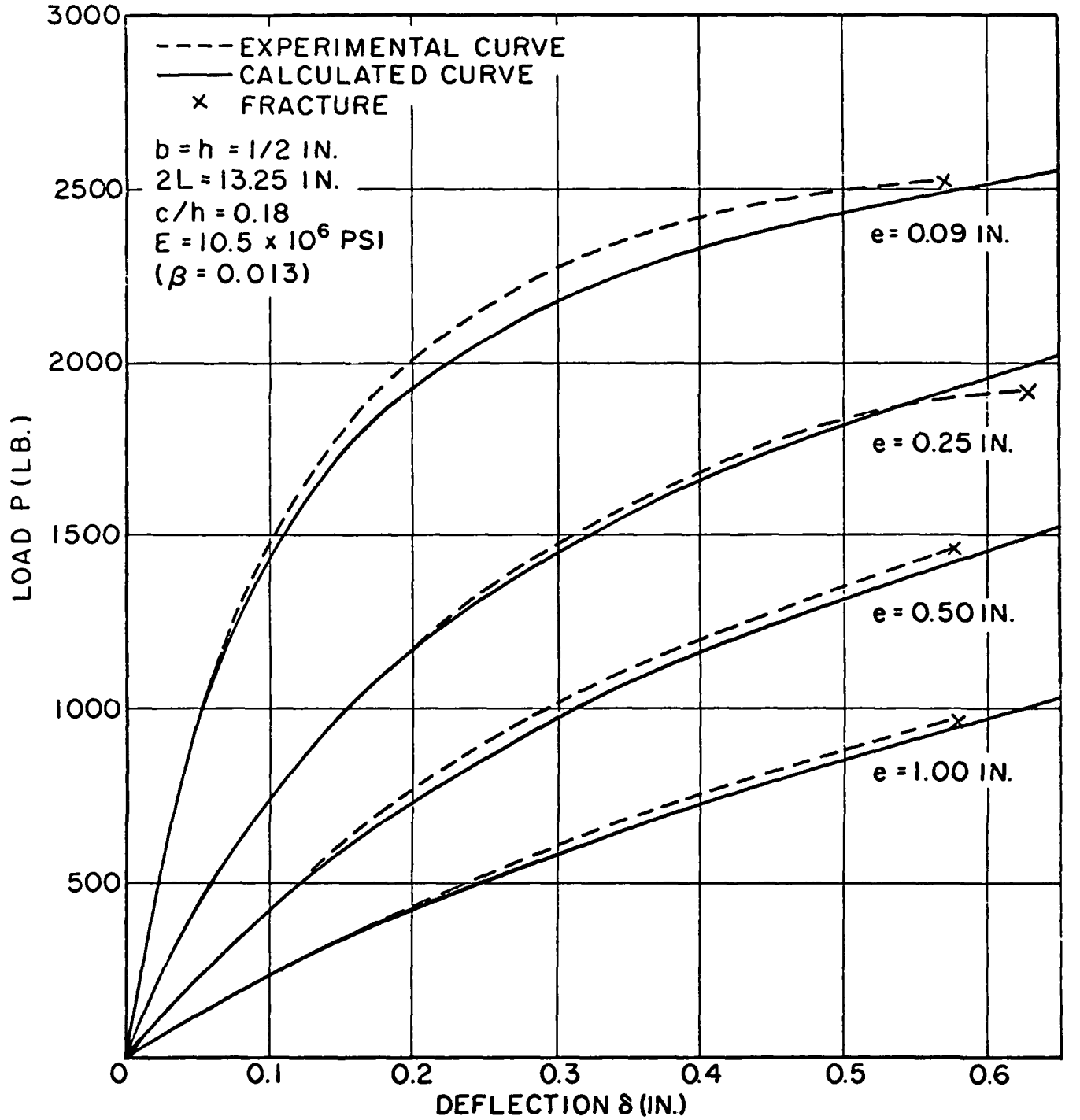

Figure 21. Load-deflection curve for a column with a 0.090-inch-deep notch with a fatigue crack extension

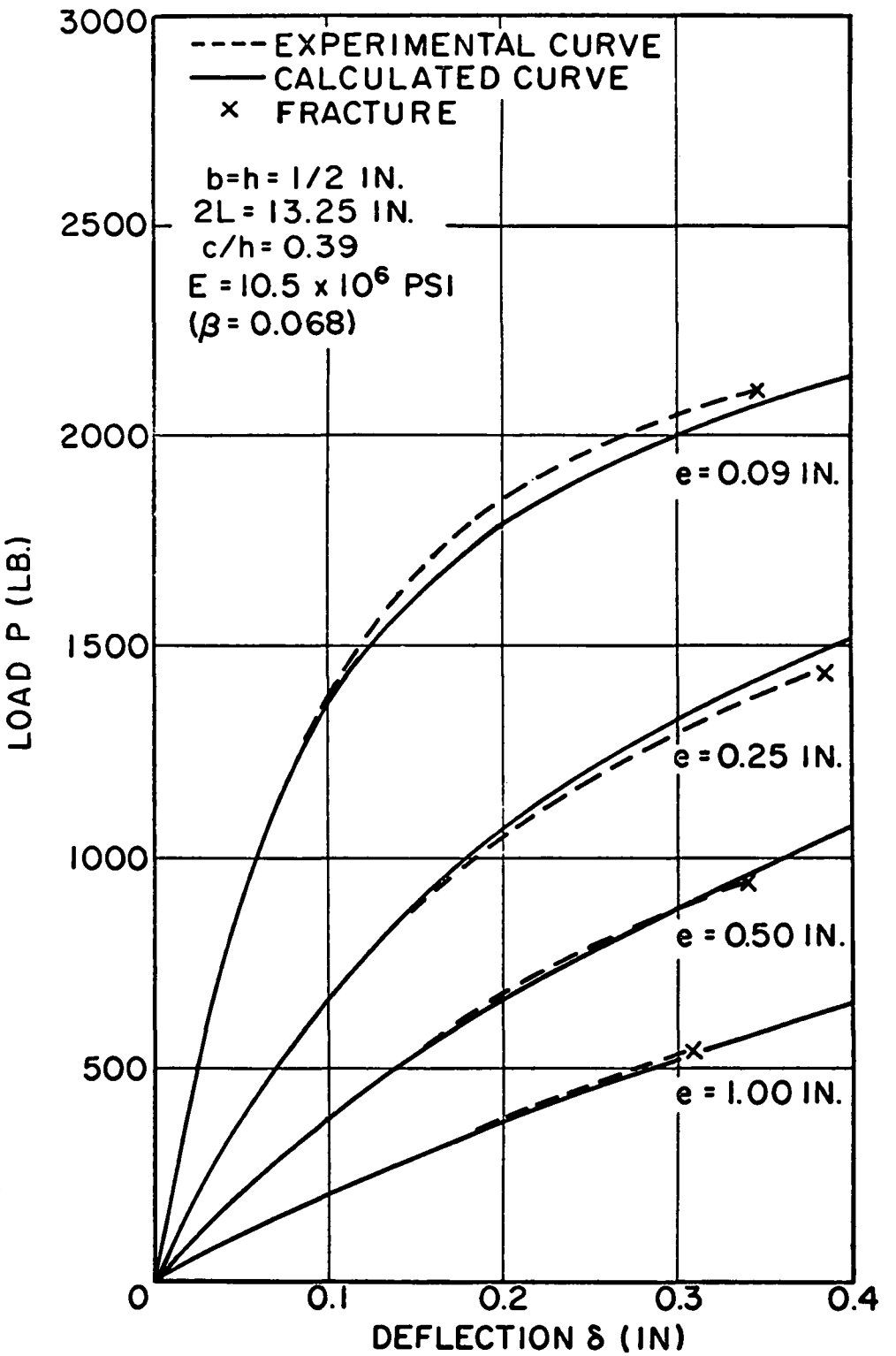

Figure 22. Load-deflection curve for a column with a 0.195-inch-deep with a fatigue crack extension

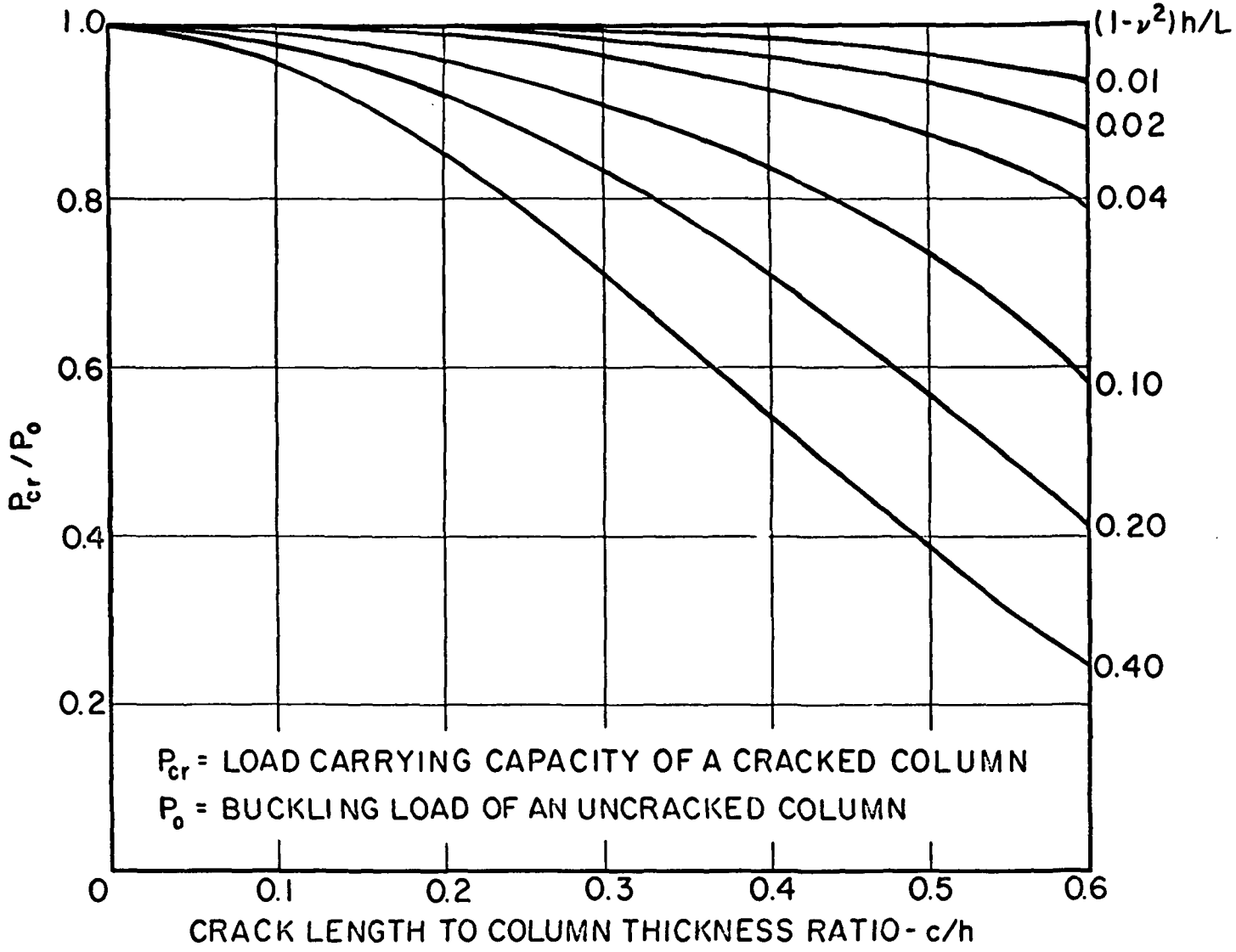

Figure 23. Load carrying capacity of a cracked column

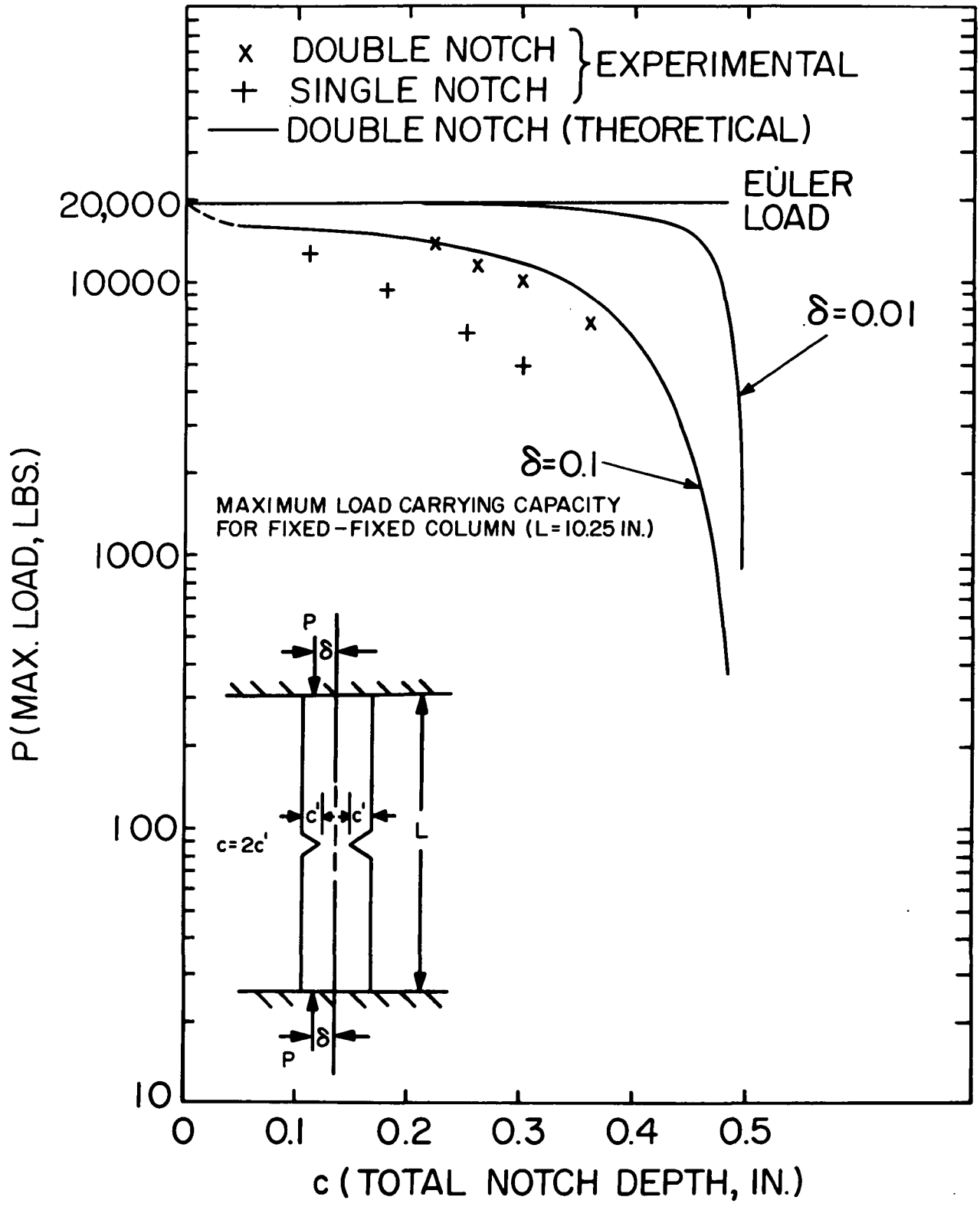

Figure 24. Maximum load vs. total notch depth in fixed-fixed column, $\delta = e = 0.01$, v.1, L=10.25

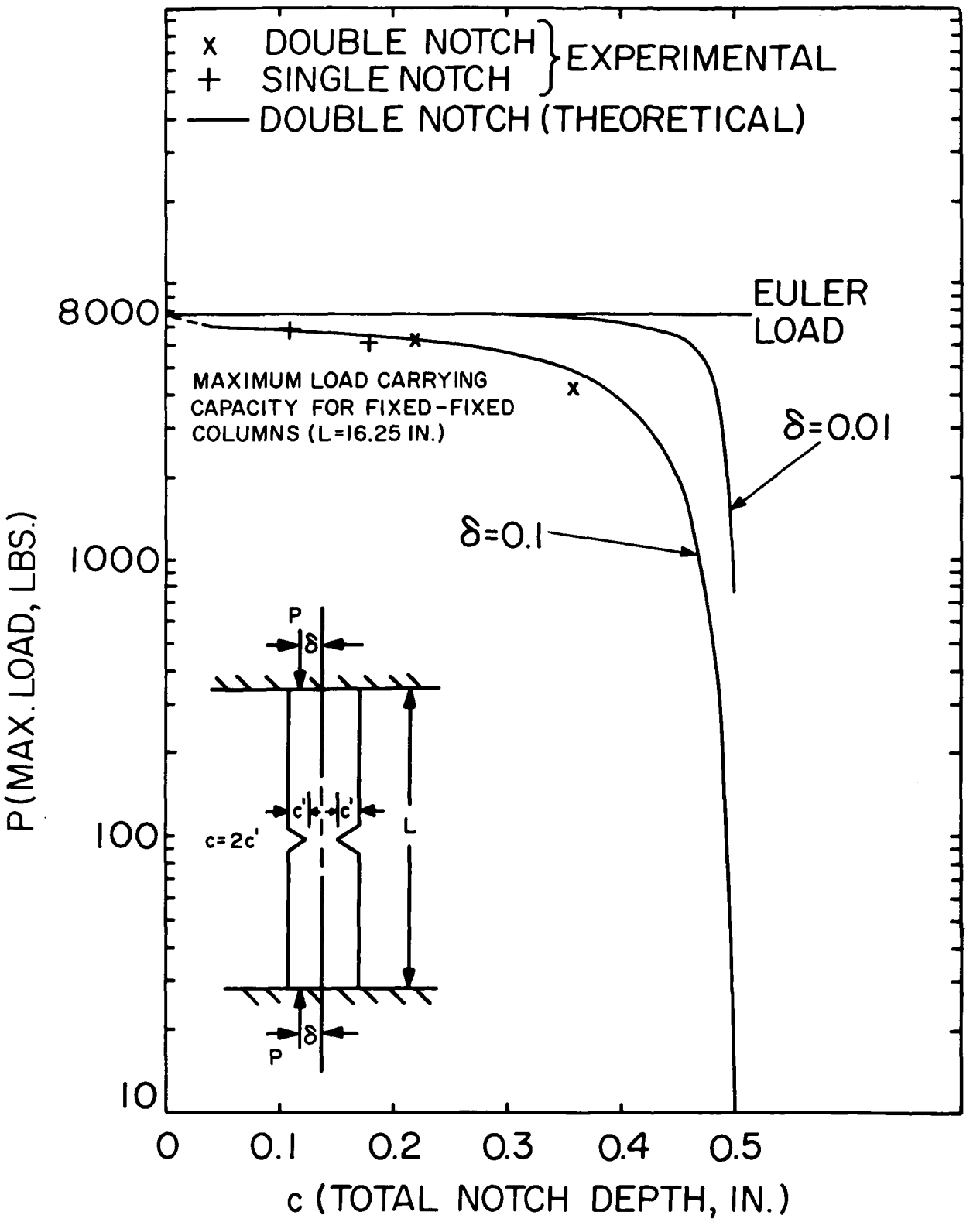

Figure 25. Maximum load vs. total notch depth in fixed-fixed column, δ=e=0.01, 0.1, L=16.25

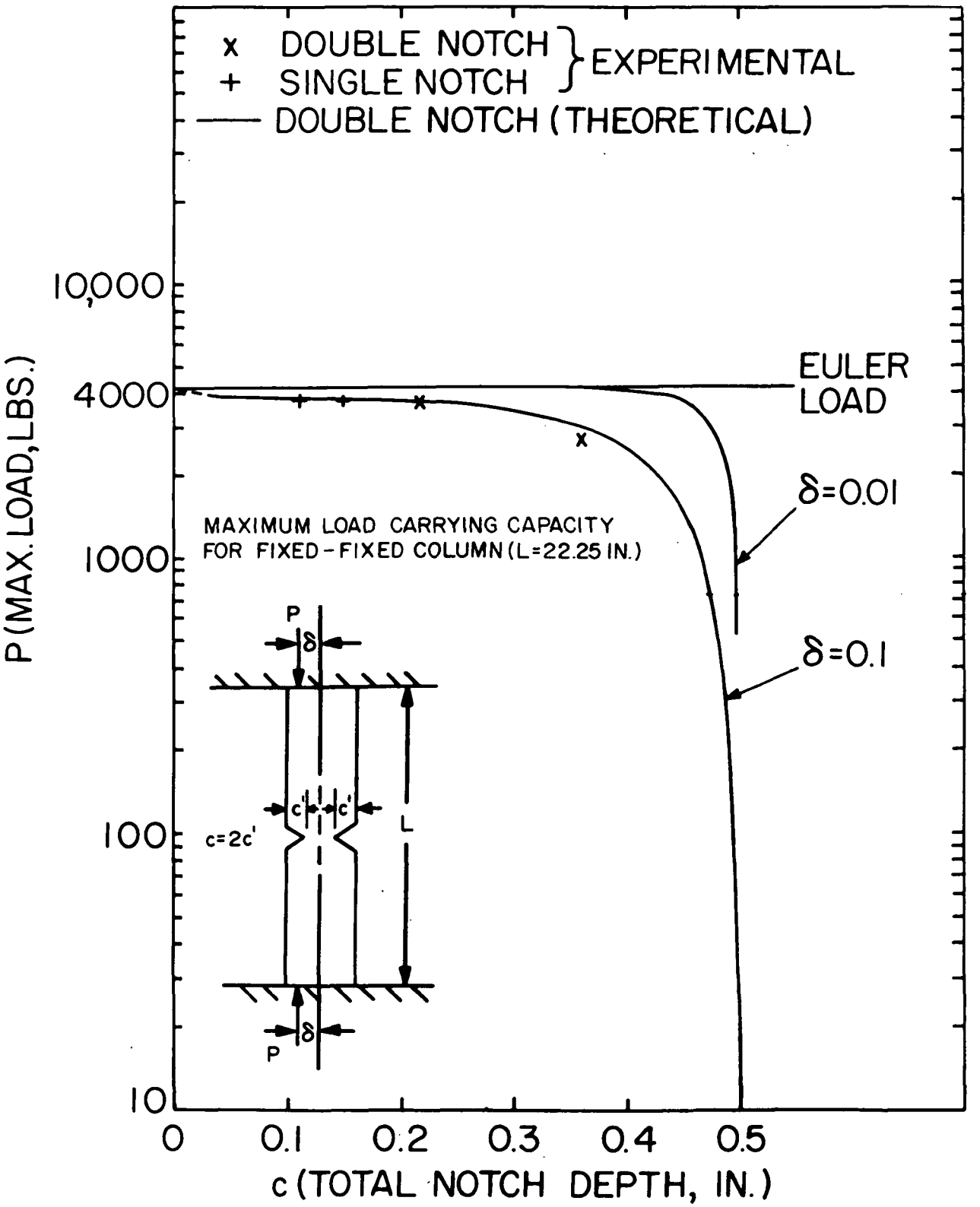

Figure 26. Maximum load vs. total notch depth in fixed-fixed column, $\delta = e = 0.01$, $L = 22.25$

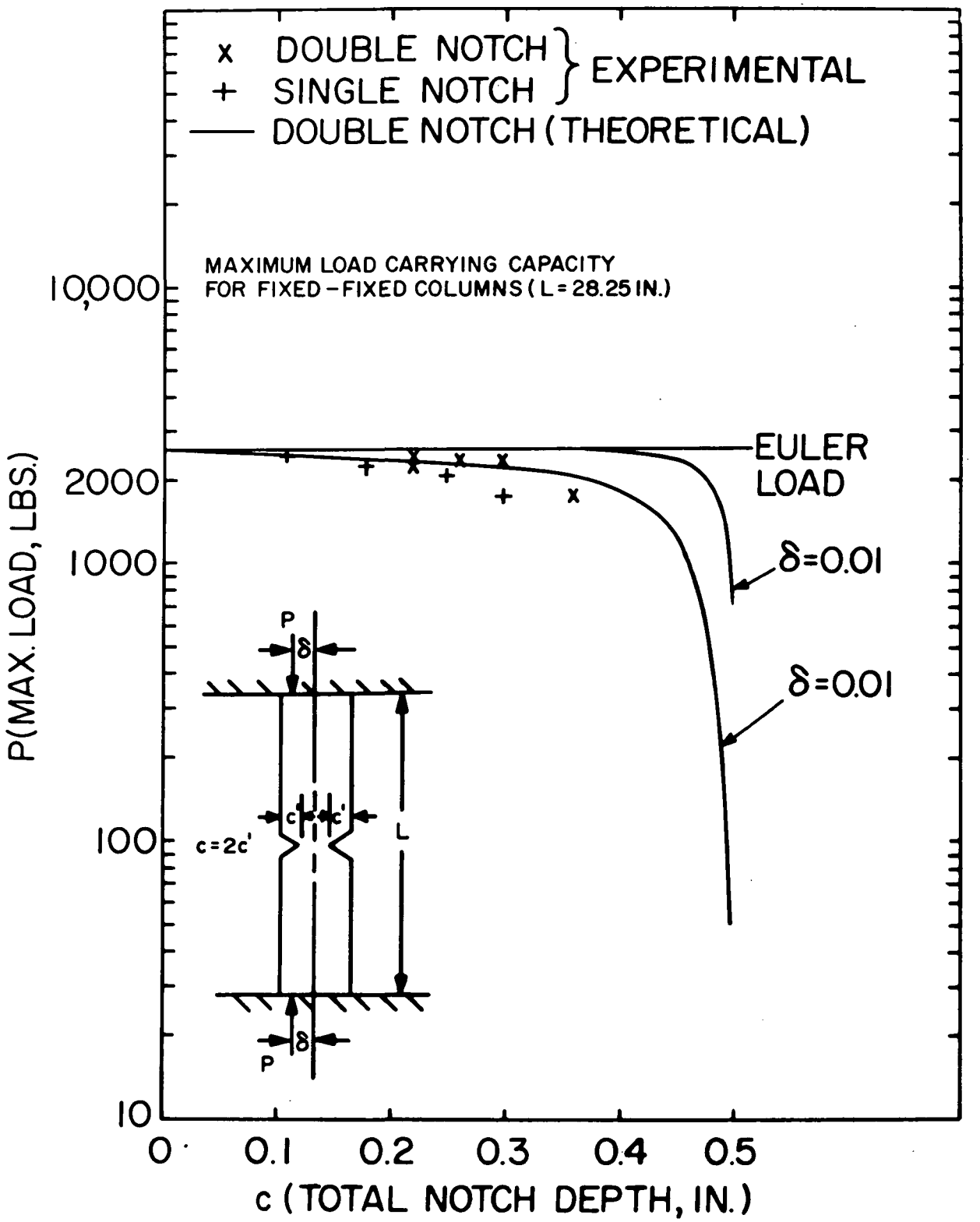

Figure 27. Maximum load vs. total notch depth in fixed-fixed column, $\delta = e = 0.01$, $L = 28.25$

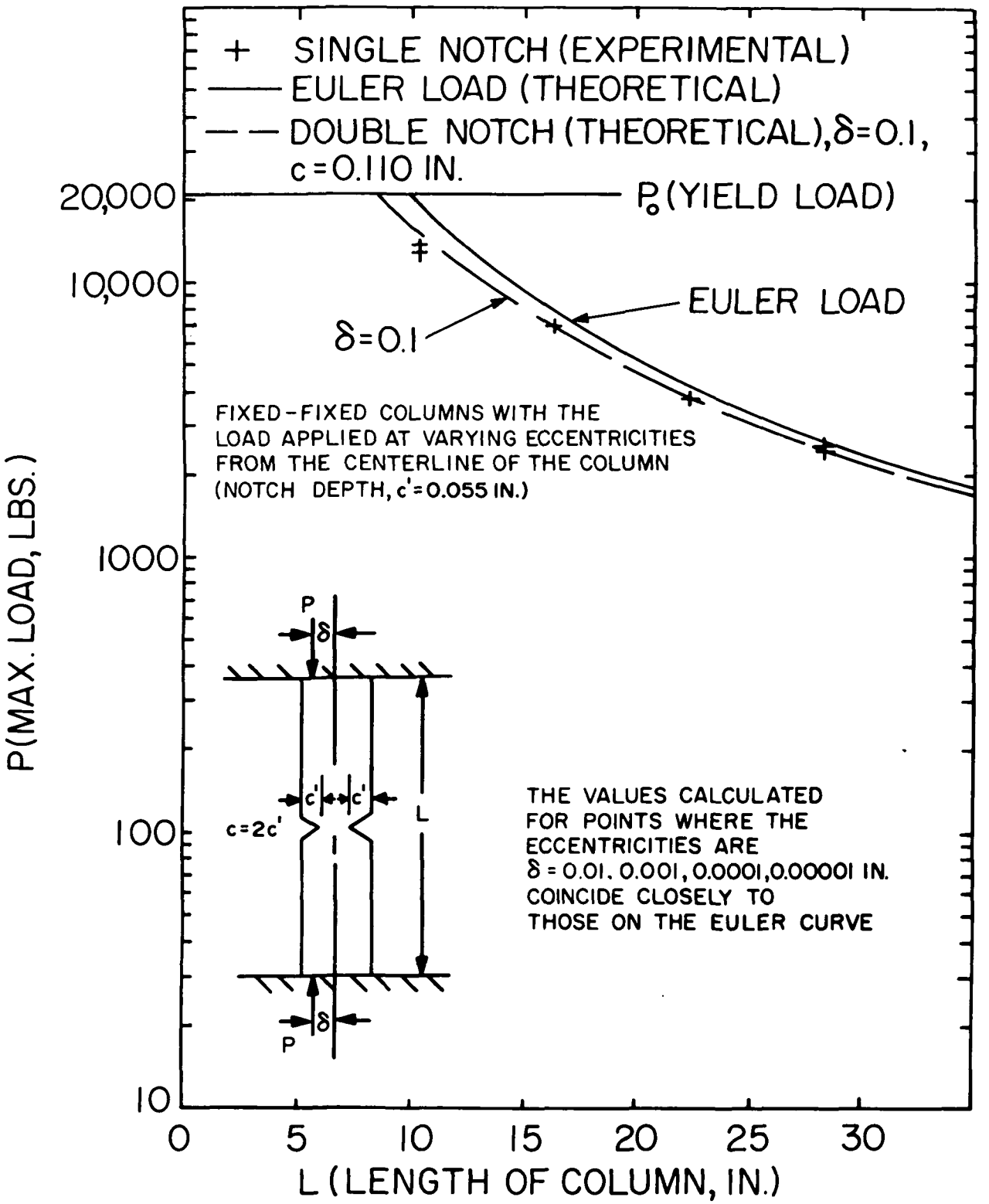

Figure 28. Maximum load vs. length of fixed-fixed column, $\delta = e = 0.1, c = 0.11$

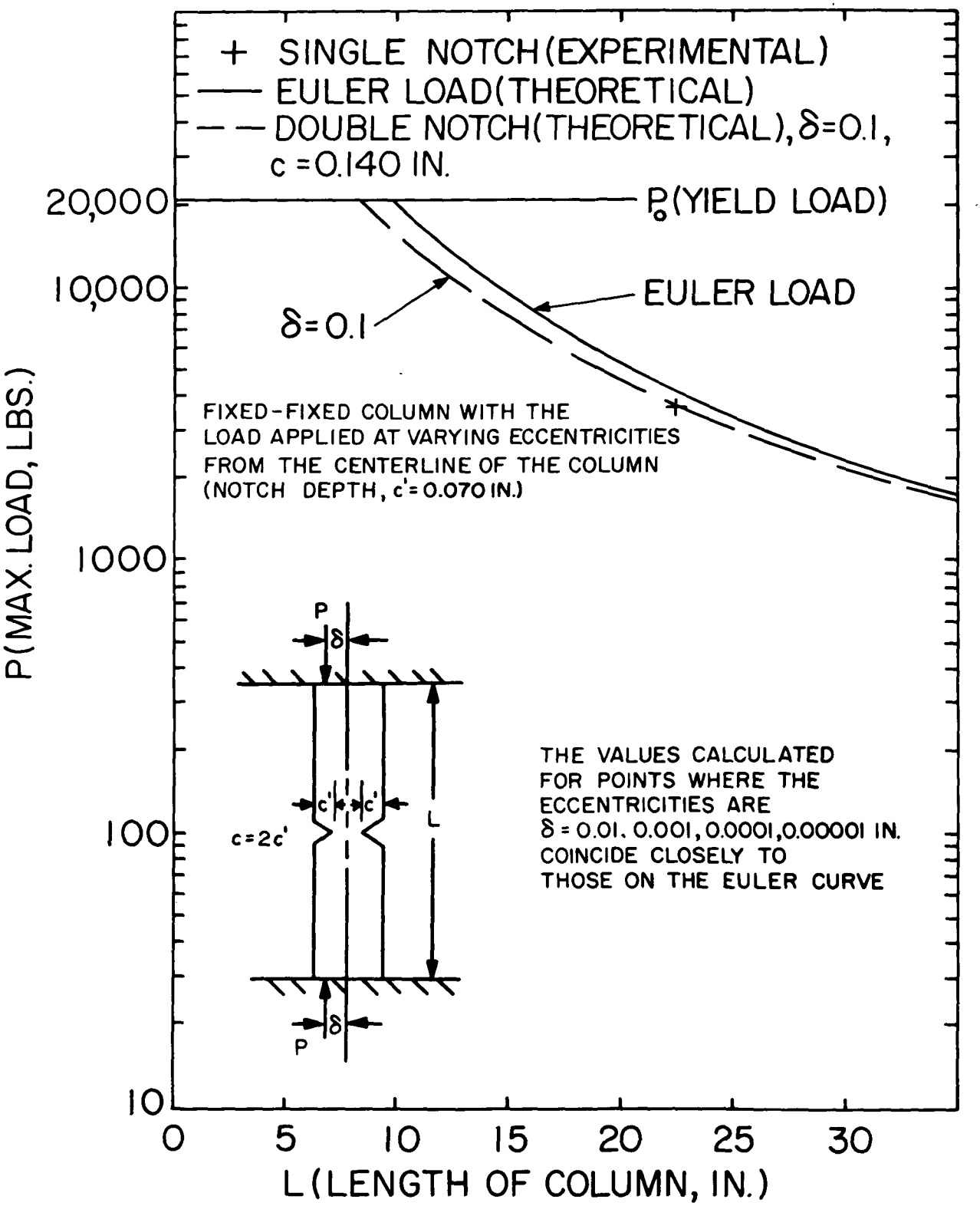

Figure 29. Maximum load vs. length of fixed-fixed column, $\delta = e = 0.1$, $c = 0.14$

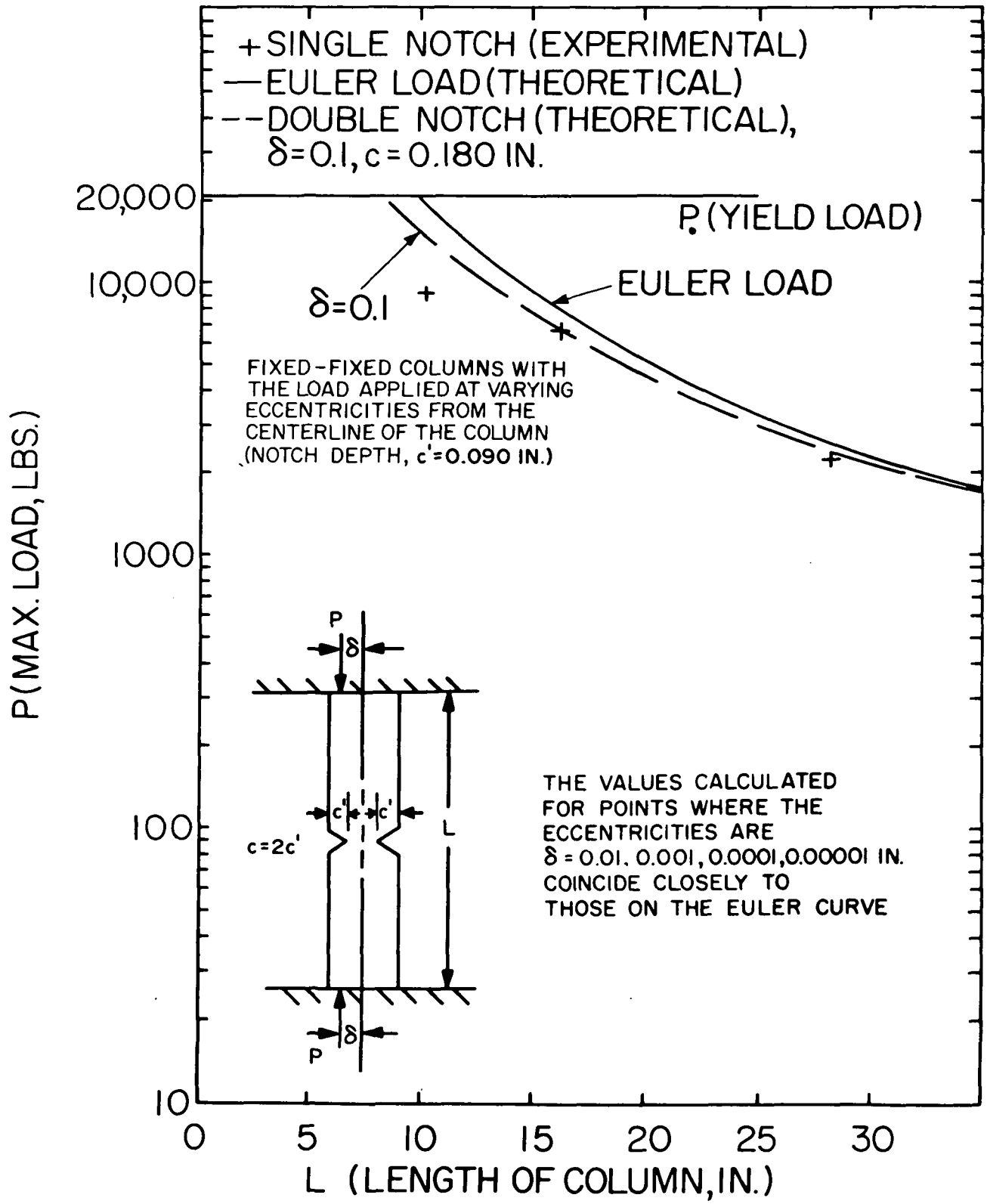

Figure 30. Maximum load vs. length of fixed-fixed column, $\delta = e = 0.1, c = 0.18$

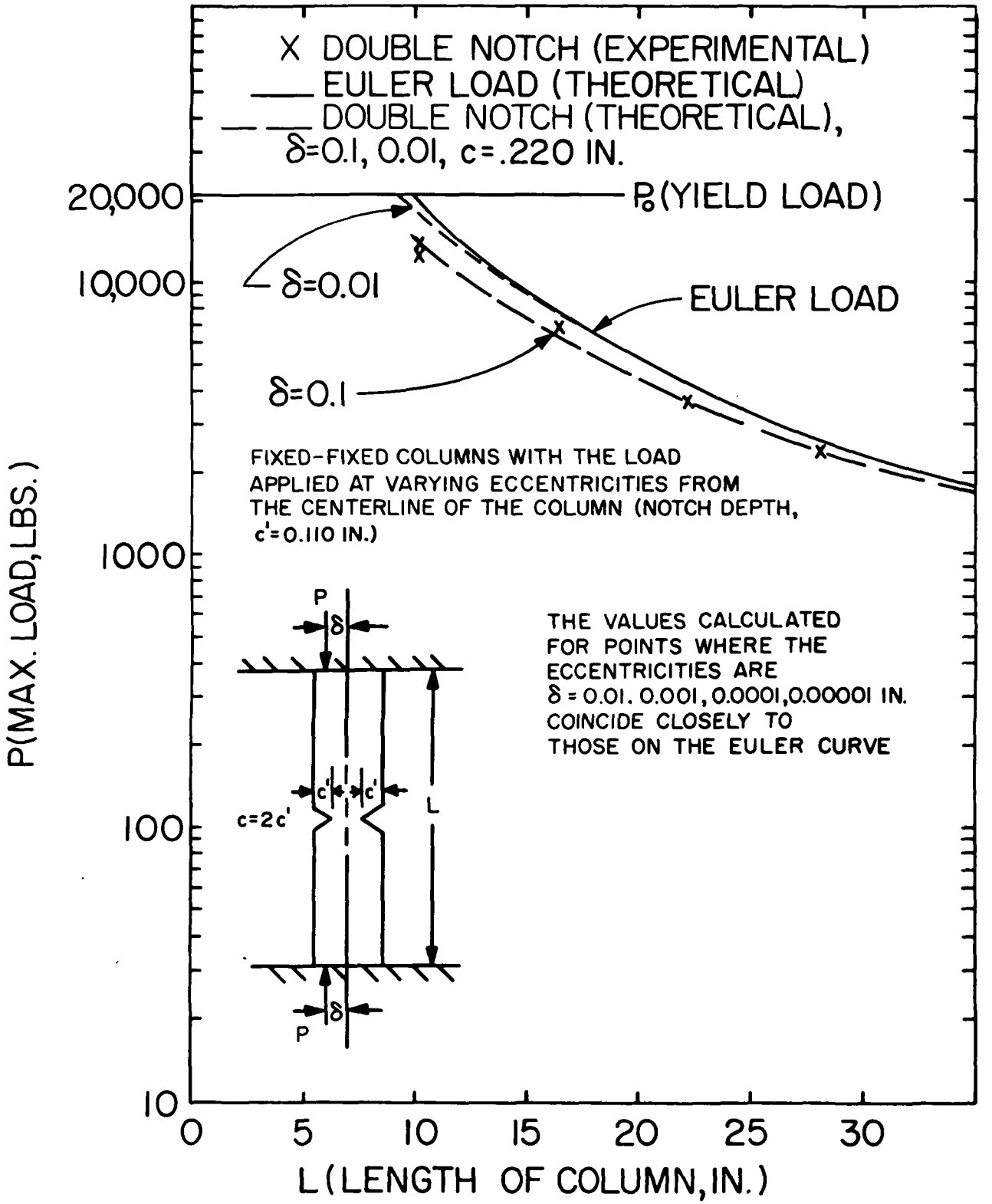

Figure 31. Maximum load vs. length of fixed-fixed column, $\delta = e = 0.1, 0.01, c = 0.22$

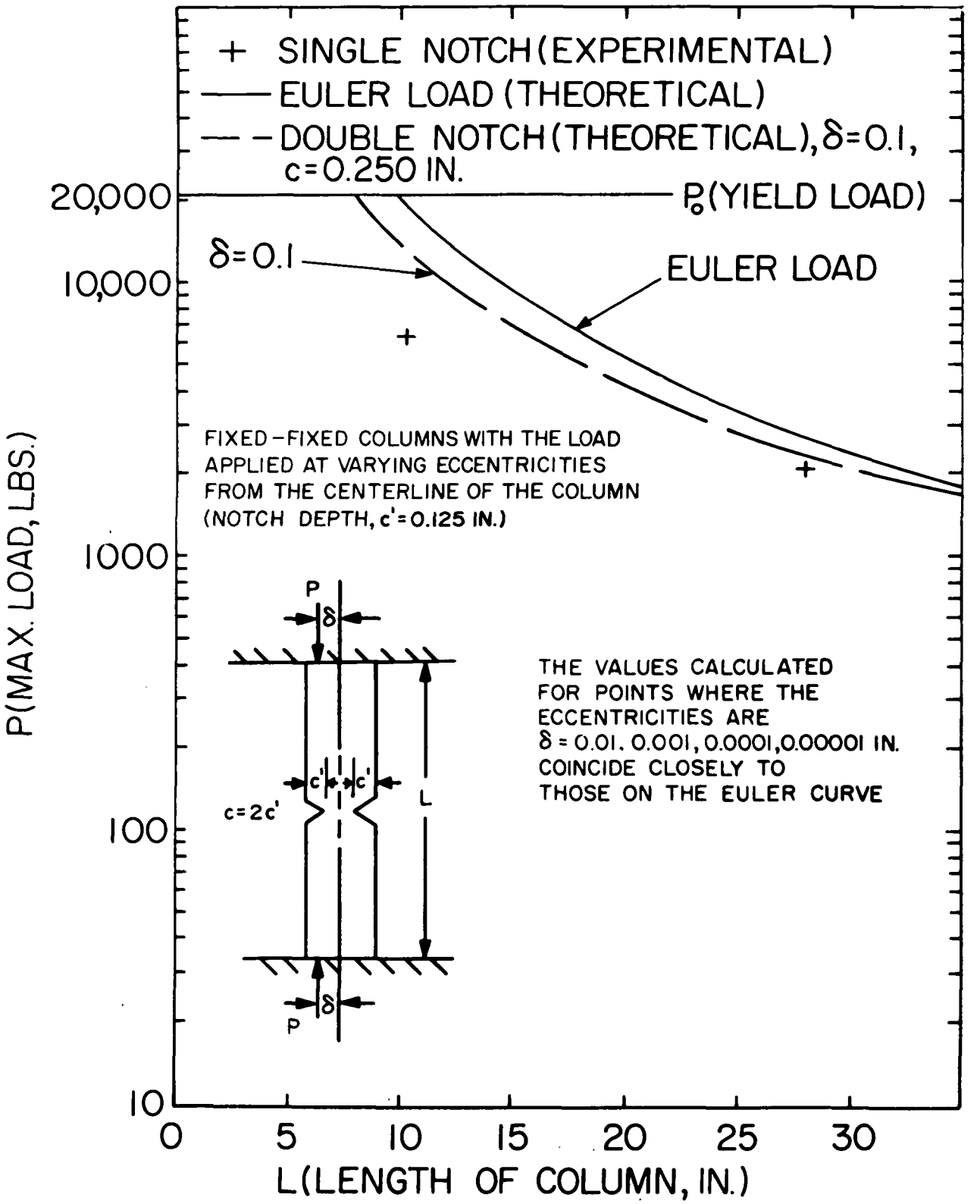

Figure 32. Maximum load vs. length of fixed-fixed column, $\delta=e=0.1, c=0.25$

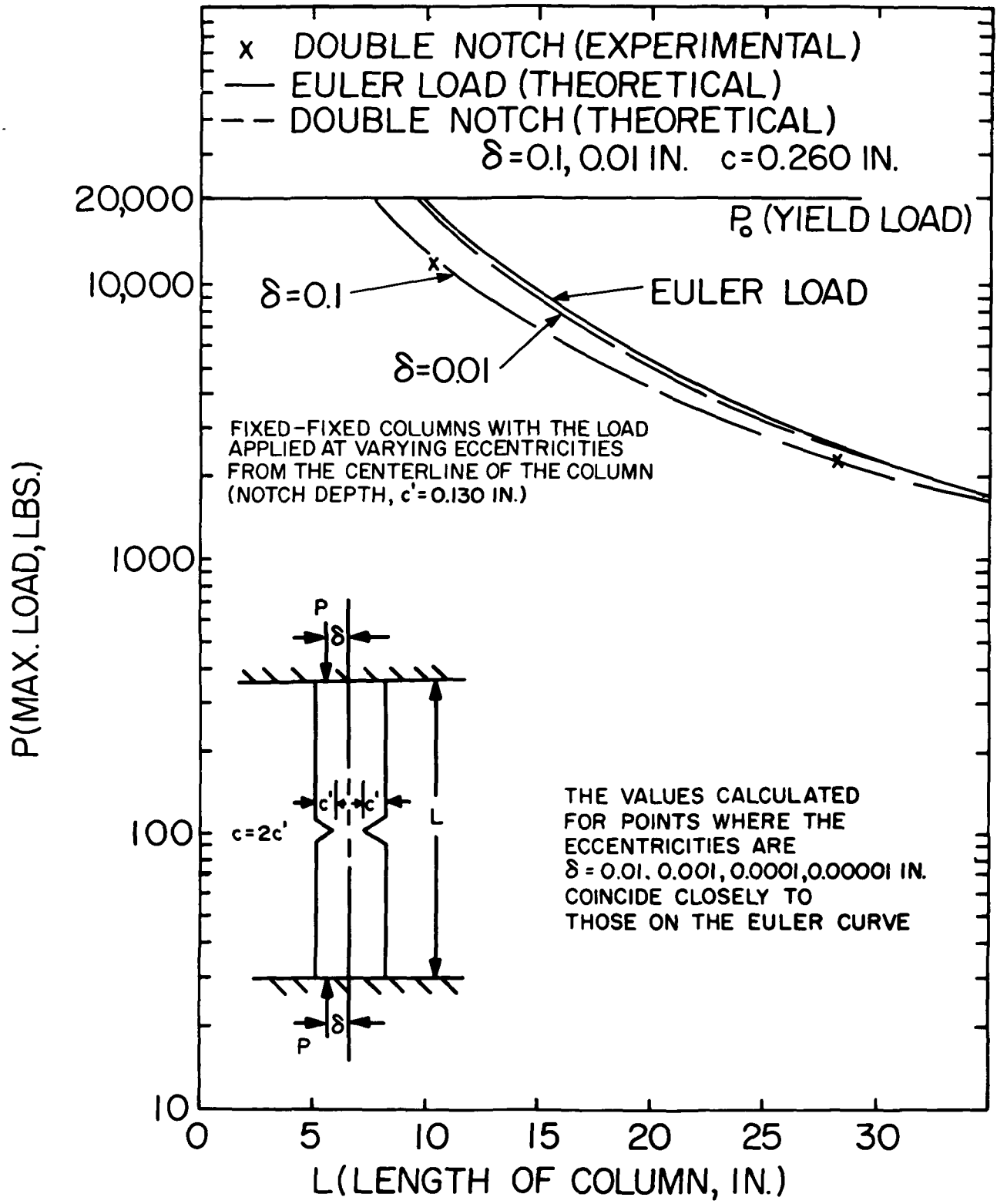

Figure 33. Maximum load vs. length of fixed-fixed column, $\delta = e = 0.1, 0.01, c = 0.26$

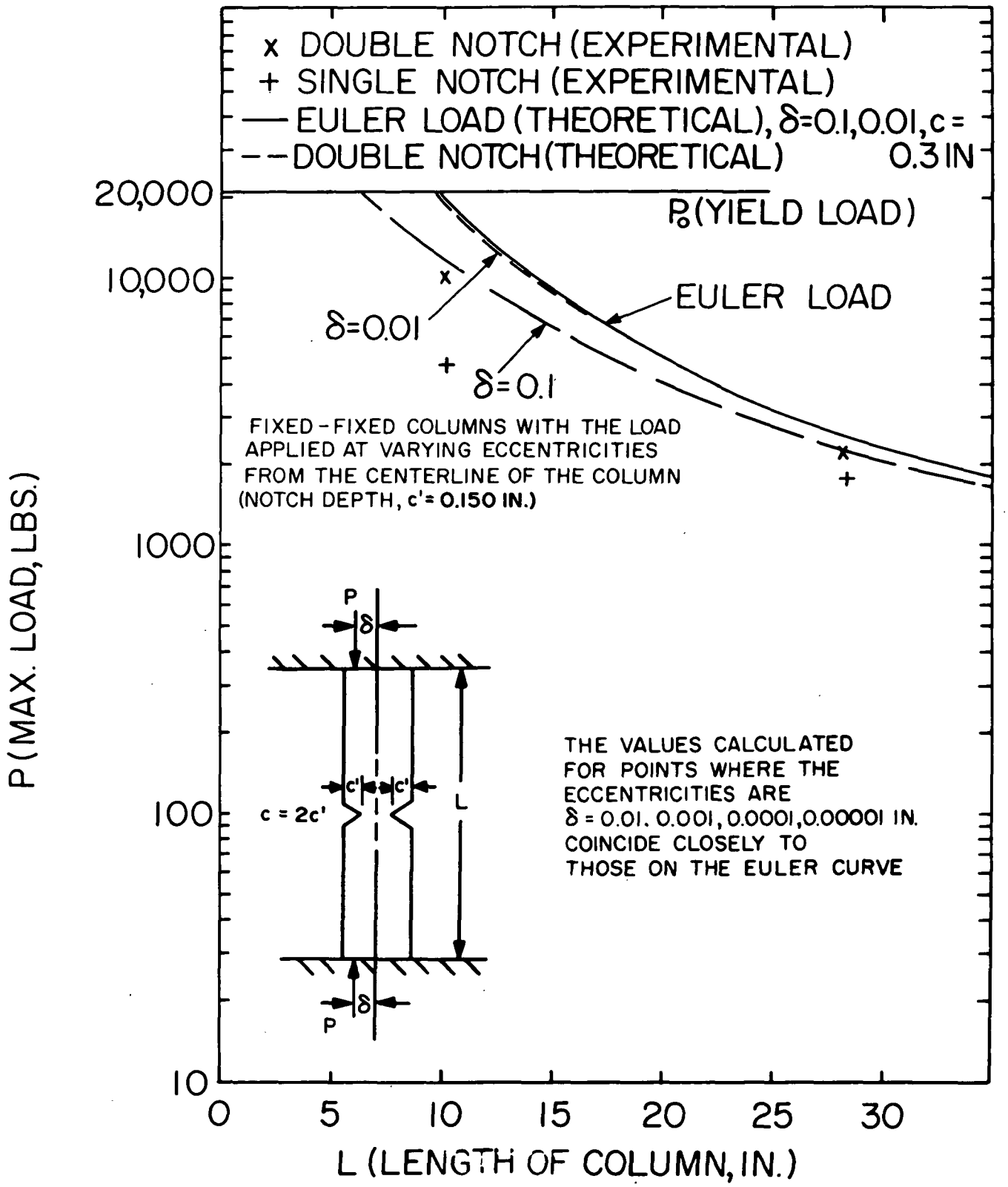

Figure 34. Maximum load vs. length of fixed-fixed column, $\delta = e = 0.1, 0.01, c = 0.30$

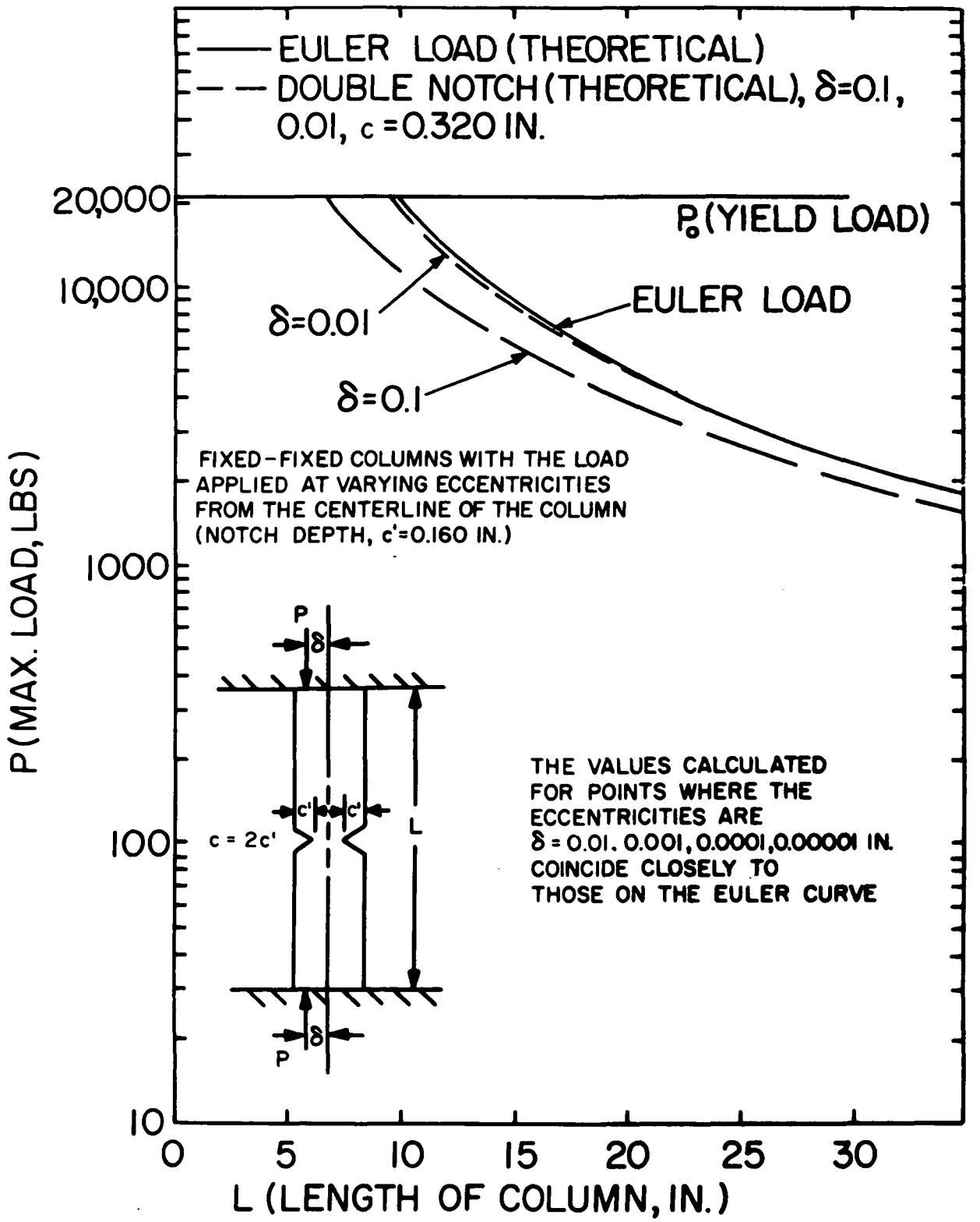

Figure 35. Maximum load vs. length of fixed-fixed column, $\delta = e = 0.1, 0.01, c = 0.32$

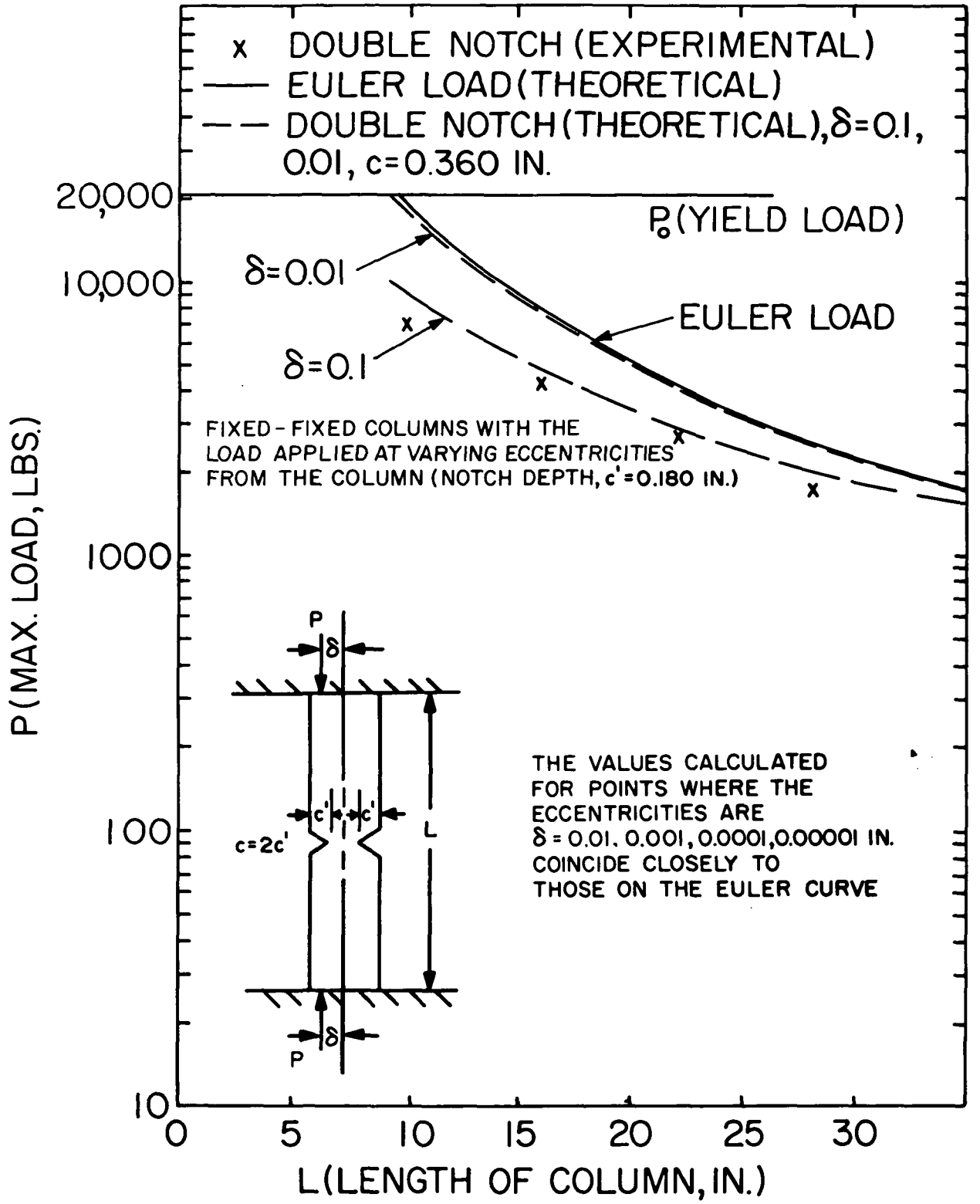

Figure 36. Maximum load vs. length of fixed-fixed column, $\delta = e = 0.1, 0.01, c = 0.36$

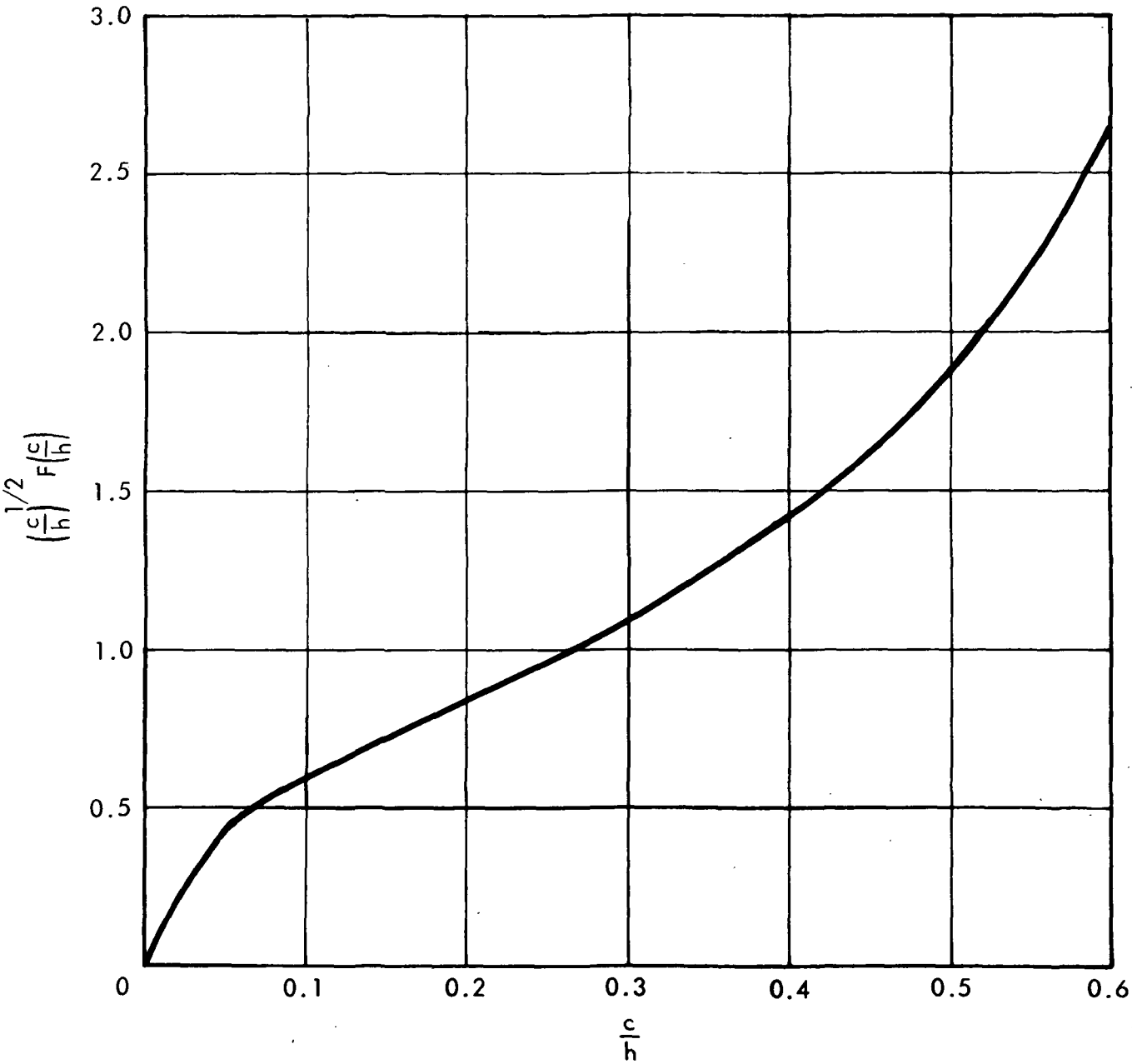

Figure 37. $(c/h)^{1/2}$ F (c/h) as a function of (c/h)

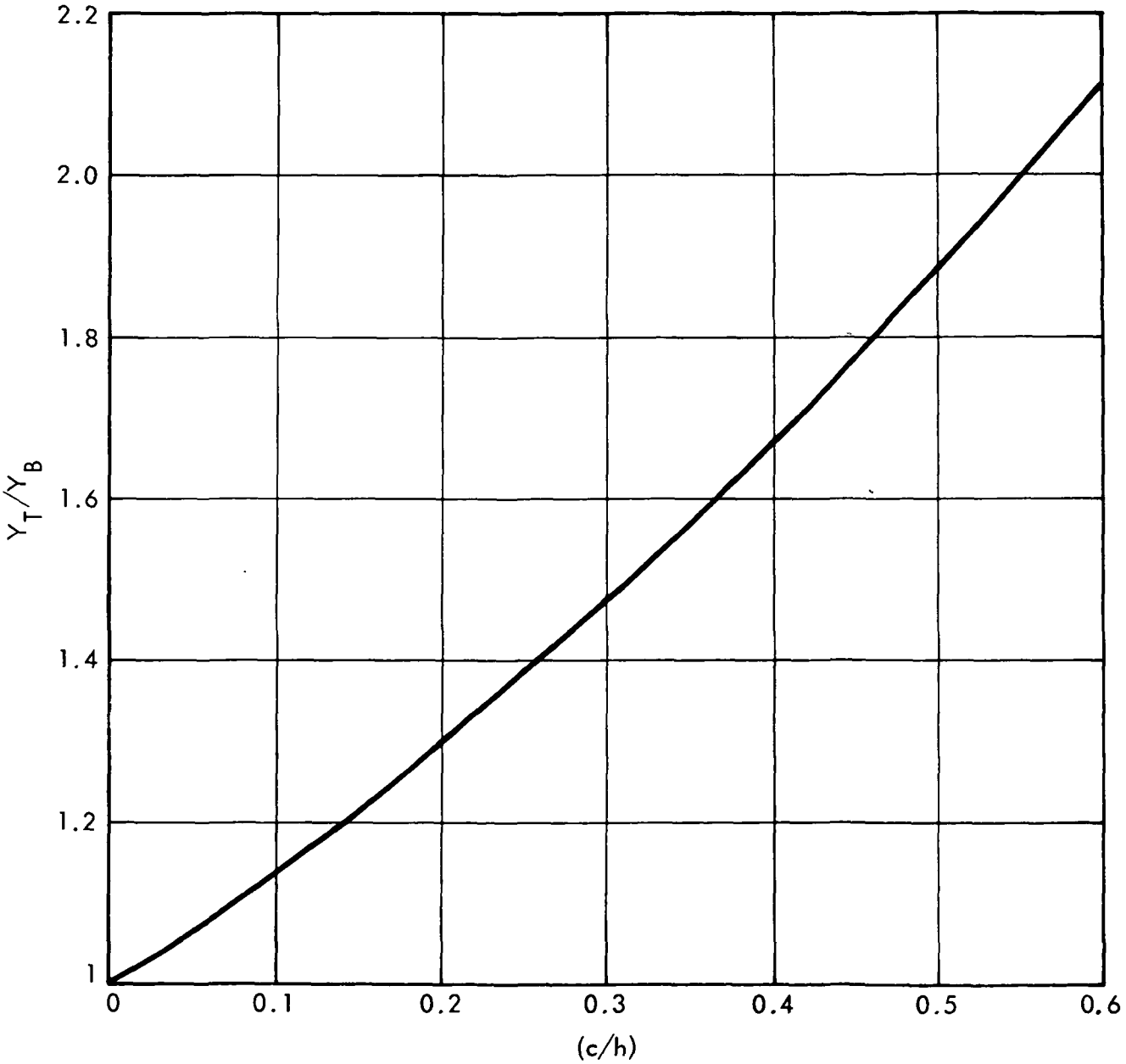

Figure 38. (Y_T/Y_B) as a function of (c/h)

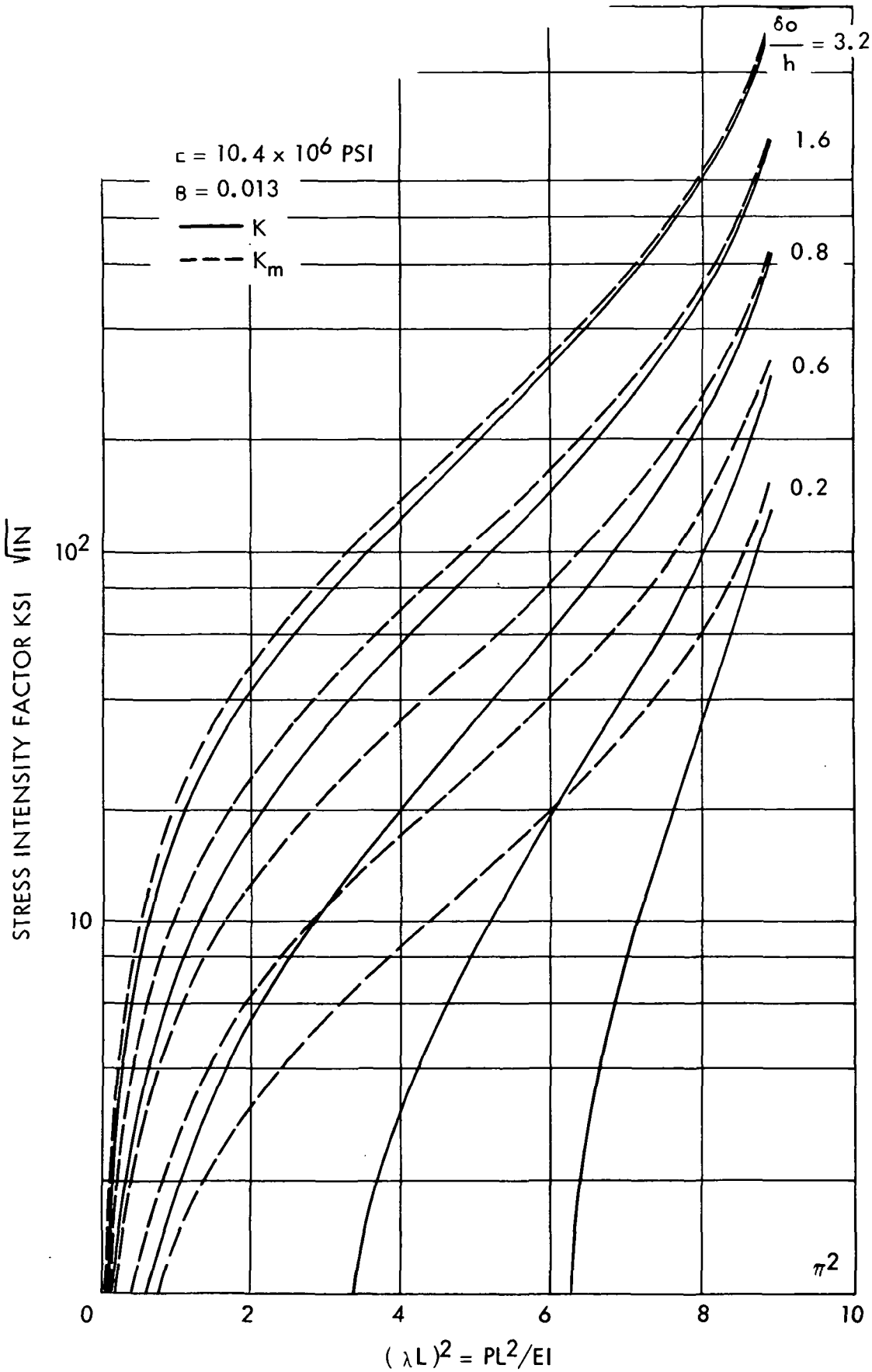

Figure 39. Stress intensity factor of a cracked column

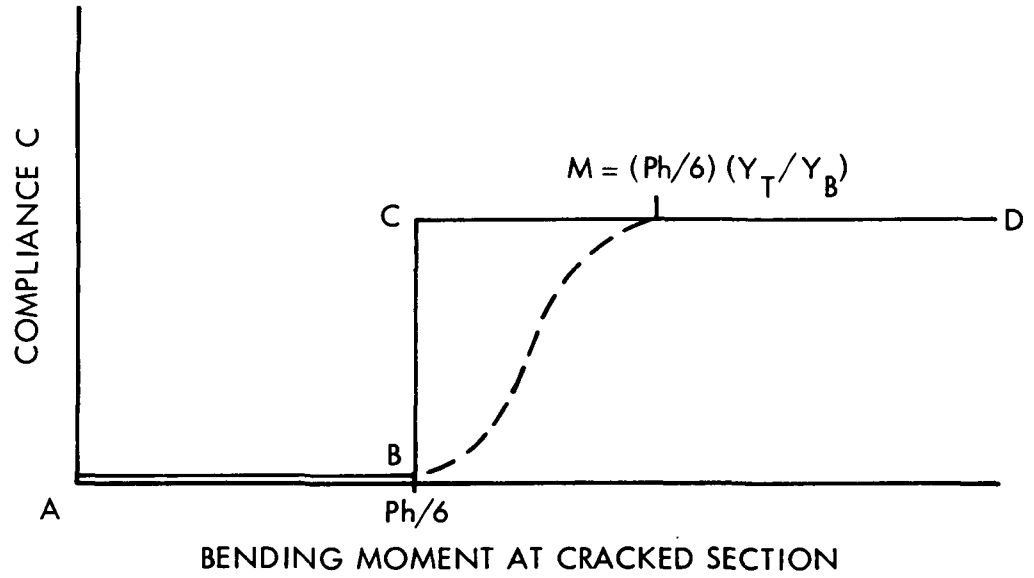

Figure 40. Compliance of a cracked column as influenced by bending moment at a cracked section

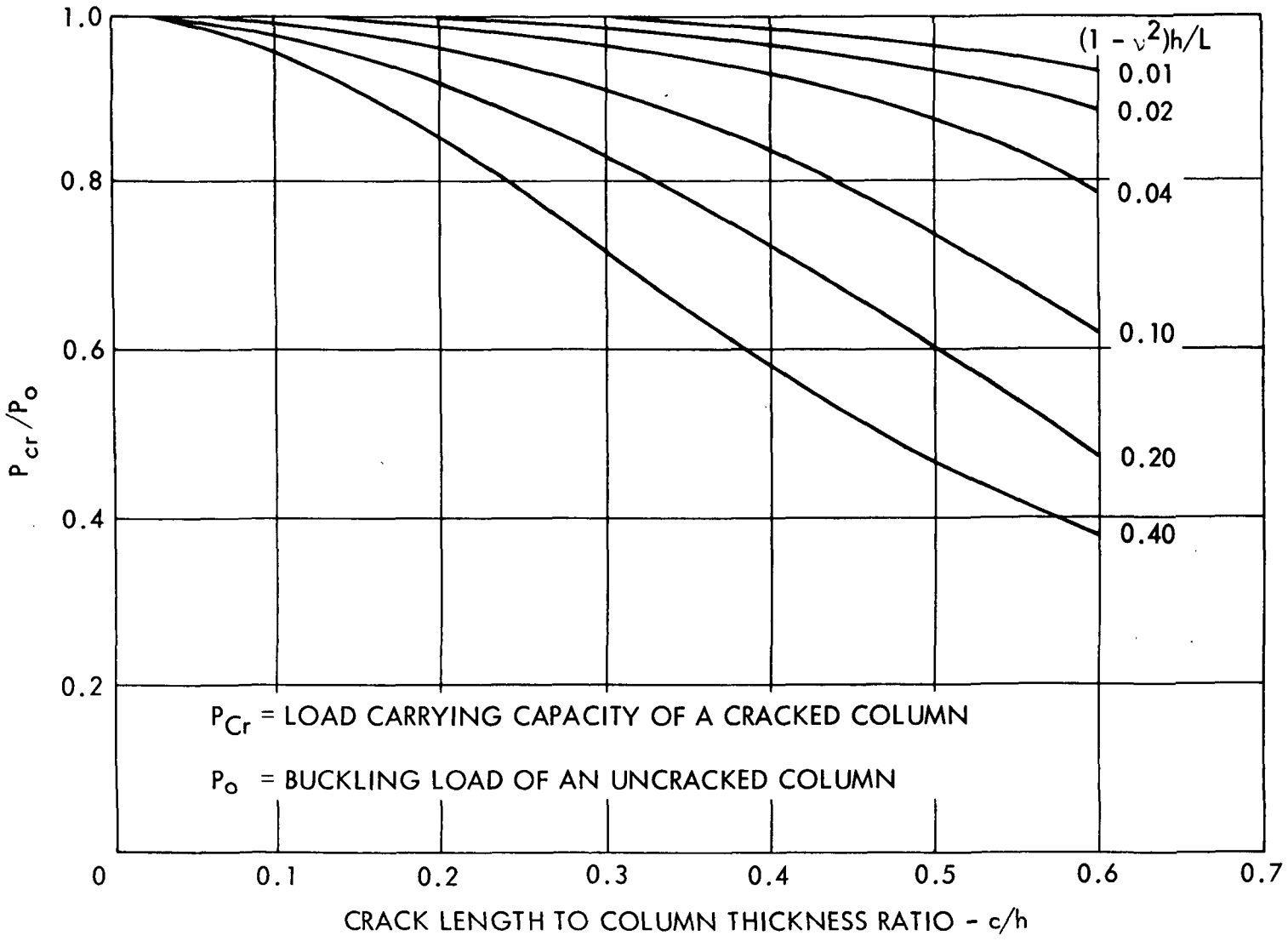

Figure 41. Load carrying capacity, P_{cr}, of a cracked column

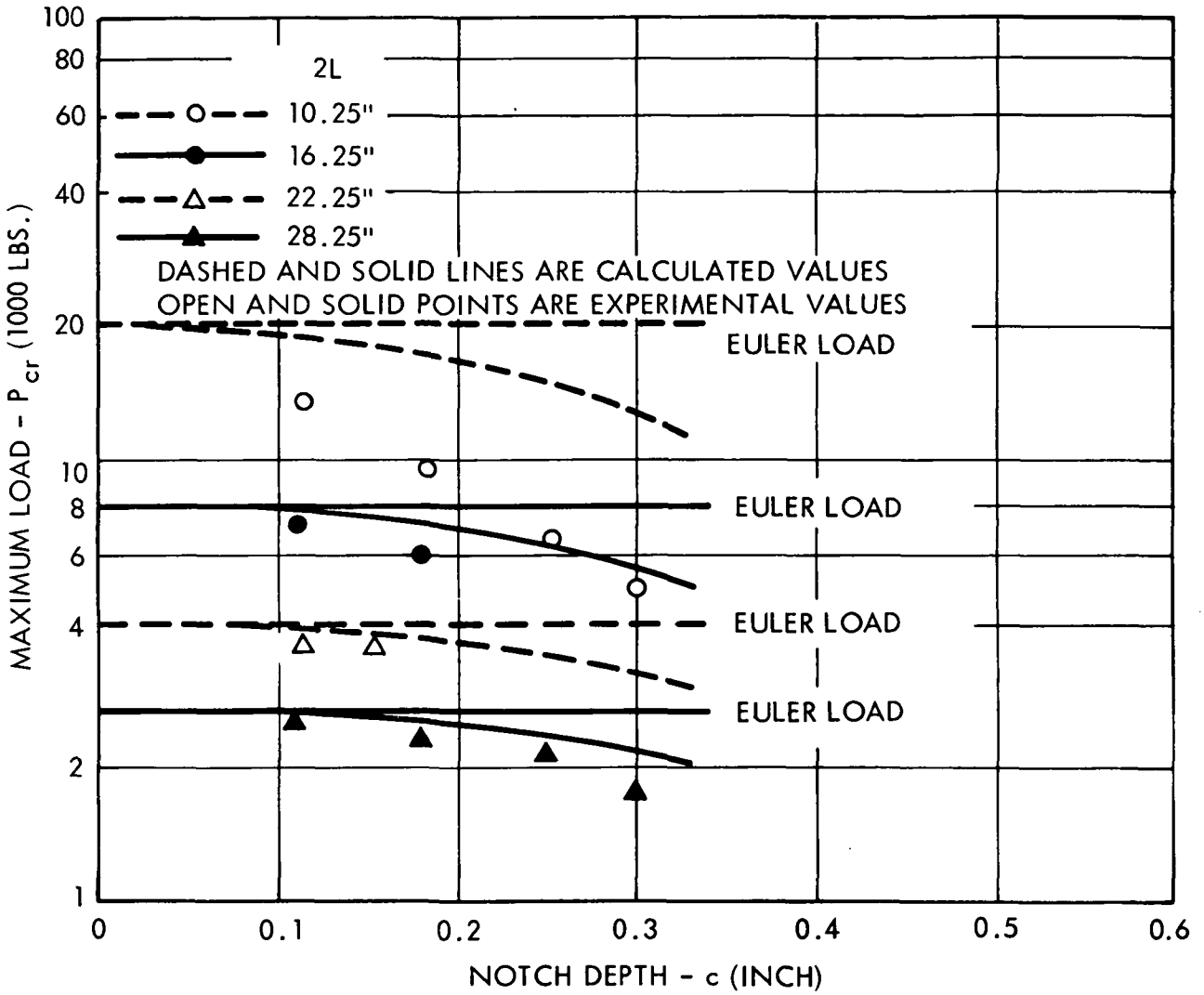

Figure 42. Load carrying capacity of single edge notched columns, (7075-T6AL)

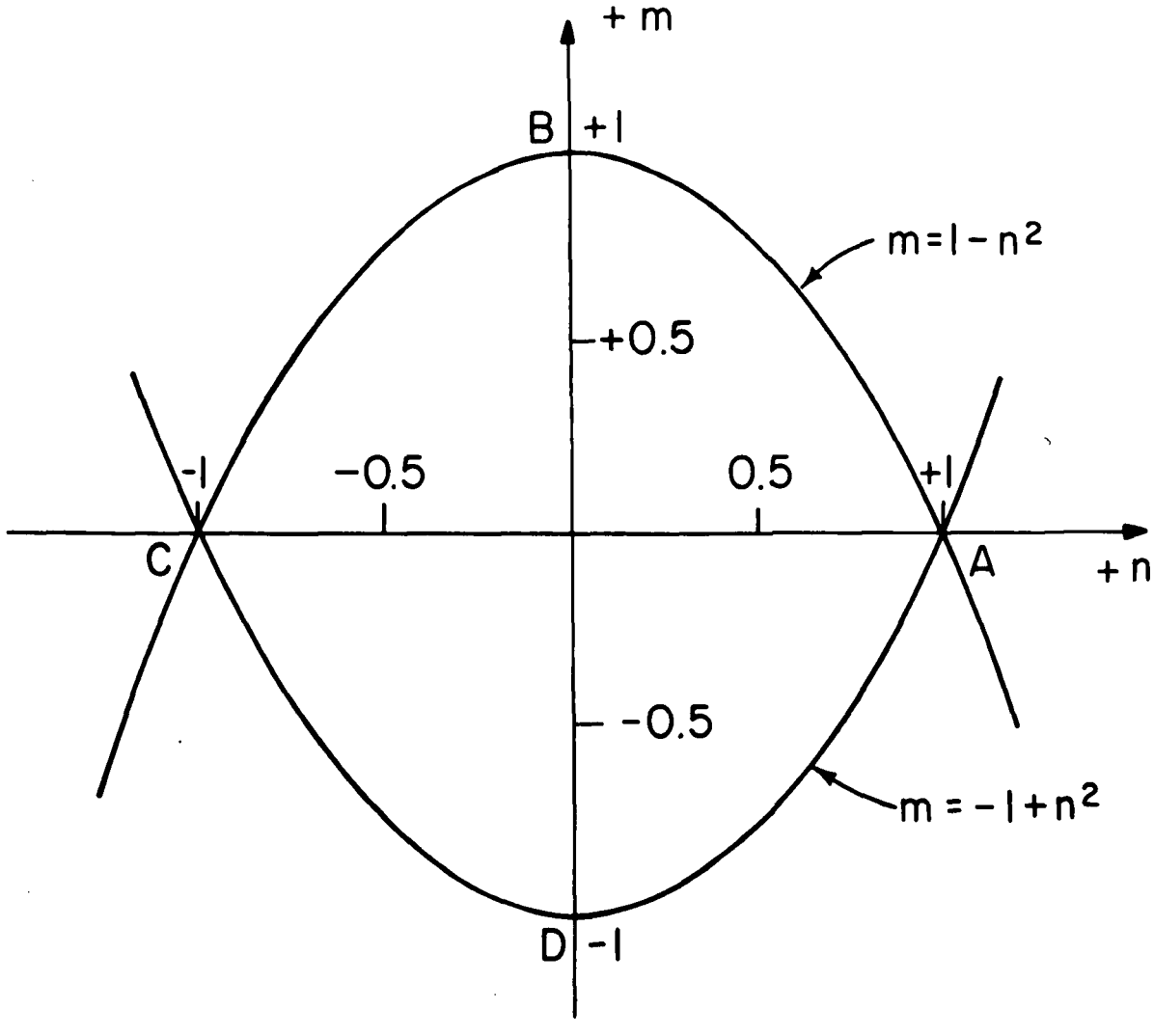

Figure 43. Interaction curve for combined axial force and bending

RATIO OF THE MAXIMUM COLUMN LOAD CARRYING CAPACITY, P_M, OVER THE COLUMN BUCKLING LOAD, P_B, VERSUS THE RATIO OF THE TOTAL NOTCH DEPTH, c, OVER THE COLUMN WIDTH, h, FOR DOUBLE NOTCHED FIXED-PINNED END COLUMNS WITH A COLUMN LENGTH, L = 11.75 IN. P_B IS DETERMINED EXPERIMENTALLY, P_B = 7540 LBS.

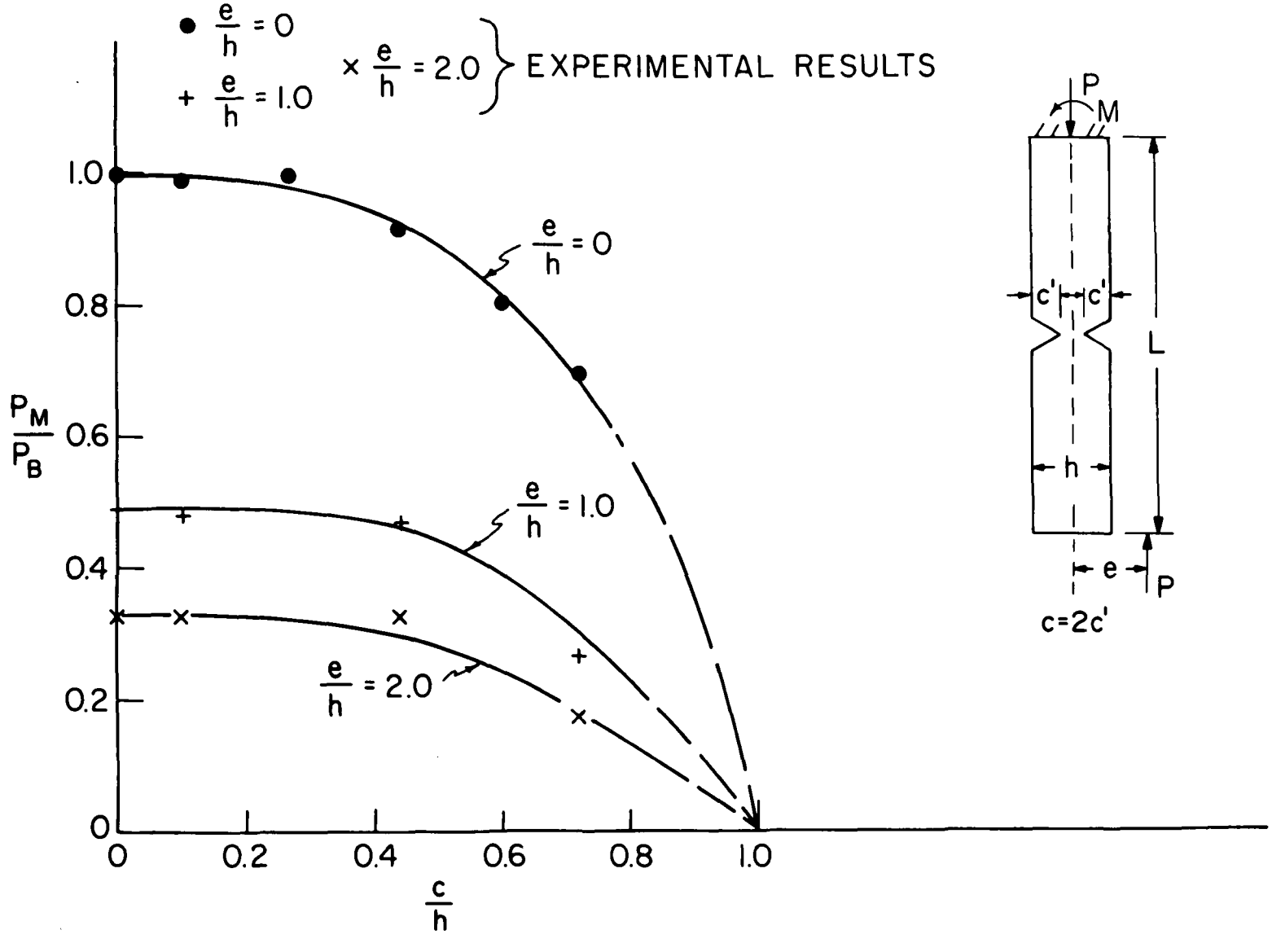

Figure 44. (P_M/P_B) vs. (c/h), when column is double-notched and L=11.75

RATIO OF THE MAXIMUM COLUMN LOAD CARRYING CAPACITY, P_M, OVER THE COLUMN BUCKLING LOAD, P_B, VERSUS THE RATIO OF THE TOTAL NOTCH DEPTH, c, OVER THE COLUMN WIDTH, h, FOR SINGLE NOTCHED FIXED-PINNED END COLUMNS WITH A COLUMN LENGTH, L = 11.75 IN.

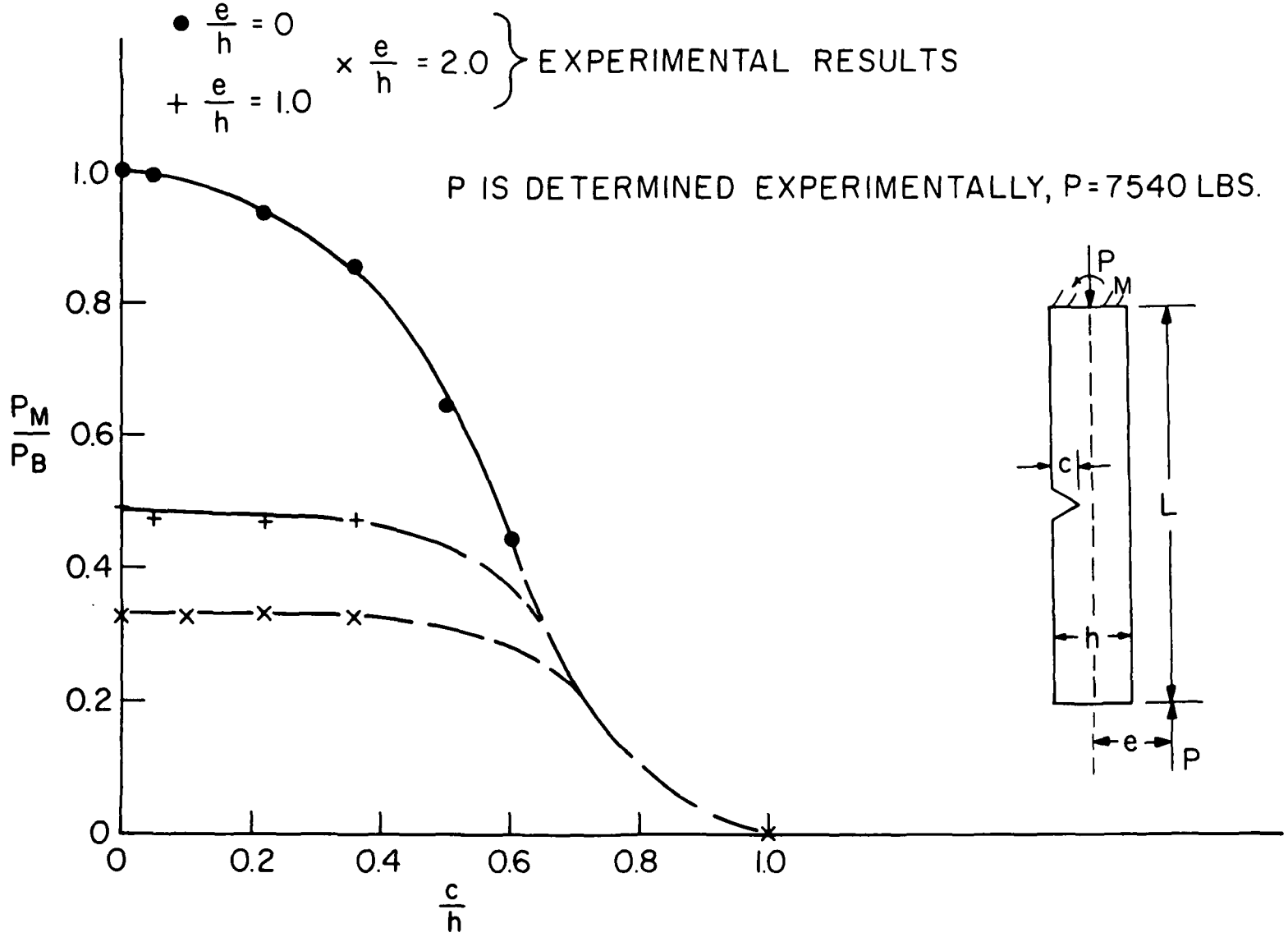

Figure 45. (P_M/P_B) vs. (c/h), when column is single-notched and L=11.75

RATIO OF THE MAXIMUM COLUMN LOAD CARRYING CAPACITY, P_M, OVER THE COLUMN BUCKLING LOAD, P_B, VERSUS THE RATIO OF THE TOTAL NOTCH DEPTH, c, OVER THE COLUMN WIDTH, h, FOR DOUBLE NOTCHED FIXED-PINNED END COLUMNS WITH A COLUMN LENGTH, L = 29.75 IN.

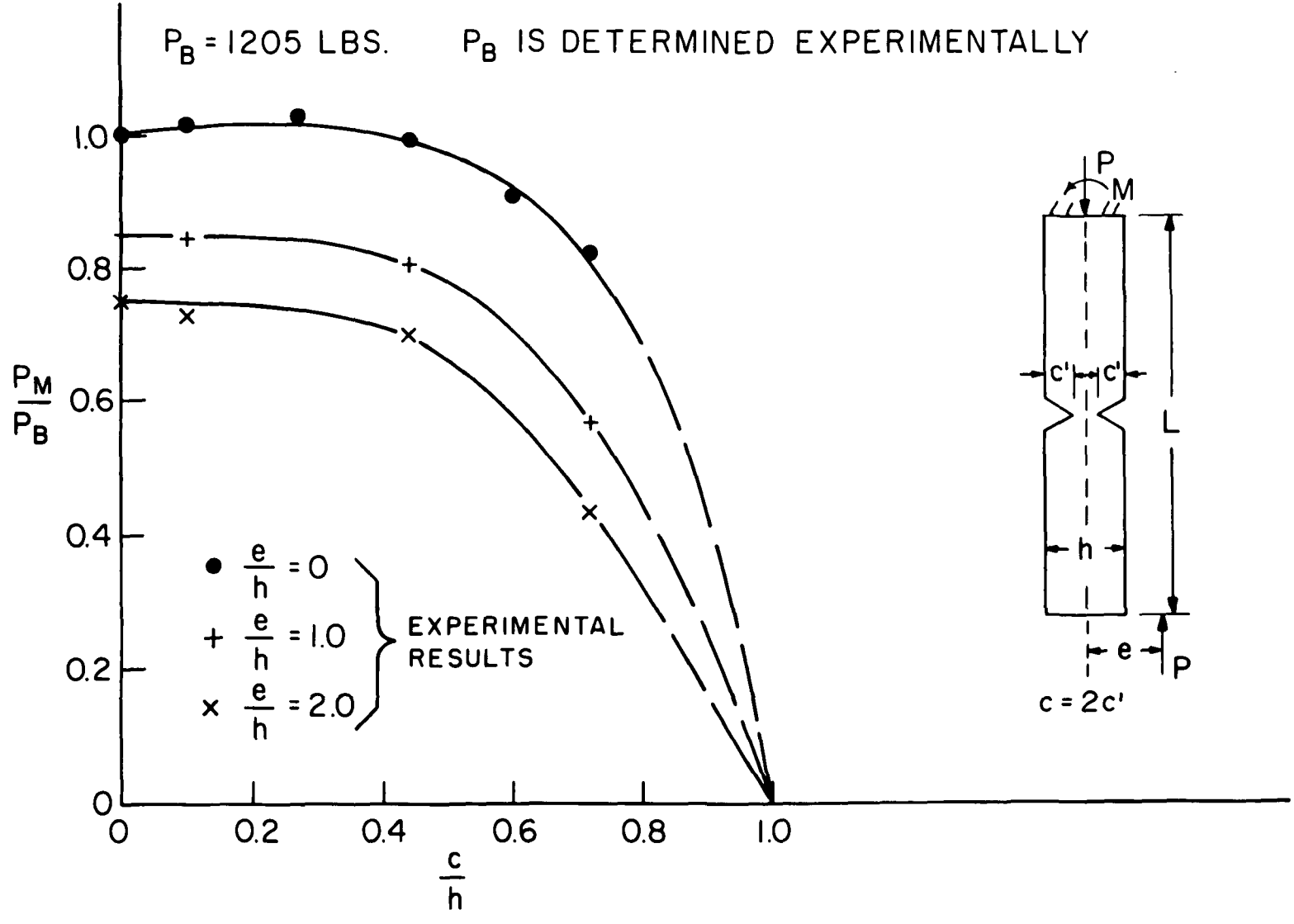

Figure 46. (P_M/P_B) vs. (c/h), when column is double-notched and L=29.75

RATIO OF THE MAXIMUM COLUMN LOAD CARRYING CAPACITY, P_M, OVER THE COLUMN BUCKLING LOAD, P_B, VERSUS THE RATIO OF THE TOTAL NOTCH DEPTH, c, OVER THE COLUMN WIDTH, h, FOR SINGLE NOTCHED FIXED-PINNED END COLUMNS WITH A COLUMN LENGTH, L = 29.75 IN.

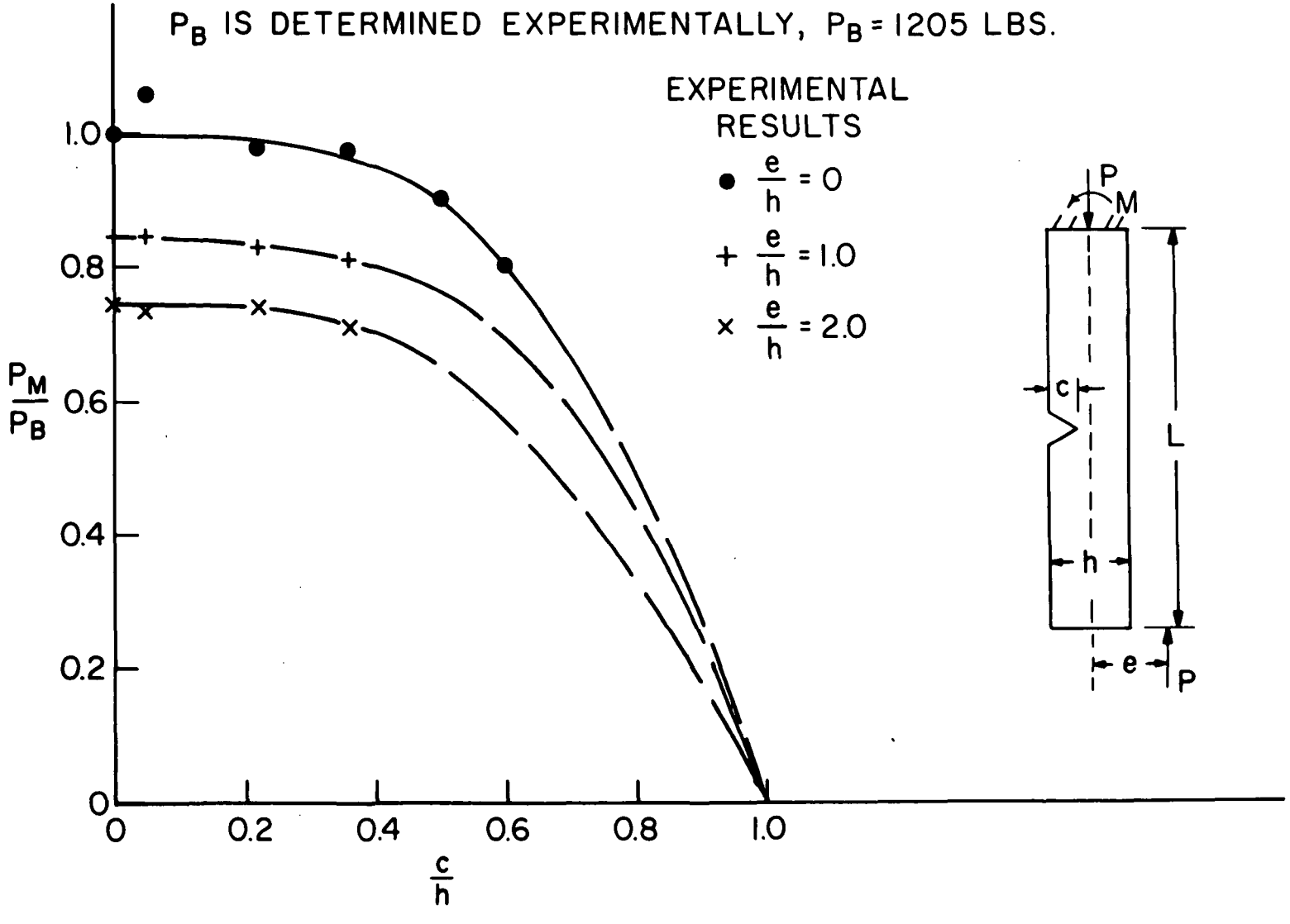

Figure 47. (P_M/P_B) vs. (c/h), when column is single-notched and L=29.75

RATIO OF THE MAXIMUM COLUMN LOAD CARRYING CAPACITY, P_M, OVER THE COLUMN BUCKLING LOAD, P_B, VERSUS THE SLENDERNESS RATIO, L/ρ, FOR DOUBLE NOTCHED FIXED-PINNED END COLUMNS

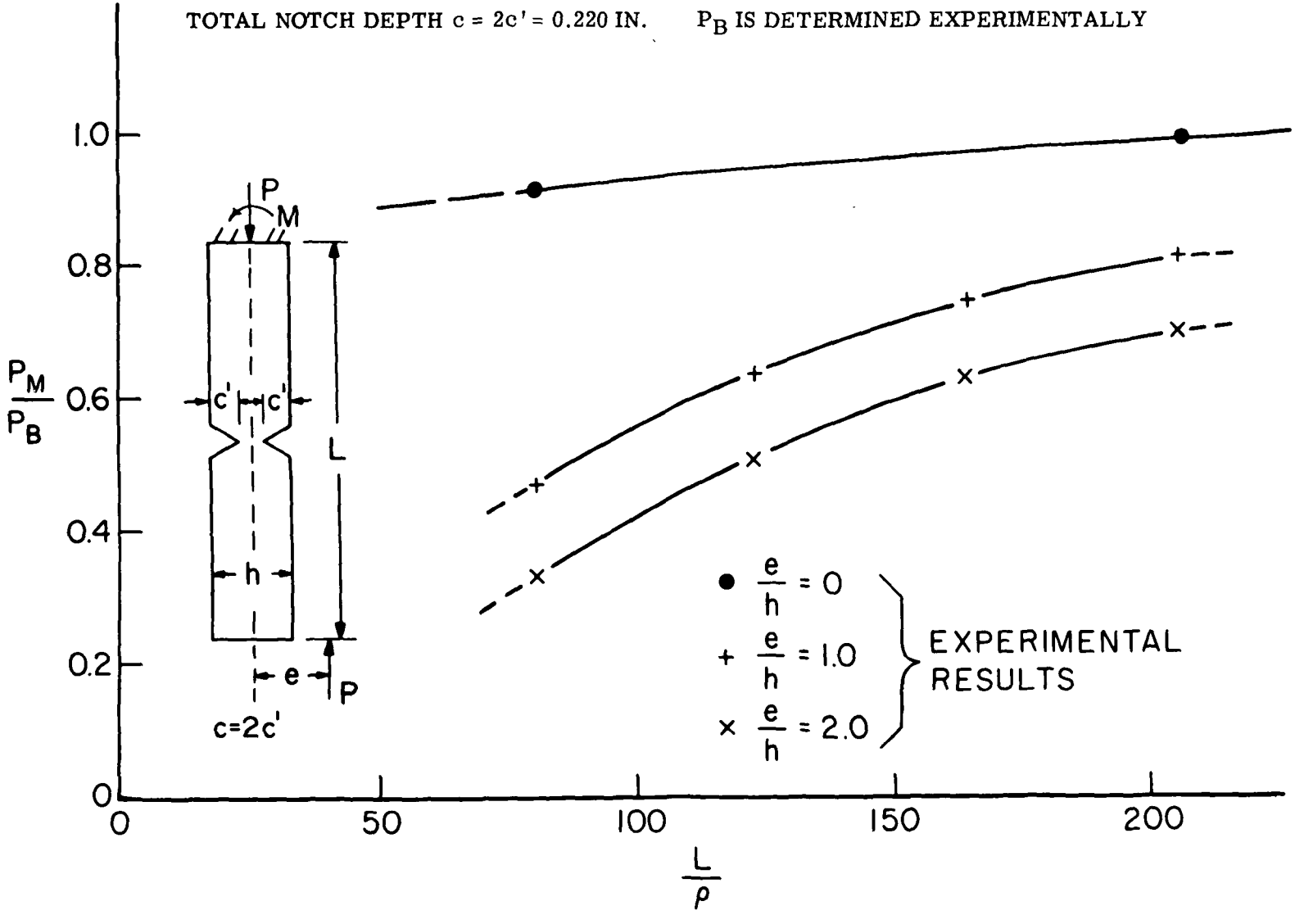

Figure 48. (P_M/P_B) vs. (L/c), when column is double-notched

RATIO OF THE MAXIMUM COLUMN LOAD CARRYING CAPACITY, P_M, OVER THE COLUMN BUCKLING LOAD, P_B, VERSUS THE SLENDERNESS RATIO, L/ρ, FOR SINGLE NOTCHED FIXED-PINNED END COLUMNS

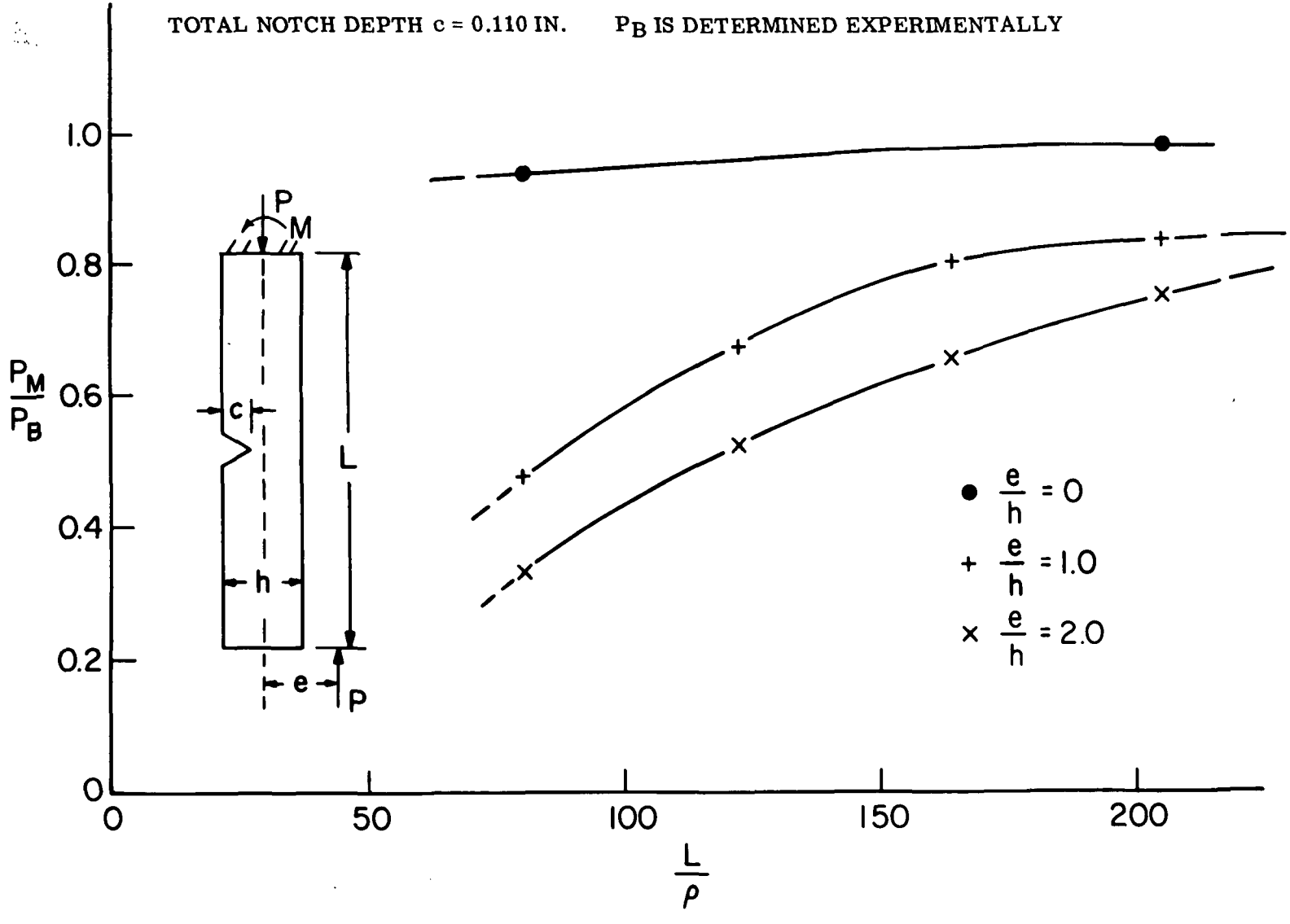

Figure 49. (P_M/P_B) vs. (L/c), when column is single-notched

RATIO OF THE MAXIMUM COLUMN LOAD CARRYING CAPACITY, P_M, OVER THE COLUMN BUCKLING LOAD, P_B, VERSUS THE RATIO OF THE TOTAL NOTCH DEPTH, c, OVER THE COLUMN WIDTH, h, FOR DOUBLE NOTCHED COLUMNS LOADED CONCENTRICALLY AND OF COMPARABLE LENGTH

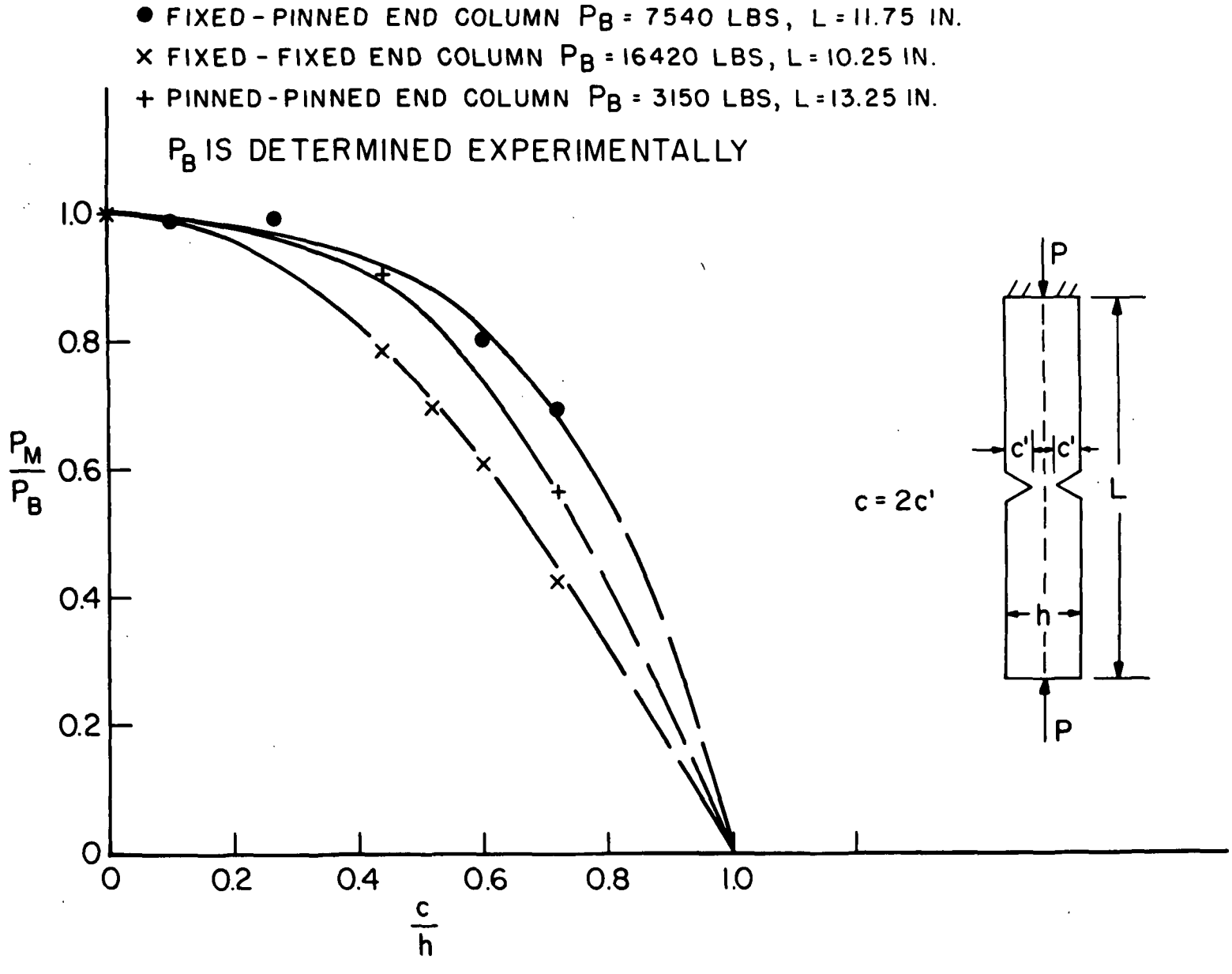

Figure 50. (P_M/P_B) vs. (c/h), various end conditions and double notch

RATIO OF THE MAXIMUM COLUMN LOAD CARRYING CAPACITY, P_M, OVER THE COLUMN BUCKLING LOAD, P_B, VERSUS THE RATIO OF THE TOTAL NOTCH DEPTH, c, OVER THE COLUMN WIDTH, h, FOR SINGLE NOTCHED COLUMNS LOADED CONCENTRICALLY AND OF COMPARABLE LENGTH

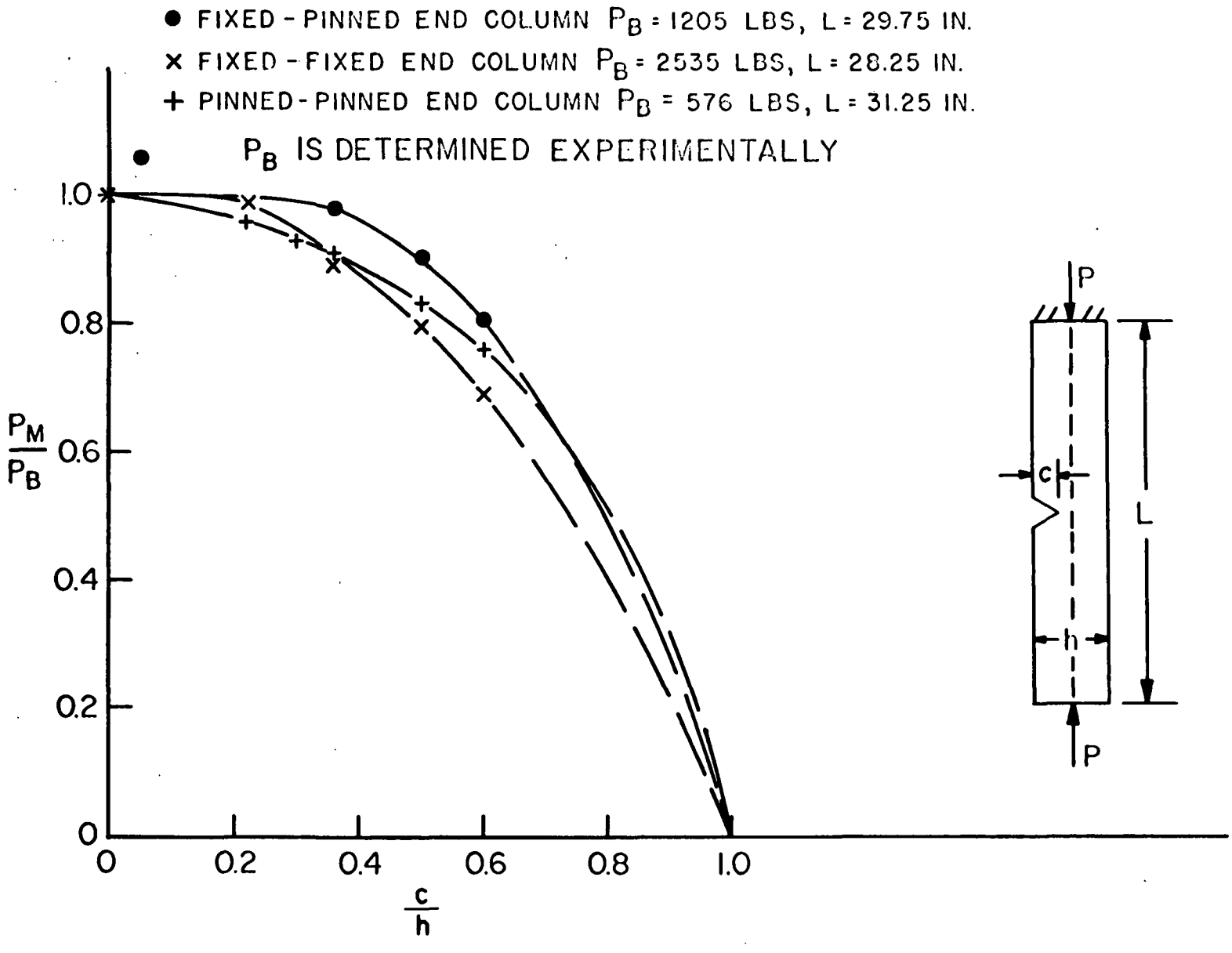

Figure 51. (P_M/P_B) vs. (c/h), various end conditions and single notch

Notch Depth (c)	Eccentricity (e)	Theoretical Maximum Load (P_{CR})	Experimental Maximum Load (P_{CR})
0.020	0.090	2548	2340
0.020	0.250	2074	1850
0.020	0.500	1613	1300
0.020	1.000	1121	1100
0.020	1.250	973	980
0.070	0.090	2417	2500
0.070	0.250	1848	1900
0.070	0.500	1355	1420
0.070	1.000	887	1050
0.070	1.250	756	980
0.090	0.090	2342	2550
0.090	0.250	1731	1920
0.090	0.500	1234	1460
0.090	1.000	784	980
0.090	1.250	633	900
0.110	0.090	2248	2470
0.110	0.250	1594	1760
0.110	0.500	1098	1400
0.110	1.000	677	950
0.110	1.250	568	720
0.170	0.090	1751	2130
0.170	0.250	1016	1530
0.170	0.500	611	1020
0.170	1.000	340	550
0.170	1.250	278	480
0.195	0.090	1359	2150
0.195	0.250	685	1460
0.195	0.500	384	960
0.195	1.000	204	540
0.195	1.250	165	470

Table I. Comparison of theoretical and experimental maximum load, pinned-pinned ends

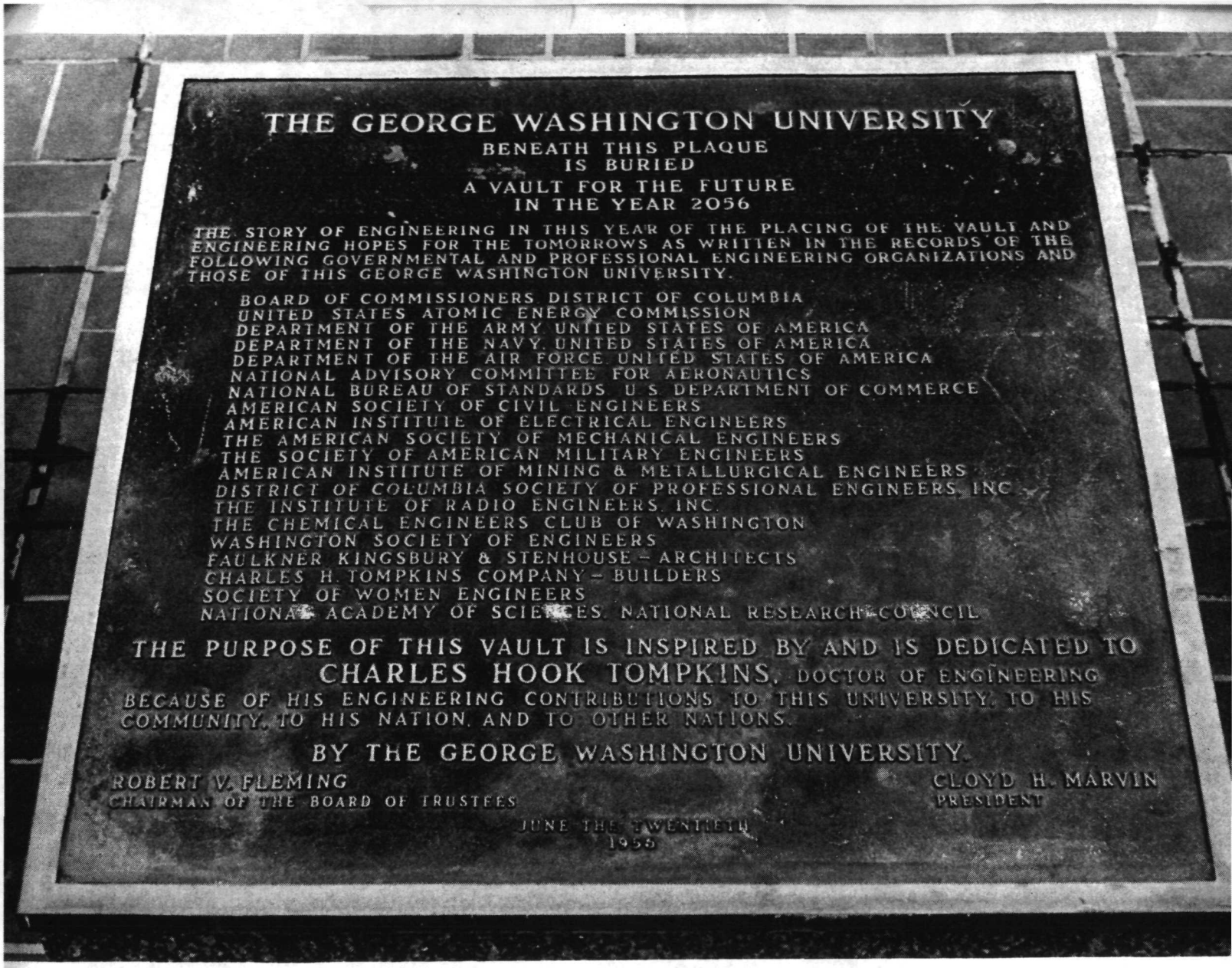
THE GEORGE WASHINGTON UNIVERSITY
BENEATH THIS PLAQUE
IS BURIED
A VAULT FOR THE FUTURE
IN THE YEAR 2056
THE STORY OF ENGINEERING IN THIS YEAR OF THE PLACING OF THE VAULT AND ENGINEERING HOPES FOR THE TOMORROWS AS WRITTEN IN THE RECORDS OF THE FOLLOWING GOVERNMENTAL AND PROFESSIONAL ENGINEERING ORGANIZATIONS AND THOSE OF THIS GEORGE WASHINGTON UNIVERSITY.
BOARD OF COMMISSIONERS DISTRICT OF COLUMBIA
UNITED STATES ATOMIC ENERGY COMMISSION
DEPARTMENT OF THE ARMY UNITED STATES OF AMERICA
DEPARTMENT OF THE NAVY UNITED STATES OF AMERICA
DEPARTMENT OF THE AIR FORCE UNITED STATES OF AMERICA
NATIONAL ADVISORY COMMITTEE FOR AERONAUTICS
NATIONAL BUREAU OF STANDARDS U S DEPARTMENT OF COMMERCE
AMERICAN SOCIETY OF CIVIL ENGINEERS
AMERICAN INSTITUTE OF ELECTRICAL ENGINEERS
THE AMERICAN SOCIETY OF MECHANICAL ENGINEERS
THE SOCIETY OF AMERICAN MILITARY ENGINEERS
AMERICAN INSTITUTE OF MINING & METALLURGICAL ENGINEERS
DISTRICT OF COLUMBIA SOCIETY OF PROFESSIONAL ENGINEERS INC
THE INSTITUTE OF RADIO ENGINEERS INC
THE CHEMICAL ENGINEERS CLUB OF WASHINGTON
WASHINGTON SOCIETY OF ENGINEERS
FAULKNER KINGSBURY & STENHOUSE – ARCHITECTS
CHARLES H TOMPKINS COMPANY – BUILDERS
SOCIETY OF WOMEN ENGINEERS
NATIONAL ACADEMY OF SCIENCES NATIONAL RESEARCH COUNCIL
THE PURPOSE OF THIS VAULT IS INSPIRED BY AND IS DEDICATED TO
CHARLES HOOK TOMPKINS, DOCTOR OF ENGINEERING
BECAUSE OF HIS ENGINEERING CONTRIBUTIONS TO THIS UNIVERSITY TO HIS COMMUNITY TO HIS NATION AND TO OTHER NATIONS.
BY THE GEORGE WASHINGTON UNIVERSITY.
ROBERT V. FLEMING
CHAIRMAN OF THE BOARD OF TRUSTEES
CLOYD H. MARVIN
PRESIDENT
JUNE THE TWENTIETH
1956

To cope with the expanding technology, our society must be assured of a continuing supply of rigorously trained and educated engineers. The School of Engineering and Applied Science is completely committed to this objective.